FACTORS AFFECTING PHYSICAL PROPERTIES AND COMPRESSIVE STRENGTH OF FLY ASH-BASED GEOPOLYMER

HONGSHENG CHENG

MASTER OF SCIENCE
IN
MATERIALS SCIENCE

SCHOOL OF SCIENCE
MAE FAH LUANG UNIVERSITY
2015

FACTORS AFFECTING PHYSICAL PROPERTIES AND COMPRESSIVE STRENGTH OF FLY ASH-BASED GEOPOLYMER

HONGSHENG CHENG

THIS THESIS IS A PARTIAL FULFILLMENT OF
THE REQUIREMENTS FOR THE DEGREE OF
MASTER OF SCIENCE
IN
MATERIALS SCIENCE

SCHOOL OF SCIENCE
MAE FAH LUANG UNIVERSITY
2015

FACTORS AFFECTING PHYSICAL PROPERTIES AND COMPRESSIVE STRENGTH OF FLY ASH-BASED GEOPOLYMER

HONGSHENG CHENG

THIS THESIS HAS BEEN APPROVED
TO BE A PARTIAL FULFILLMENT OF THE REQUIREMENTS
FOR THE DEGREE OF MASTER OF SCIENCE
IN
MATERIALS SCIENCE
2015

EXAMINATION COMMITTEE

.....CHAIRPERSON
(Nattakan Soykeabkaew, Ph. D.)

.....ADVISOR
(Asst. Prof. Suthee Wattanasiriwech, Ph. D.)

.....CO-ADVISOR
(Assoc. Prof. Darunee Wattanasiriwech, Ph. D.)

.....EXAMINER
(Nattaya Tawichai, Ph. D.)

.....EXTERNAL EXAMINER
(Pavadee Aungkavattana, Ph. D.)

ACKNOWLEDGEMENTS

This thesis would not have been completed without much assistance, encouragement and support from many people. I would like sincerely to take this opportunity to express my cordial thanks to those who have granted me invaluable instructions during the process of experiment and thesis writing.

First and foremost, I extend my greatest gratitude to Assistant Professor Dr. Suthee Wattanasiriwech, my advisor and Associate Professor Dr. Darunee Wattanasiriwech, my co-advisor, for their insightful guidance, earnest help and providing financial support to me by doing research assistant. They advised me to think over the selection of the subject and to carry out a series of relevant research at a very early time; and during the process of writing, they spent a lot of time guiding me in a right direction and provided many useful suggestions. It is under their strenuous help that I could complete this thesis in time.

Moreover, my sincere thanks go to Miss Haswipa Maimon and Mr. Keattipong Daikarn for their patience, instructions and professional advice in techniques all the time. Besides, I would like to be grateful acknowledge to Mae Fah Luang University and Higher Education Research Promotion, Office of the Higher Education Commission for financial support. I also express my thanks to Dr. Uraiwan Intatha for her providing me an opportunity to do a research assistant to solve some financial problems.

Last but not least, I am deeply in debt to my beloved parents for their understanding, support and endless love during my life.

Hongsheng Cheng

Thesis Title	Factors Affecting Physical Properties and Compressive Strength of Fly Ash-based Geopolymer
Author	Hongsheng Cheng
Degree	Master of Science (Materials Science)
Advisor	Asst. Prof. Suthee Wattanasiriwech, Ph. D.
Co-Advisor	Assoc. Prof. Darunee Wattanasiriwech, Ph. D.

ABSTRACT

Fly ash particle size distribution and curing conditions, such as curing atmosphere, activation temperature and initial water content, are important for mechanical properties of fly ash-based geopolymer. This work has been done to study the relationship between the factors above and compressive strength, as well as the physical properties including apparent density, bulk density and porosity. To make sure the study was consistent, the Si:Al:Na molar ratio was kept as constant at 2.46:1:1.38 throughout this research. The effect of cuing atmosphere on compressive strength and physical properties was evaluated by comparing the specimens kept either in saturated or open condition. Activation temperatures of 60, 75 and 90 ℃ in parallel with various initial water content of 29, 34 and 44 wt% were selected in finding the optimum activation condition. Finally, as received fly ash and fly ash with milling time of 10 min were chosen to study effect of particle size on compressive strength and physical properties. Compressive strength has been studied by universal testing machine (UTM). To observe the microstructure, scanning electron microscope (SEM) has been used. Following ASTM C 642-06, physical property values were

obtained. X-ray diffraction (XRD) has been used for roughly analyzing the phase. In summary, the highest compressive strength was obtained at the activation temperature of 75 ℃ compared to 60 ℃ and 90 ℃, under saturated condition, using finer fly ash and with lower initial water content.

Keywords: Fly ash/Geopolymer/Compressive strength/Density/Saturated/Initial water/Particle size/Activation temperature

TABLE OF CONTENTS

TABLE OF CONTENTS (continued)

TABLE OF CONTENTS (continued)

TABLE OF CONTENTS (continued)

LIST OF TABLES

LIST OF FIGURES

LIST OF FIGURES (continued)

LIST OF FIGURES (continued)

LIST OF FIGURES (continued)

LIST OF FIGURES (continued)

LIST OF FIGURES (continued)

CHAPTER 1

INTRODUCTION

Geopolymers are chains or networks of inorganic molecules linked with co-valent bonds. In the late 1970's, Joseph Davidovits, the inventor and developer of geopolymerization, gave the term "geopolymer" to classify the newly discovered geosynthesis that produces inorganic polymeric materials now used for a number of industrial applications. In details, geopolymer is a kind of inorganic polymer made from silicon and aluminum sources activated by alkaline liquid medium. The source could be metakaolin or fly ash which consists of silicon and aluminum. The alkaline liquid medium could be potassium hydroxide (KOH) or sodium hydroxide (NaOH).

Geopolymer is a potential alternative construction material. It is expected to replace Portland cement due to its high strength, very low creep and shrinkage, heat and cold resistance and chemical resistance. Most importantly, geopolymer is claimed to be more environmental friendly than Portland cement. This is because a lot of carbon dioxide (CO_2) is generated and it costs large amount of energy in the production of portland cement. According to Armstrong's statistics review (Armstrong, 2013), the production of 1 tonne of portland cement produces 1 tonne of CO_2 emissions. Global portland cement production is responsible for 5-8% of total man made CO_2 (greenhouse gas) emissions. Figure 1.1 shows that in 2012, global cement production was 3.7 billion tonnes, and cement consumption continues to increase with world growth. Such demand would cause a continuing rise in the global CO_2 level unless the cement production process is changed to a "cleaner" method.

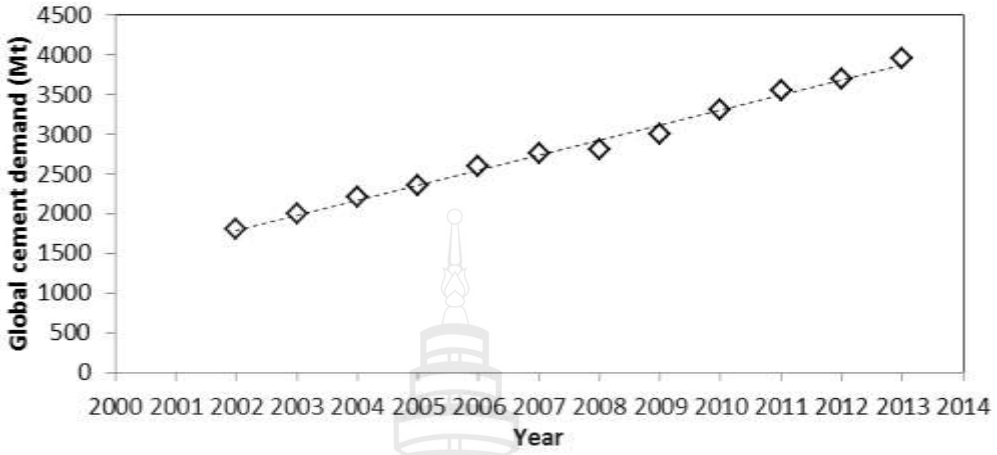

Source Armstrong (2013).

Figure 1.1 An Overview of Global Cement Sector Trends

Meanwhile, geopolymer can be made from fly ash which is a kind of waste material produced by coal combustion and it is nontoxic, environmental friendly and cheap. Fly ash is used to be source for geopolymerization due to its large of active silicate and aluminate parts. Due to the two reasons mentioned above, geopolymer is getting more and more important nowadays.

The mechanical property, especially compressive strength, of geopolymer is brought into focus of researcher since it is always used to be construction materials. Table 1.1 is adapted according to *code for design of concrete structures* (2010), which shows that the requirement of compressive strength for most applications varies from 10 MPa to 50.2 MPa. Many researchers have studied geopolymer and tried to obtain higher compressive strength (Chanh et al., 2008; Bakri et al., 2011; Jaarsveld et al., 2002; Izquierdo et al., 2010; Xie & Kayali, 2013; Criado et al., 2010; Temuujin et al., 2009; Joseph & Mathew, 2012; Bohlooli et al., 2012; Pangdaeng et al., 2014; Chindaprasirt et al., 2007; Arioz et al., 2012; Alvarez-Ayuso et al., 2008; Vora & Dave, 2013; Nazari et al., 2011; Guo et al., 2010; Arioz et al., 2012; Rajamma et al., 2012; Chindaprasirt et al., 2009; Ryu et al., 2013; Rattanasak & Chindaprasirt, 2009;

Somaratna et al., 2010; Phoo-ngernkham et al., 2014; Chi & Huang, 2013; Kumar & Kumar, 2011; Temuujin et al., 2009). However, the compressive strength was less than 50 MPa in most works. The higher compressive strength was mainly obtained on geopolymer motars (Joseph & Mathew, 2012; Chindaprasirt et al., 2007; Rattanasak & Chindaprasirt, 2009). Only a few works on pure geopolymer could get the compressive strength greater than 50 MPa (Bakri et al., 2011; Temuujin et al., 2009; Kumar & Kumar, 2011).

Table 1.1 Standard Compressive Strength of Concrete

Concrete Type	15	20	25	30	35	40	45	50	55	60	65	70	75	80
Compressive strength (MPa)	0.0	3.4	6.7	0.1	3.4	6.8	9.6	2.4	5.5	8.5	1.5	4.5	7.4	0.2

Source Code for design of concrete structures, China, GB50010-2010 (2010).

To improve compressive strength of geopolymer, the factors which can affect compressive strength have been done. The factors are fly ash particle size, sodium hydroxide concentration, the ratio of sodium silicate to sodium hydroxide, initial water content, controlling of humidity, activation temperature, activation time and testing time. Most factors have been studied with clear results and valuable information has been achieved. However, some factors have not been studied systematically such as initial water content. Some factors still neither unclear nor contradictory result was obtained.

In order to clarify the factors mentioned above and further improve the compressive strength, activation conditions will be optimized in this work. Once the processing condition is optimized, the compressive strength of 55 MPa is expected which can be used for most applications such as building and road construction.

CHAPTER 2

LITERATURE REVIEW

2.1 Concept of Geopolymerization

The geopolymer is a poly(sialate) network, consists of SiO_4 and AlO_4 tetrahedral chemical geometry. Sodium ions (Na^+) are present in the framework to balance the negative charge of Al in tetrahedral structure. Na-Poly(sialate) has the following empirical formula:

$$Na_n\,(-(SiO_2)_z - AlO_2)_n, wH_2O$$

where w is amount of water, z is 1, 2, 3 or higher and n is a degree of polycondensation.

Davidovits (2011, pp. 25, 141-143) summarized the basic principles of the synthetic reactions and hardening process by equations as follows:

$$(Si_2O_5, Al_2O_2)_n + 3nH_2O \xrightarrow{OH^-} n(OH)_3 - Si - O - Al^-(OH)_3 \quad (2.1)$$

$$n(OH)_3 - Si - O - Al^-(OH)_3 \rightarrow (-SiO - O - Al^-O - O-)_n \quad (2.2)$$

where $(Si_2O_5,\ Al_2O_2)_n$ represents Si, Al materials, $(OH)_3$-Si-O-Al-$(OH)_3$ is sialate, and $(-SiO-O-Al-O-O-)_n$ represents poly(sialate).

Equation 2.1 shows the mechanism of fly ash dissolution under alkaline condition. Si part and Al part are dissolved and reorganized into a monomer, sialate, which is basic species for polycondensation. Equation 2.2 shows that a lot of monomers are linked to form geopolymer networks of poly(sialate).

2.2 Factors in Controlling of Compressive Strength of Fly Ash-Based Geopolymer

2.2.1 Fly Ash Particle Size

Particle size is a very important factor that can affect the mechanical properties. This is because finer fly ash particles have larger surface area. Fly ash is easily dissolved in the alkaline solution because of high surface area. Furthermore, more dissolved monomers increase the geopolymerization reaction.

Researchers demonstrated that the compressive strength increased rapidly with increasing milling time of fly ash (Kumar & Kumar, 2011). The relationship between compressive strength and specific surface area, Figure 2.2, was adapted from Figure 2.1 and Table 2.1. According to Figure 2.2, the compressive strength of samples cured at 27 ℃ for 24 h increased from 5 MPa to 40 MPa with increasing specific surface area of fly ash from 0.969 m^2/g to 2.57 m^2/g. At the same time, the compressive strength of samples cured at 60 ℃ for 4 h increased from 10 MPa to 68 MPa with the specific surface area increased from 0.969 m^2/g to 2.57 m^2/g. It was also shown that compressive strength was increased linearly with the rise of fly ash specific surface area in both cases mentioned above (Figure 2.2).

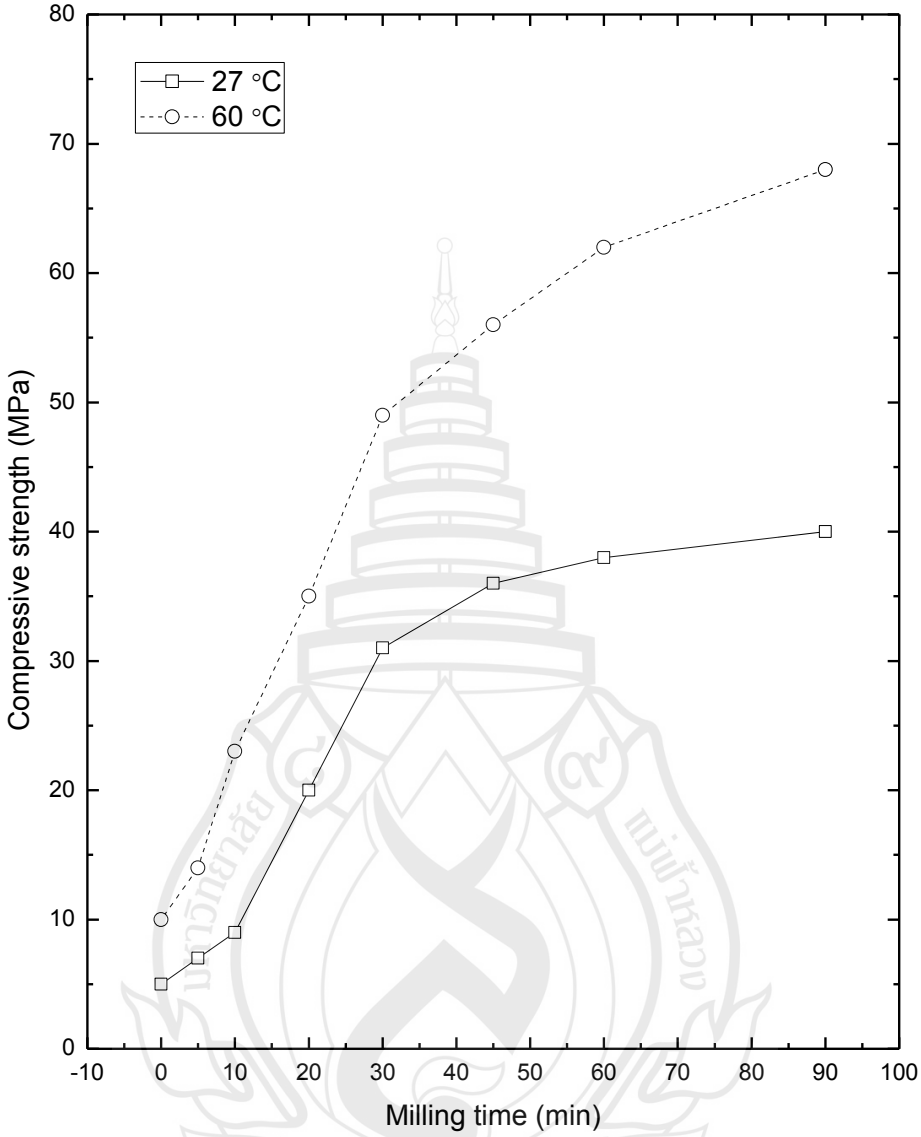

Source Adapted from Kumar et al. (2011).

Figure 2.1 Variation of Compressive Strength of the Samples Milled for Different Time and Cured at 27 ℃ and 60 ℃

Table 2.1 Specific Surface Area of Fly Ash Milled for Different Time

Milling time (min)	0	5	10	20	30	45	60	90
Specific surface area (m^2/g)	0.969	1.439	1.502	1.781	2.065	2.316	2.333	2.57

Source Kumar et al. (2011).

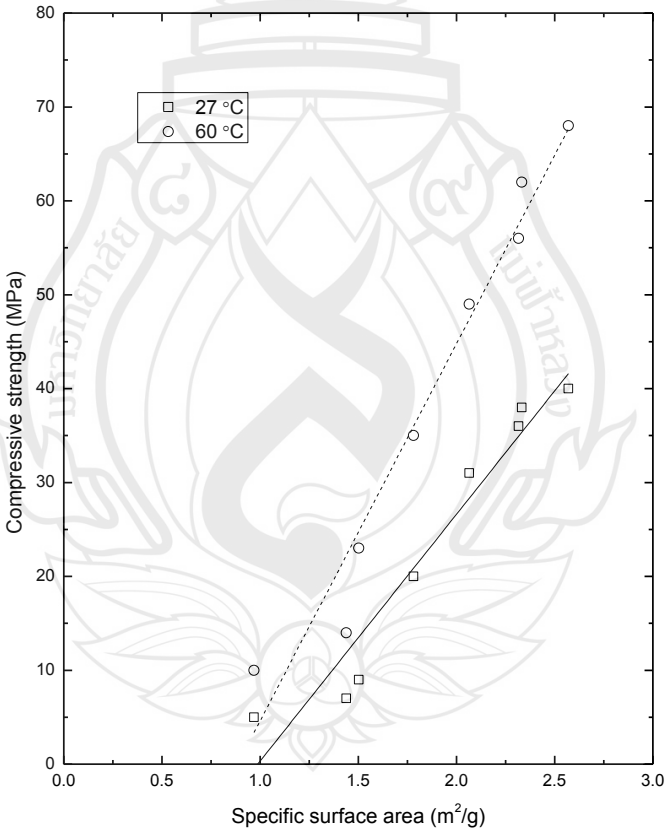

Source Kumar et al. (2011)**.**

Figure 2.2 Relationship between Compressive Strength and Fly Ash Specific Surface Area

The maximum compressive strength, 44 MPa, was obtained in the mixture of 3 μm fly ash at 70% by weight and 7 μm rice husk bark ash at 30% by weight in accordance with Table 1.2. Furthermore, the minimum compressive strength value of 24 MPa was obtained in the mixture of 75 μm fly ash at 70% by weight and 90 μm rice husk bark ash at 30% by weight. It was obvious that small fly ash particle size contributed to high compressive strength of geopolymer (Bohlooli et al., 2012). Temuujin et al. also supported this conclusion that small fly ash particle size contributed to high compressive strength of geopolymer. The work showed that compressive strength of samples cured at room temperature for 28 days increased from 16 MPa to 45 MPa when the fly ash median size, d50, decreased from 14.4 μm to 6.8 μm (Temuujin et al., 2009).

Table 2.2 Effect of Fly Ash Particle Size on the 7th Day Compressive Strength Cured at 80 ℃ for 36 h (FA-fly ash; RHBA-rice husk bark ash)

FA-3μm (wt%)	FA-75μm (wt%)	RHBA-7μm (wt%)	RHBA-90μm (wt%)	Compressive strength (MPa)
70	-	30	-	44
70	-	-	30	40
-	70	30	-	32
-	70	-	30	24

Source Bohlooli et al. (2012).

2.2.2 Sodium Hydroxide Concentration

Sodium hydroxide (NaOH) concentration is an important factor which affects compressive strength of fly ash-based geopolymer. According to geopolymerization shown in topic (section 2.1), there are two main steps which are dissolution and condensation in order. On the one hand, it is hard to completely dissolve fly ash in a low concentration of NaOH. On the other hand, the high velocity due to gel formation can hinder condensation step in a high concentration of NaOH.

Figure 2.3 was adapted from data based on various related work (Joseph & Mathew, 2012; Bohlooli et al., 2012; Chindaprasirt et al., 2007; Alvarez-Ayuso et al., 2008; Vora & Dave, 2013; Nazari et al., 2011; Arioz et al., 2012; Chindaprasirt et al., 2009; Ryu et al., 2013; Rattanasak & Chinadaprasirt, 2009; Somaratna et al., 2010). It was observed that in most cases, the compressive strength was increased and then decreased with increasing sodium hydroxide concentration. However, sodium hydroxide concentration was not only factor affecting compressive strength. Even though there was no specific optimum value of sodium hydroxide concentration, the optimum range existed. It also indicated that the maximum value of compressive strength was obtained at the sodium hydroxide concentration range between 10M to 15M.

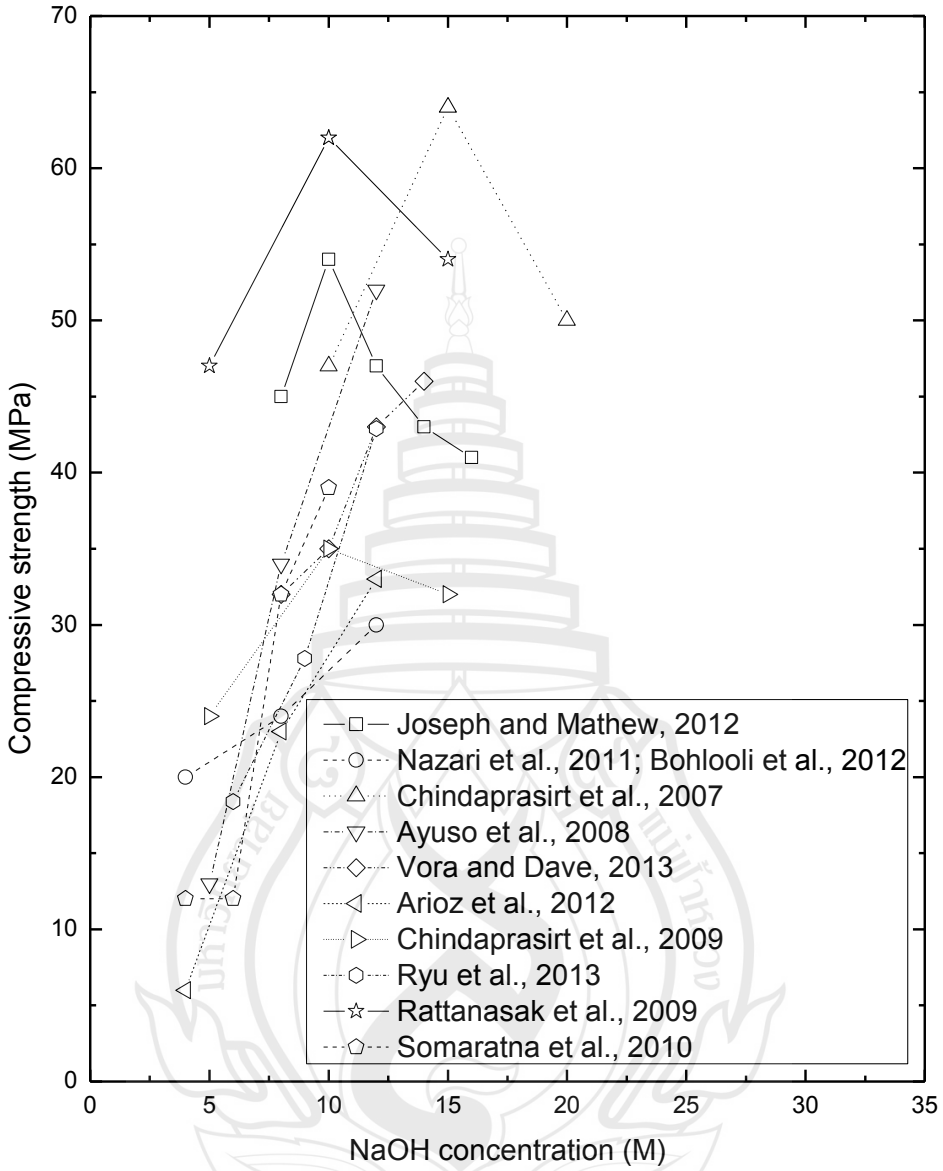

Source Joseph & Mathew (2012); Bohlooli et al. (2012); Nazari et al. (2011); Chindaprasirt et al. (2007); Ayuso et al. (2008); Vora & Dave (2013); Arioz et al. (2012); Chindaprasirt et al. (2009); Ryu et al. (2013); Rattanasak et al. (2009); Somaratna et al. (2010).

Figure 2.3 The Effect of NaOH Concentration on Compressive Strength

2.2.3 The Ratio of Sodium Silicate to Sodium Hydroxide

From Figure 2.4, the compressive strength increased and then decreased with increasing the ratio of sodium silicate to sodium hydroxide. The maximum compressive strength was obtained at the sodium silicate to sodium hydroxide ratio of 1. The compressive strength decreased slowly as the ratio of sodium silicate to sodium hydroxide is further increased beyond the optimum ratio of 1.

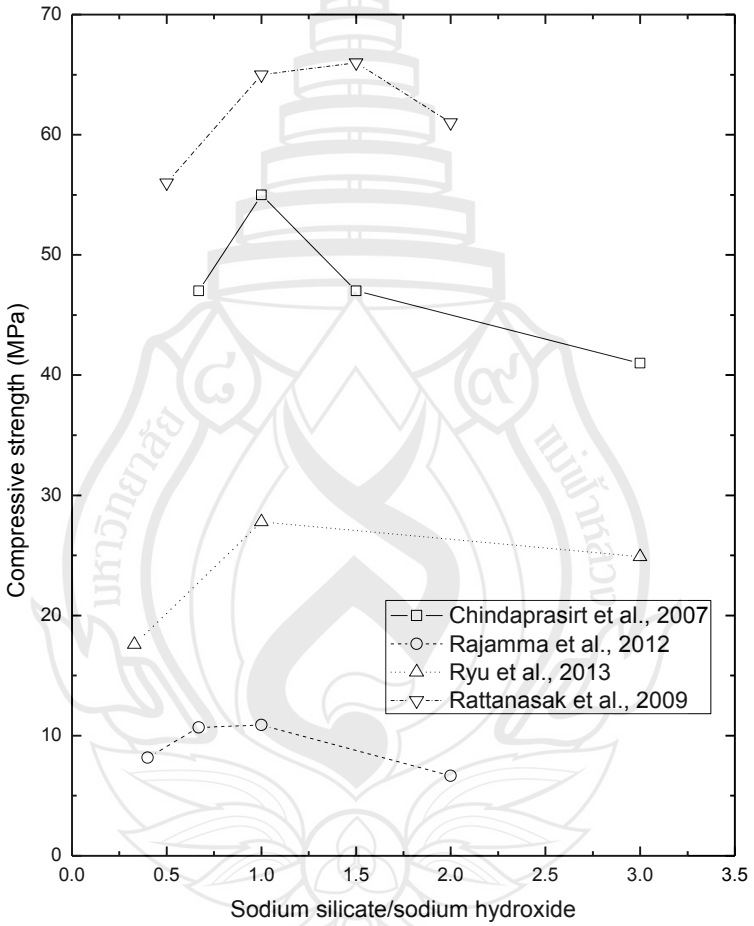

Source Chindaprasirt et al. (2007); Rajamma et al. (2012); Ryu et al. (2013); Rattanasak et al. (2009).

Figure 2.4 The Effect of Sodium Silicate to Sodium Hydroxide Ratio on the Compressive Strength of Fly Ash-Based Geopolymer

2.2.4 Initial Water Content

Water is the reaction medium for ions transportation in the geopolymerization process. In geopolymerization, some water is a part of the network while the excess of water is expelled from three dimensional networks. Ferone et al.'s work showed that with curing at 60 ℃ for 7 days, increasing the initial water content from 28% to 45% resulted in a very strong reduction of compressive strength, from 30 MPa to 17 MPa (Ferone et al., 2011). Temuujin et al. also demonstrated that the compressive strength reduced from 25 MPa to 16 MPa with increasing initial water content from 19% to 25% (Temuujin et al., 2009). Another work showed that compressive strength of geopolymer concrete reduced from 30 MPa to 20 MPa with increasing the ratio of water to geopolymer solids from 1: 10 to 1: 5 (Vora & Dave, 2013). In conclusion, the compressive strength seemed to decrease with increasing initial water content. However, the former two studies were neither detailed nor systematic and the later one was about concrete which included coarse and fine aggregates. Therefore, the proper initial water content was still unclear.

2.2.5 Control of Humidity

As we knew, initial water content was very important for compressive strength development. Too small amount of water resulted in insufficient media for transportation and reaction between ions (e.g. Na^+, OH^-). On the contrary, too much water leaves micro-voids after evaporation. Micro-voids are actually the weak point so crack propagation can easily occur. Meanwhile, low concentration of NaOH makes dissolution step slow and incomplete, as described in detail in another topic (section 2.2.2). Therefore, closed atmosphere could prevent water from evaporation which is good for strength development, but open atmosphere could accelerate water evaporating which could be harm to compressive strength.

Izquierdo et al.'s work studied effect of open and closed curing condition on compressive strength of fly ash-based geopolymer mortar (Izquierdo et al., 2010). The maximum compressive strength value of 52 MPa, which was twice as large as that from the open activation condition, was obtained from the closed condition at a period of 28 days (Figure 2.5).

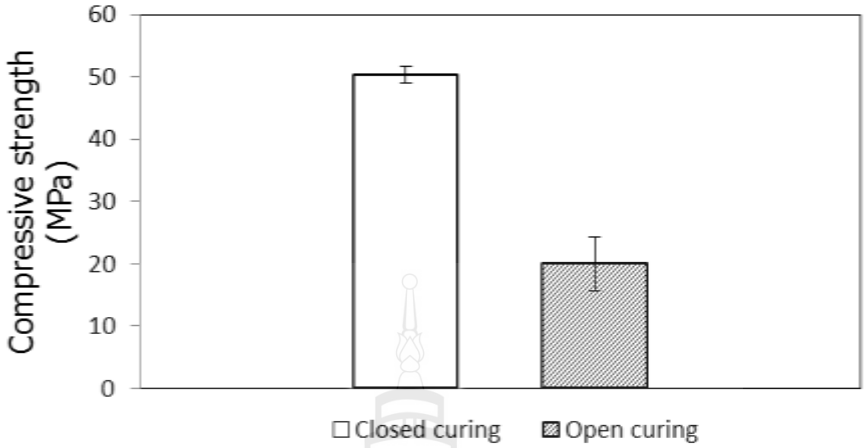

Source Izquierdo et al. (2010).

Figure 2.5 The Effect of Curing Condition on the 28th Day Compressive Strength of Fly Ash-Based Geopolymer Cured at Room Temperature

However, another work showed that the compressive strength was not related to activation treatment (Jaarsveld et al., 2002). In their study, it was observed that the samples activated at higher humidity in closed plastic bags did not always exhibit improved compressive strengths (Figure 2.6).

To sum up, one work showed that higher compressive strength was obtained at closed treatment that the samples were wrapped with cling film, while the lower compressive strength was obtained at open treatment that the samples were exposure to air condition. To the opposite, another work indicated that there was no relationship between compressive strength and activation treatment.

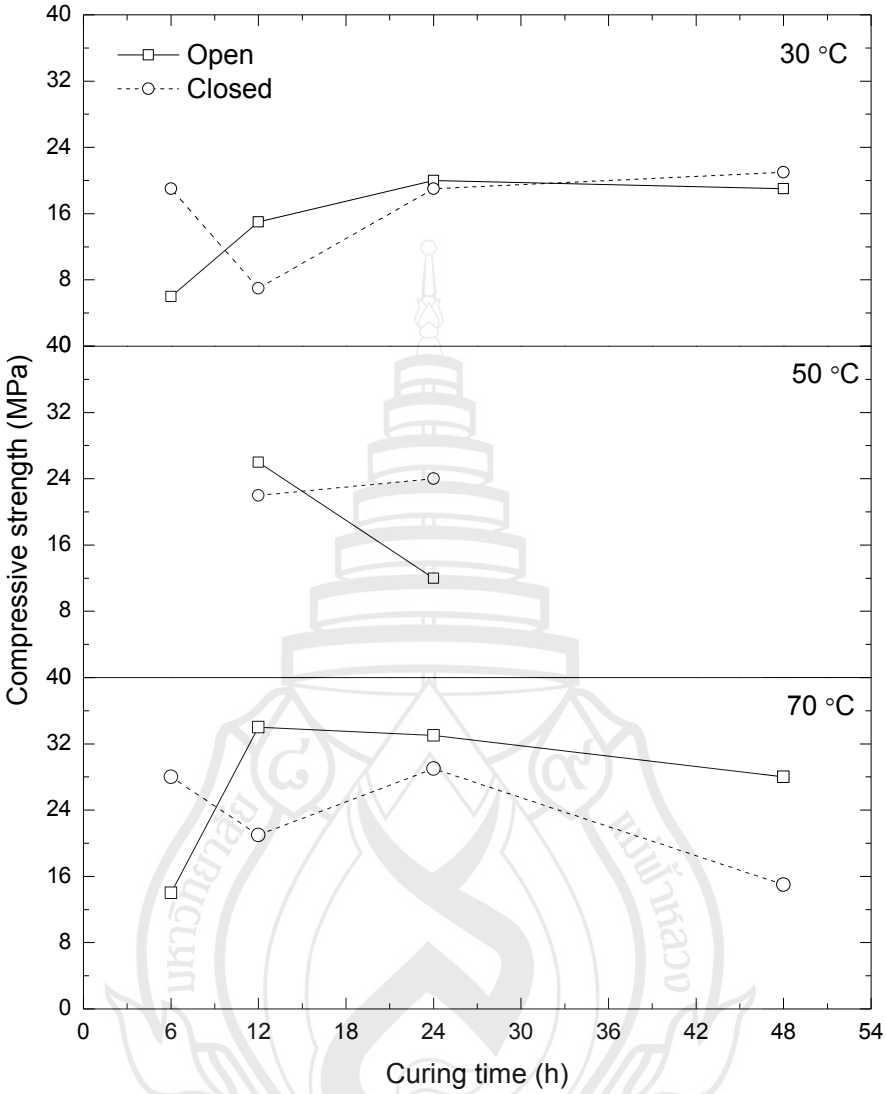

Source Jaarsveld et al. (2002).

Figure 2.6 The Effect of Curing Condition on the 14th Day Compressive Strength of Fly Ash-Based Geopolymer Cured at 30 ℃, 50 ℃ or 70 ℃

2.2.6 Activation Temperature

Temperature is a key factor in most chemical reaction because it can accelerate the reaction rate. In the case of geopolymer, temperature could have three functions. First, the high activation temperature promotes fly ash dissolution and ions

movement. Secondly, it promotes the water evaporation leading to a higher NaOH concentration which has been detailed in topic (section 2.2.2). The last one is the high activation temperature generates large extract force in period of condensation which results in cracks.

To obtain the relationship between compressive strength and activation temperature, some previous work has been analyzed and two contrasting results have been obtained. One was that compressive strength increased and then dropped with increasing activation temperature (Bakri et al., 2011; Joseph & Mathew, 2012; Chindaprasirt et al., 2007; Guo et al., 2010). Another was that compressive strength had an increasing trend with rising activation temperature (Chanh et al., 2008; Jaarsveld et al., 2002; Xie & Kayali, 2013; Temuujin et al., 2009; Arioz et al., 2012; Alvarez-Ayuso et al., 2008; Vora & Dave, 2013). Both contradictory results would be presented first and summarized later.

2.2.6.1 Compressive Strength Increasing and Decreasing with Increasing Activation Temperature

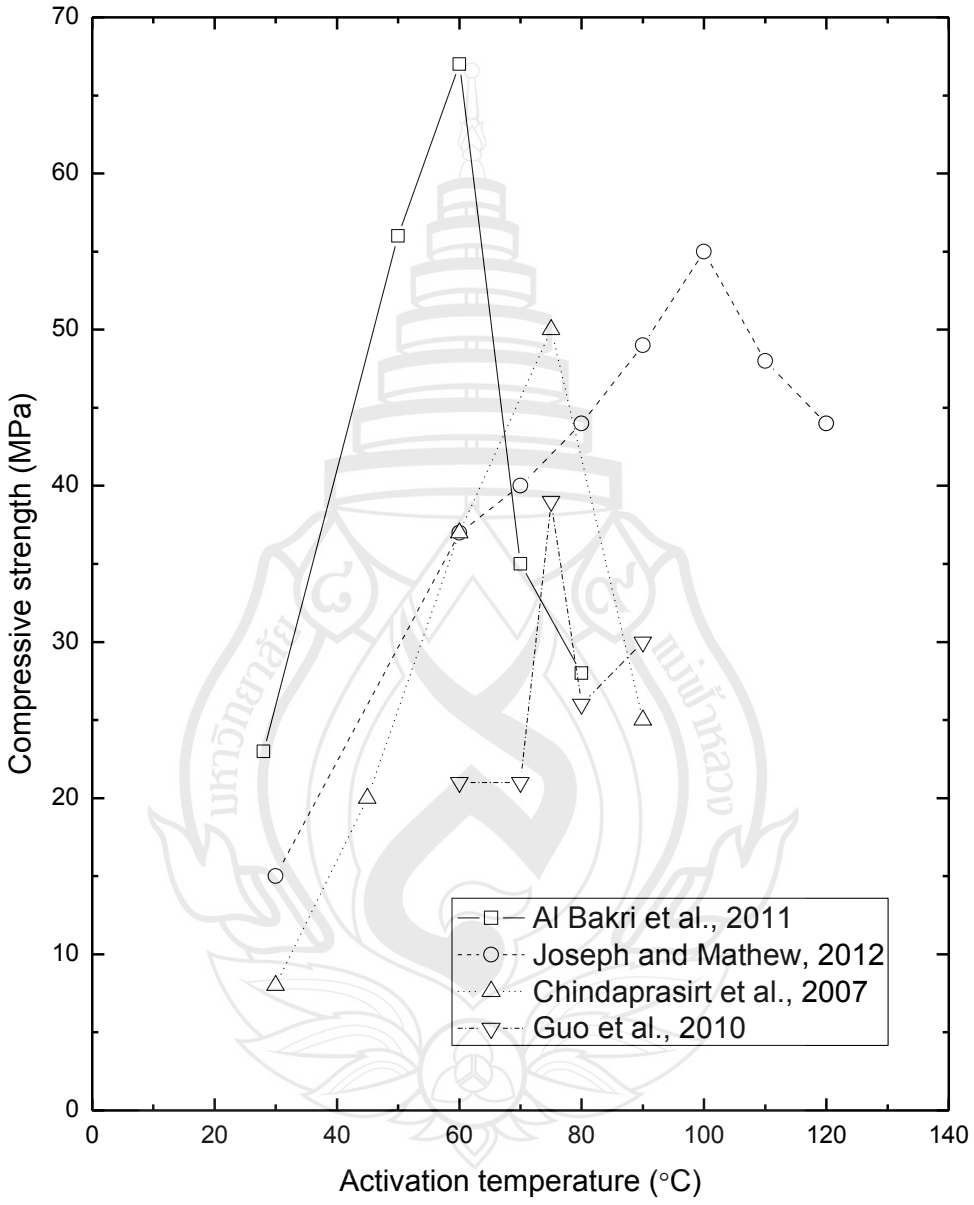

Source Al Bakri et al. (2011); Joseph & Mathew (2012); Chindaprasirt et al. (2007); Guo et al. (2010).

Figure 2.7 Effect of Activation Temperature on Compressive Strength

2.2.6.2 Compressive Strength Increasing with Increasing Activation Temperature

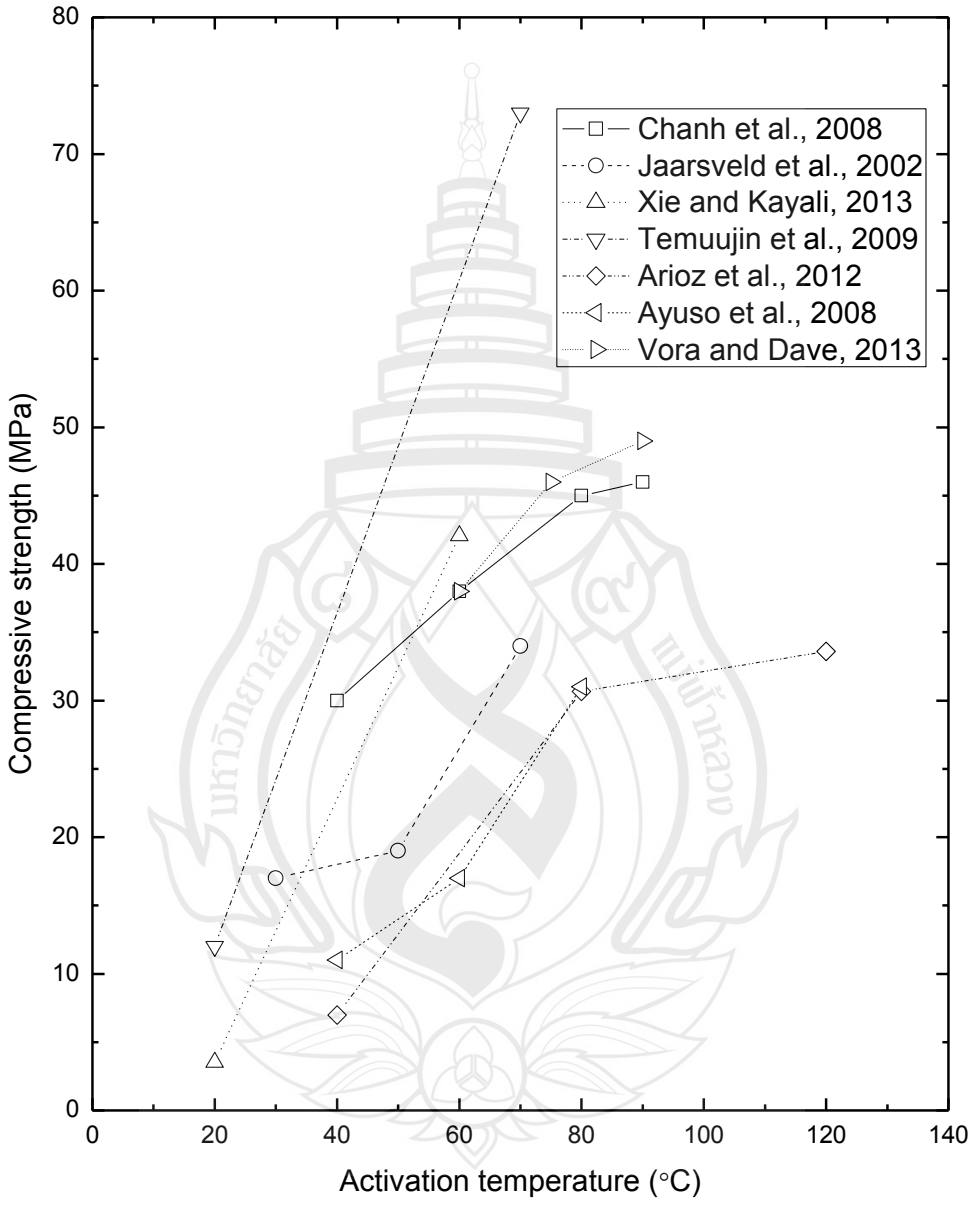

Source Jaarsveld et al. (2002); Xie & Kayali (2013); Temuujin et al. (2009); Arioz et al. (2012); Ayuso et al. (2008); Vora & Dave (2013); Chanh et al. (2008)**.**

Figure 2.8 Effect of Activation Temperature on Compressive Strength

From Figure 2.7 and Figure 2.8, activation temperature was one of the most important factors which affected the compressive strength of fly ash-based geopolymer. Figure 2.8 showed that the compressive strength was increased with increasing activation temperature at the range from 30 to 100 ℃. It was worth noting that the compressive strength increased from 15 MPa to 70 MPa with increasing activation temperature from 20 to 70 ℃. However, the different result was obtained from Figure 2.7 which was that the compressive strength was increasing and then decreasing with increasing curing temperature at the range from 30 to 100 ℃. The mechanism was not quite clear.

2.2.7 Activation Time

Activation time is a factor related reaction time. As we known, any chemical reaction needs time until it is completed. Less time is insufficient for complete reaction whereas more time is a waste. There was an agreement in some work (Chanh et al., 2008; Xie & Kayali, 2013; Criado et al., 2010; Joseph & Mathew, 2012; Chindaprasirt et al., 2007; Alvarez-Ayuso et al., 2008; Guo et al., 2010). Figure 2.9 was adapted by collecting and analyzing data from work mentioned above. It was observed that the compressive strength value was increasing with prolonging activation time but the speed was different. The compressive strength increased rapidly with prolonging activation time until 24 h and was kept almost constant after 24 h.

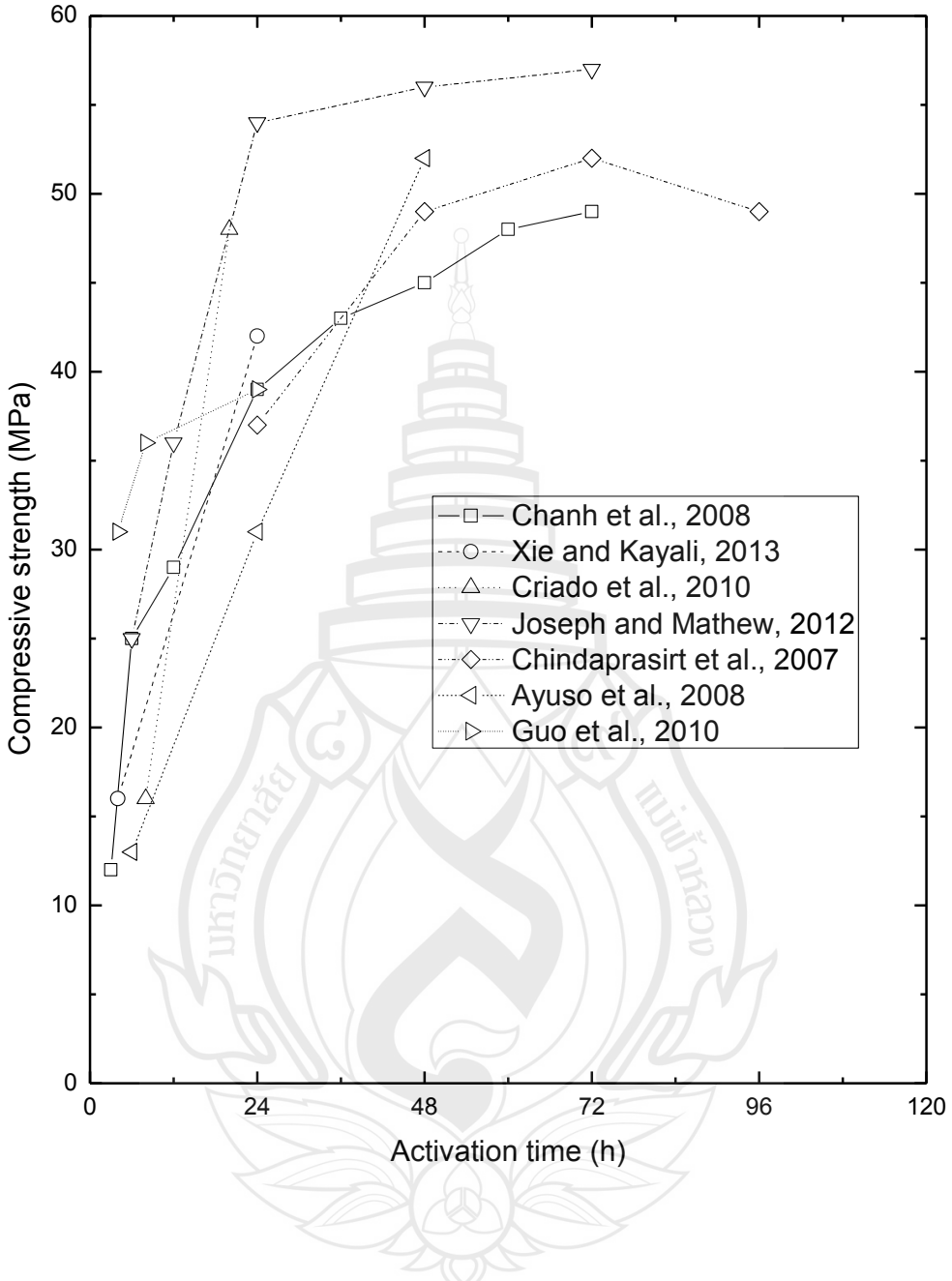

Source Xie & Kayali (2013); Criado et al. (2010); Joseph & Mathew (2012); Chindaprasirt et al. (2007); Ayuso et al. (2008); Guo et al. (2010); Chanh et al. (2008).

Figure 2.9 Effect of Activation Time on Compressive Strength

2.2.8 Testing Time

Testing time is an important index for compressive strength of cement because reaction continues with time. Similarly, testing time is a factor that we need to concern. Geopolymerization continues with time and a maximum value exists. Some related work demonstrated that an optimum testing day existed (Pangdaeng et al., 2014; Ryu et al., 2013; Phoo-ngernkham et al., 2014; Chi & Huang, 2013). Figure 2.10 was obtained by collecting and selecting data from works mentioned above. It was observed that the compressive strength started to increase with testing time sharply increased before the testing time of 7 days before increasing slowly after 7 days.

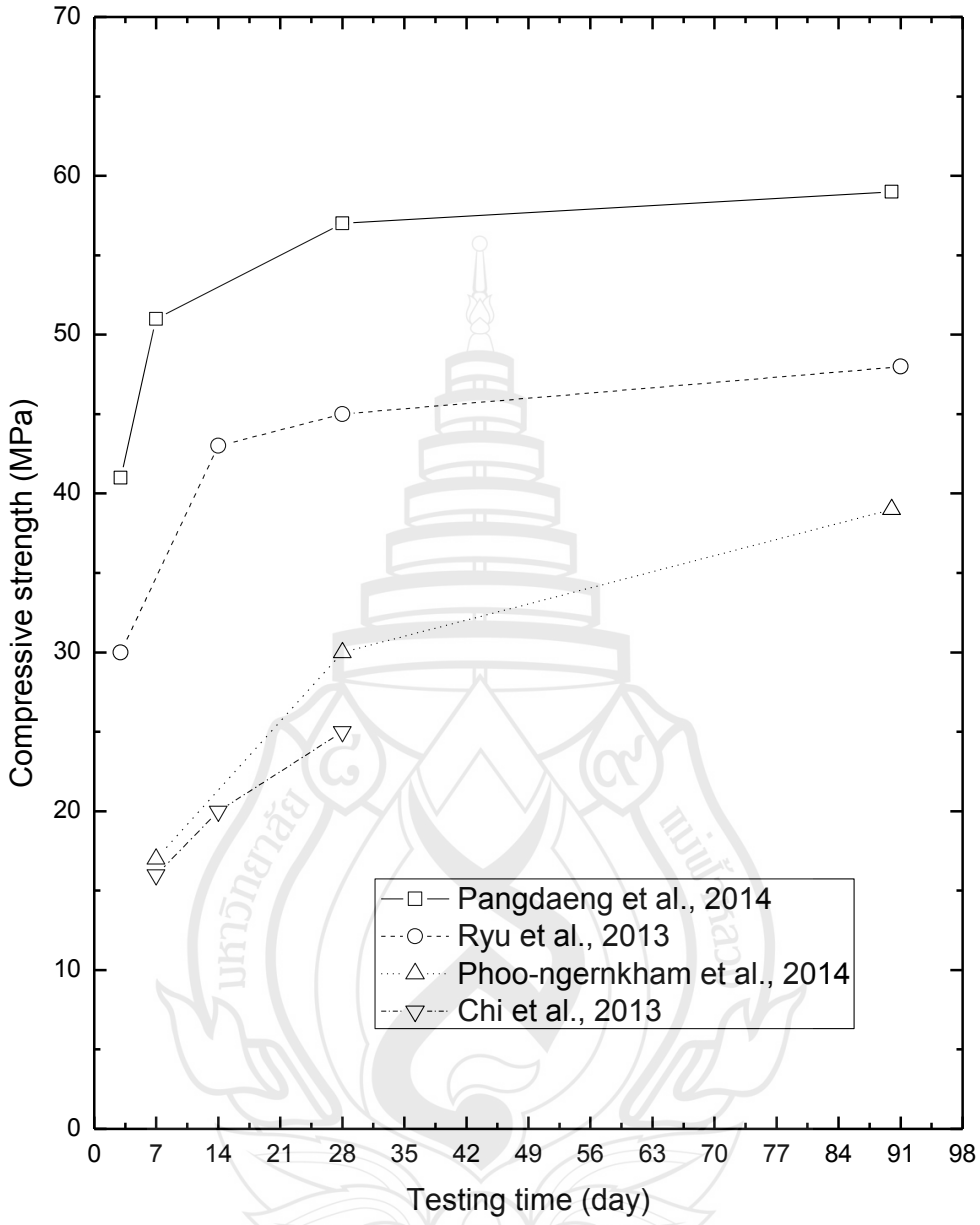

Source Pangdaeng et al. (2014); Ryu et al. (2013); Phoo-ngernkham et al. (2014); Chi et al. (2013).

Figure 2.10 Effect of Aging on Compressive Strength of Fly Ash-Based Geopolymer

CHAPTER 3

GENERAL PREPARATION OF FLY ASH-BASED GEOPOLYMER

3.1 Mixing

NaOH solution and Na_2SiO_3 solution were mixed in a beaker and stirred until the mixed solution was to become homogenous, as shown in Figure 3.1(a) and (b). Then the solution of NaOH and Na_2SiO_3 and fly ash (FA) powder were thoroughly mixed until no obvious agglomerate could be observed by eyes (Figure 3.1(c) and (d)).

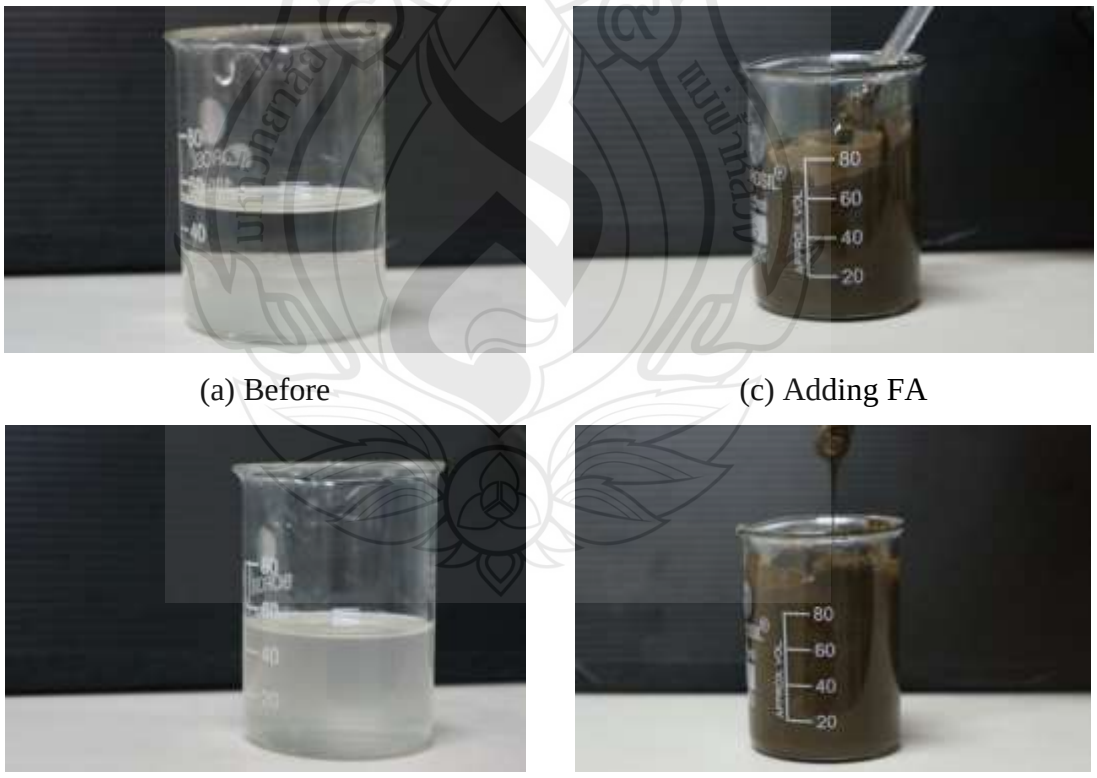

(a) Before (c) Adding FA

(b) After (d) Final mixture

Figure 3.1 Mixture of NaOH and Na_2SiO_3 Solution and FA

3.2 Pouring

The mixture of NaOH, Na_2SiO_3 and FA were poured into mold as slowly as possible in case that bubbles occurred inside. Figure 3.2 showed the operation of pouring mixture into a cylindrical shape plastic mold with 11.6 mm diameter and 29 mm height.

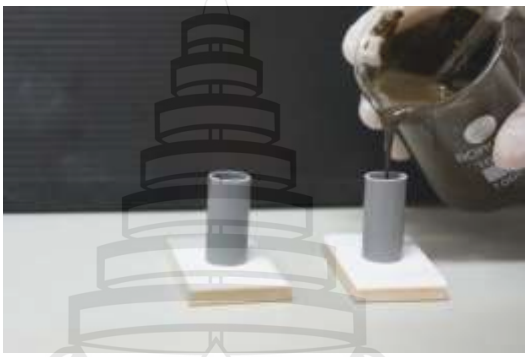

Figure 3.2 Pouring Mixture into Mold

3.3 Providing Saturated Condition

A cup of water was put in container to generate the saturated atmosphere, as shown in Figure 3.3.

Figure 3.3 Samples with Water in the Container

3.4 Activation and Curing

Samples were kept in a sealed container. Then the container was put in an oven, as shown in Figure 3.4.

Sealed

Activated

Figure 3.4 Samples in A Sealed Container and Activated in An Oven

3.5 Demolding

The samples would shrink after activation and curing, so it was easy to demold. However, if the shrinkage was too small, samples would be exerted a pressure with positive direction and mold would be given an opposite direction (Figure 3.5).

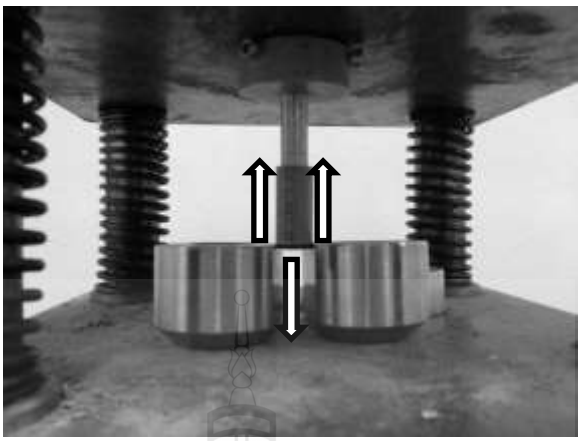

Figure 3.5 Demolding Hardened Fly Ash-Based Geopolymer (The arrows stood for the direction of force)

CHAPTER 4

THE EFFECT OF OPEN AND SATURATED CONDITION ON PHYSICAL PROPERTIES AND COMPRESSIVE STRENGTH OF FLY ASH-BASED GEOPOLYMER

4.1 Abstract

This work has been done to study the effect of open and saturated condition on physical properties and compressive strength of fly ash-based geopolymer. The mass difference before and after curing has been recorded. It showed that water evaporated from samples for open condition but it was kept inside samples for saturated condition. Open curing condition was used as control group which meant that the samples were activated at 60, 75 or 90 ℃ for 24 h under saturated condition and then cured at 40 ℃ under open condition for 6 days. Saturated condition was used as experimental group which meant that samples were activated at 60, 75 or 90 ℃ for 24 h and then cured at 40 ℃ under saturated condition for 1, 2 and 3 days, finally cured at 40 ℃ under open condition for 5, 4 and 3 days, respectively. Physical properties, such as apparent density, bulk density, geometric density and porosity were tested. Compressive strength was tested using universal testing machine (UTM). To observe the microstructure of samples, scanning electron microscope (SEM) was used. X-ray diffraction (XRD) was used to characterize the phase of hardened fly ash-based geopolymer. It was concluded that compressive strength of fly ash-based geopolymer was higher for saturated condition compared to open condition. Furthermore, the compressive strength had an increasing trend with prolonging curing time under saturated condition. Almost the same value of apparent density, bulk density, geometric density and porosity were obtained for samples cured under both open and saturated conditions. SEM images showed that the distribution of crack and the width of crack were similar for saturated condition compared to open condition.

The reacted matrix for open condition was coarse and the reacted matrix for saturated condition was smooth.

4.2 Introduction

From literature review (section 2.2.5), Izquierdo et al. (2010) showed that higher compressive strength was obtained at saturated condition in which the samples were wrapped with cling film, while the lower compressive strength was obtained with open air condition. In contrast, another work (Jaarsveld et al., 2002) indicated that there was no specific relationship between compressive strength and moisture-control activation treatment. In order to clarify the effect of atmospheric water on compressive strength, saturated and open conditions have been used in preparation of geopolymer.

4.3 Experiment

4.3.1 Materials

Fly ash (source: Mae Moh, Lampang, Thailand) has been selected as the raw material in our geopolymer production. The concentration of 10 mole/liter (M/L) of sodium hydroxide solution (10M NaOH) and sodium silicate solution (Na_2SiO_3) has been selected as alkaline liquid to dissolve fly ash and supply sodium and silicon.

4.3.2 Preparation of Fly Ash-Based Geopolymer

10M NaOH and Na_2SiO_3 solution (APPENDIX E: Table E3) were mixed following the weight ratio of 1 and stirred by magnetic stirrer for 3 min. Fly ash powders were added into alkaline solution following the solution to fly ash weight ratio of 3:5 and stirred for 30 s until no obvious agglomerate was observed. The mixture was poured into a cylindrical shape plastic mold with 11.6 mm diameter and 29 mm height. The mold continued to be kept in a sealed container with water saturated atmosphere by supplying 160 mL extra water called saturated condition (Figure 4.1(b)). The container was kept in the oven and activated either at 60, 75 or

90 ℃ for 24 h with saturated condition. All samples at same temperature were divided into 2 groups. One group called control group continued to be cured at 40 ℃ under open condition for 6 days. The other group called experimental group continued to be cured at 40 ℃ under saturated condition for 1, 2 or 3 days. The group was kept at 40 ℃ under open condition, which meant samples were kept in an open container without supplying extra water (Figure 4.1(a)), until the total curing period of 6 days was achieved, respectively. Finally, the samples were removed from mold for characterization (Figure 4.2).

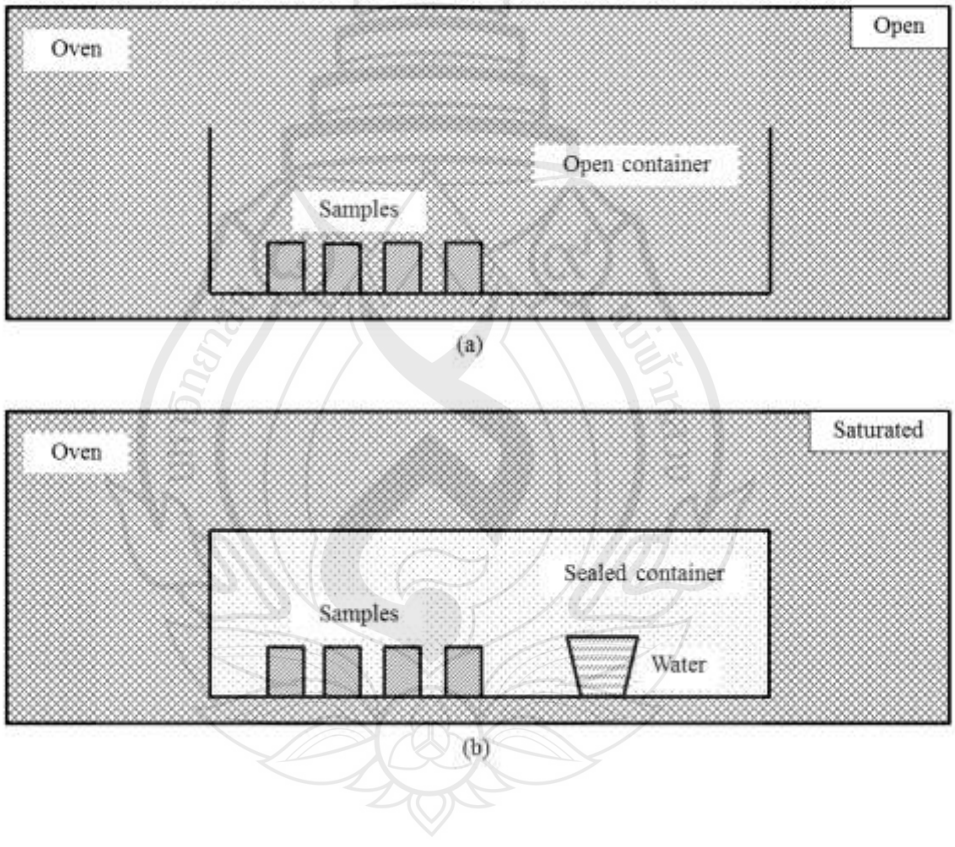

Figure 4.1 Diagram of (a) Open Condition and (b) Saturated Condition

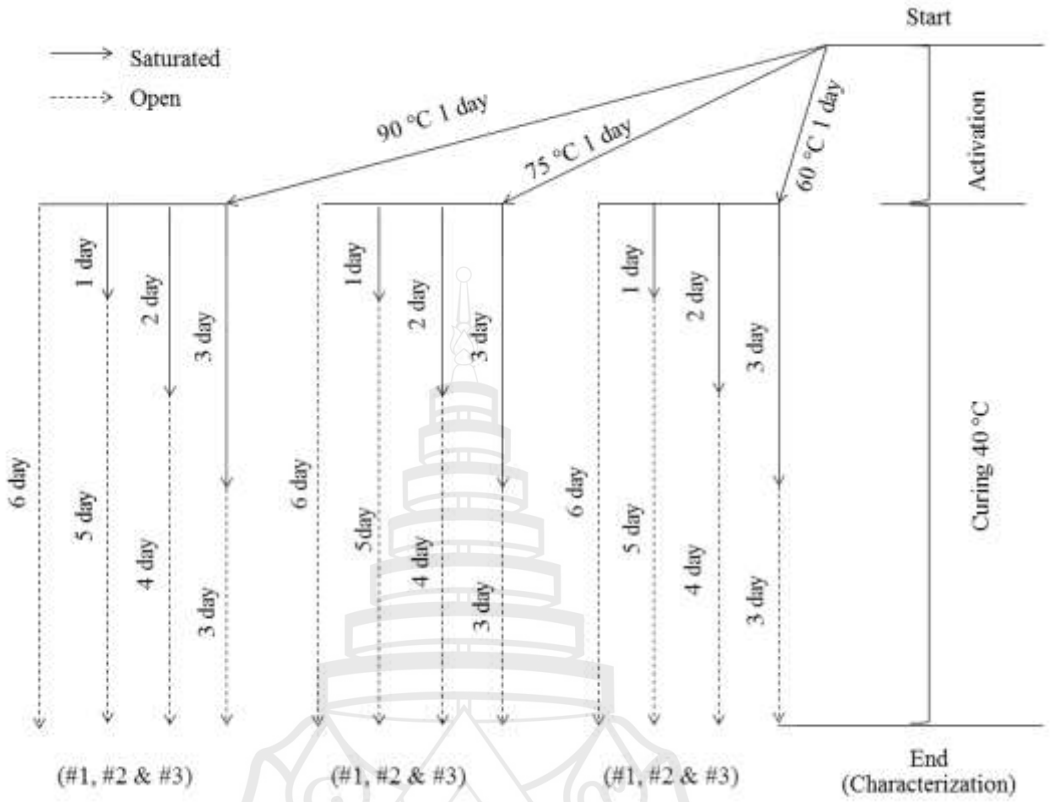

Figure 4.2 Diagram of Experimental Preparation (Control group with curing under open condition for 6 days; Experimental group with curing under saturated condition for 1, 2 or 3 days)

4.3.3 Characterization

4.3.3.1 Weight Change

The weight change (ΔW) was calculated by using the following equation:

$$\Delta W = W_f - W_i \tag{4.1}$$

where W_f is final weight of samples and W_i is initial weight of samples.

The initial weight of samples was recorded at the time when samples were set up immediately. The final weight of samples was recorded when samples were activated for 24 h and cured for 3 days. In this experiment, samples were activated at 60, 75 and 90 ℃ under saturated condition for 24 h and then samples were divided

two groups, open group and saturated group. Open group was cured at 40 ℃ under open condition for 3 days. Saturated group was continuously cured at 40 ℃ under saturated condition for 3 days. Weight change was calculated using Equation 4.1.

4.3.3.2 Compressive Strength

Compressive strength at 7th day was characterized by universal testing machine (INSTRON 5566). The top and the bottom faces of each cylindrical sample were polished on abrasive paper P320 with a rotational speed of 200 rpm till they were parallel prior to testing. The loading speed was set at 1.0 mm/min and the maximum load of 10.0 kN was used. The measurement was following ASTM C39-04a.The results were the average values of five samples. In the graphs throughout this thesis, #1, #2 and #3 represented each repeating experiment.

4.3.3.3 Physical Properties

1. Apparent Density, Bulk Density and Porosity

Samples were dried in oven at 105 ℃ for 24 h and recorded the oven-dry mass as A. Then samples were immersed in water at ambient temperature for 24 h and recorded the saturated mass after immersion as B. Finally, the buoyancy of samples immersed in water was tested and recorded as F. Apparent density, bulk density and porosity were tested following ASTM C 642-06. The results were the average of five samples.

Apparent density (g_2) was calculated by the following equation:

$$g_2 = \frac{A}{A + F - B} \times \rho_{H_2O} \tag{4.2}$$

Bulk density (g_1) was calculated by the following equation:

$$g_1 = \frac{A}{F} \times \rho_{H_2O} \tag{4.3}$$

where ρ_{H_2O} is density of water.

Porosity (p) was calculated by the following equation:

$$p = \frac{g_2 - g_1}{g_2} \times 100\% \quad (4.4)$$

2. Geometric Density

Geometric density was tested using balance and vernier caliper. Geometric density (g_3) was calculated by the following equation:

$$g_3 = \frac{W}{\pi \times (D/2)^2 \times H} \quad (4.5)$$

where W is weight of hardened samples measured using a digital balance, D is diameter of hardened samples measured using a digital vernier caliper, and H is height of hardened samples measured using a digital vernier caliper.

4.3.3.4 Microstructure

Scanning electron microscope (LEO 1450 VP) was used for observing the microstructure. Samples were polished on abrasive paper P600 for 1 min with a rotational speed of 180 rpm and then on abrasive paper P1200 for 30 s with a rotational speed of 200 rpm. The received samples were finally polished using 6 μm diamond particles for 60s with rotational speed of 220 rpm.

4.3.3.5 Phase Composition

X-ray Diffraction instrument (PANalytical, X'Pert PRO) was used for analyzing the phase composition of hardened fly ash-based geopolymer. The surface of sample was polished on abrasive paper P320 for 30 s.

4.4 Results and Discussion

4.4.1 Weight Change

For all samples cured under open condition, weight loss was observed. The weight changes of samples activated at 60, 75 and 90 ℃ were -2.6±0.2 wt%, -3.8±1.1 wt% and -3.9±0.1 wt%, respectively. On the other hand, for samples cured under saturated condition, the weight gain was observed. The weight changes of samples activated at 60, 75 and 90 ℃ were 5.3±0.3 wt%, 3.0±0.4 wt% and 3.5±0.3 wt%, respectively. The results showed that the weight changes of samples cured under open condition were negative while that of samples cured under saturated condition were positive which means that curing under saturated condition prevent initial water from evaporation (Figure 4.3).

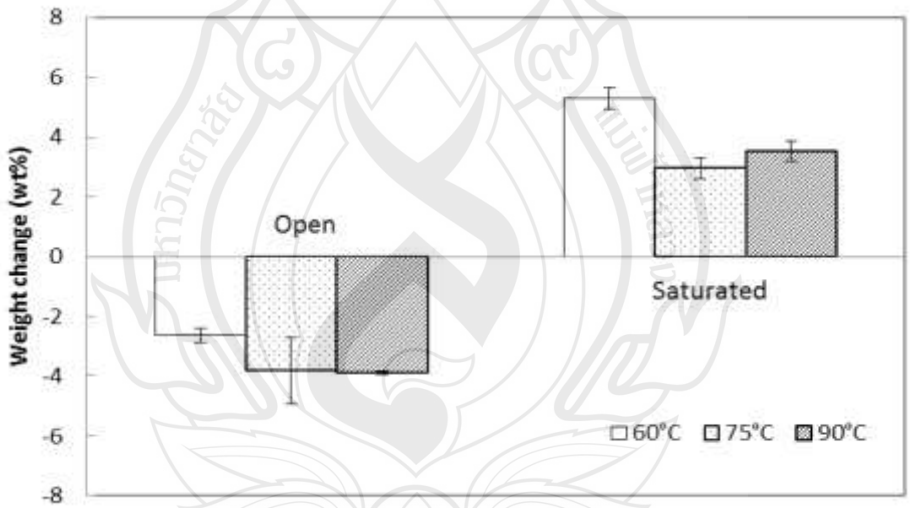

Figure 4.3 Effect of Open and Saturated Condition on Weight Change of Fly Ash-Based Geopolymer

4.4.2 Open and Saturated Condition

For compressive strength, the value from saturated condition (including saturated time for 1, 2 or 3 day) was always increasing compared to open condition for activation temperature of 60 ℃ (#1, #2 and #3), for 75 ℃ (#1, #2 and #3) and for

90 ℃ (#2 and #3). Decreasing compressive strength was obtained for samples from open to saturated time for 1 day in the case of 90 ℃ (#1). Therefore, saturated condition contributed to higher compressive strength compared to open condition. Furthermore, compressive strength exactly increased with increasing saturated time (Figure 4.4). The results showed the same trend to previous work (Izquierdo et al., 2010).

Apparent density was slightly increasing with increasing saturated time for activation temperature of 60 ℃ (#1 and #3), for 75 ℃ (#3) and for 90 ℃ (#2). Decreasing apparent density occurred in the case of 60 ℃ (#2) and 90 ℃ (#3). Increasing and then decreasing apparent density occurred for 75 ℃ (#1 and #2). Apparent density was almost constant in the case of 90 ℃ (#1). However, either increasing trend or decreasing trend was slight. Therefore, generally it was believed that the apparent density was kept almost constant with changing saturated time (Figure 4.5).

Bulk density was almost kept constant with increasing saturated time for 60 ℃ (#2 and #3), for 75 ℃ (#1, #2 and #3) and for 90 ℃ (#1, #2 and #3). Increasing bulk density occurred in the case of activation temperature of 90 ℃ (#1). Therefore, generally it was believed that the bulk density was kept almost constant with changing saturated time (Figure 4.6).

Geometric density was slightly increasing with increasing saturated time for activation temperature of 60 ℃ (#1 and #2), for 75 ℃ (#1 and #2) and for 90 ℃ (#2). Decreasing and then increasing geometric density occurred for 90 ℃ (#1). However, either increasing trend or decreasing trend was slight. Therefore, generally it was believed that the apparent density was kept almost constant with changing saturated time (Figure 4.7).

Porosity was slightly decreasing with increasing saturated time for activation temperature of 60 ℃ (#1) and for 90 ℃ (#3). Increasing porosity occurred in the case of 60 ℃ (#3), 75 ℃ (#3) and 90 ℃ (#2). Increasing and then decreasing porosity occurred for 75 ℃ (#2). Decreasing and then slight increasing porosity was observed for 60 ℃ (#2). It was showed that the porosity performed decreasing, then increasing and finally decreasing trend for 75 ℃ (#1) and 90 ℃ (#1). However, either increasing

trend or decreasing trend was slight. Therefore, generally it was believed that the apparent density was kept almost constant with changing saturated time (Figure 4.8).

A higher compressive strength was obtained for samples cured under saturated condition and the lower one was obtained for open condition. Furthermore, the compressive strength increased with prolonging the curing time under saturated condition. It was believed that curing under saturated condition was good for geopolymerization. However, almost the same value of apparent density, bulk density, geometric density and porosity were obtained for samples cured under both open and saturated conditions. It was likely that the atmospheric water prevented initial water from evaporation so that the reaction occurred more completely. Furthermore, effect of atmospheric water on apparent, bulk, geometric density and porosity of hardened fly ash-based geopolymer paste could be negligible.

From SEM image, the distribution of crack and the width of crack were similar on surface of fly ash-based geopolymer with a magnification of 50X, as shown in Figure 4.8 and Figure 4.10. In an image with a magnification of 200X, as shown in Figure 4.9 and Figure 4.11, two obvious phenomena were observed. The first one was that the distribution of crack and the width of crack were similar compared to open condition (Figure 4.10 (a) and Figure 4.12 (a)) to saturated condition (Figure 4.10 (b) and Figure 4.12 (b)), which was supported by Figure 4.9 and Figure 4.11. The second was that the reacted matrix for open condition was coarse, shown in Figure 4.10 (a), while the reacted matrix for saturated condition was smooth, as shown in Figure 4.10 (b).

X-ray diffraction analysis was used for analyzing the crystallinity and phase of fly ash-based geopolymerization. Figure 4.13 showed that for fly ash, anhydrite ($CaSO_4$), magnetite low (Fe_3O_4) and quartz alpha (SiO_2) were observed. Magnesioferrite ($MgFe_2O_4$), cancrinite ($3NaAlSO_4 \cdot NaOH$), calcite ($CaCO_3$) and quartz (SiO_2) were observed in geopolymer cured under open condition. Magnesioferrite ($MgFe_2O_4$), quartz (SiO_2) and enstatite ($MgSiO_3$) were observed in geopolymer cured under saturated condition. Compared to raw material, fly ash, after geopolymerization under both open and saturated condition, magnesioferrite phase

occurred. For open condition, cancrinite existed which meant some NaOH did not react.

4.5 Conclusions

Compressive strength of fly ash-based geopolymer was higher for saturated condition compared to open condition. Furthermore, the compressive strength had an increasing trend with prolonging curing time under saturated condition. Almost the same value of apparent density, bulk density, geometric density and porosity were obtained for samples cured under both open and saturated conditions. SEM images showed that the distribution of crack and the width of crack were similar for saturated condition compared to open condition. However, the reacted matrix for open condition was coarse and the reacted matrix for saturated condition was smooth.

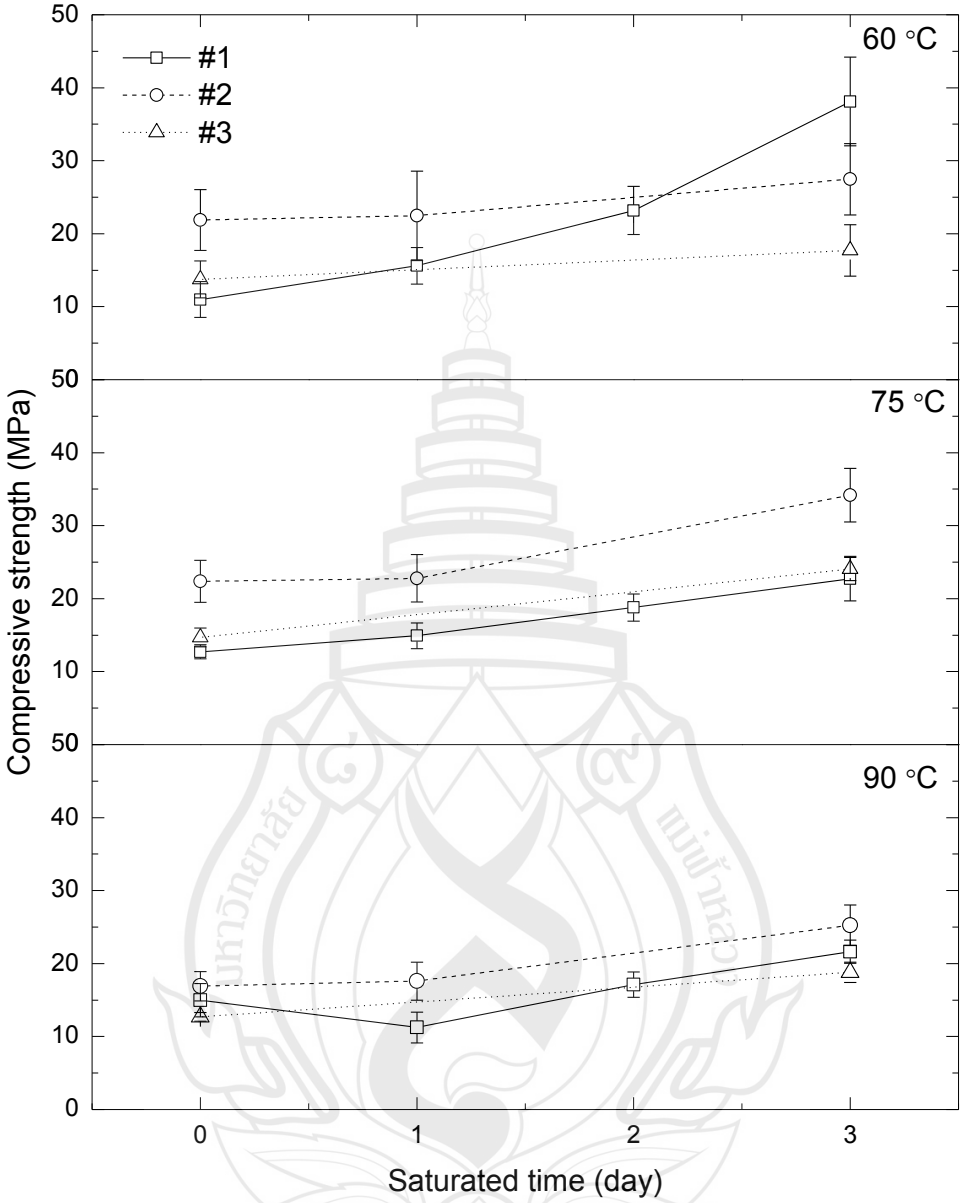

Figure 4.4 Effect of Open and Saturated Condition on Compressive Strength of Fly Ash-Based Geopolymer

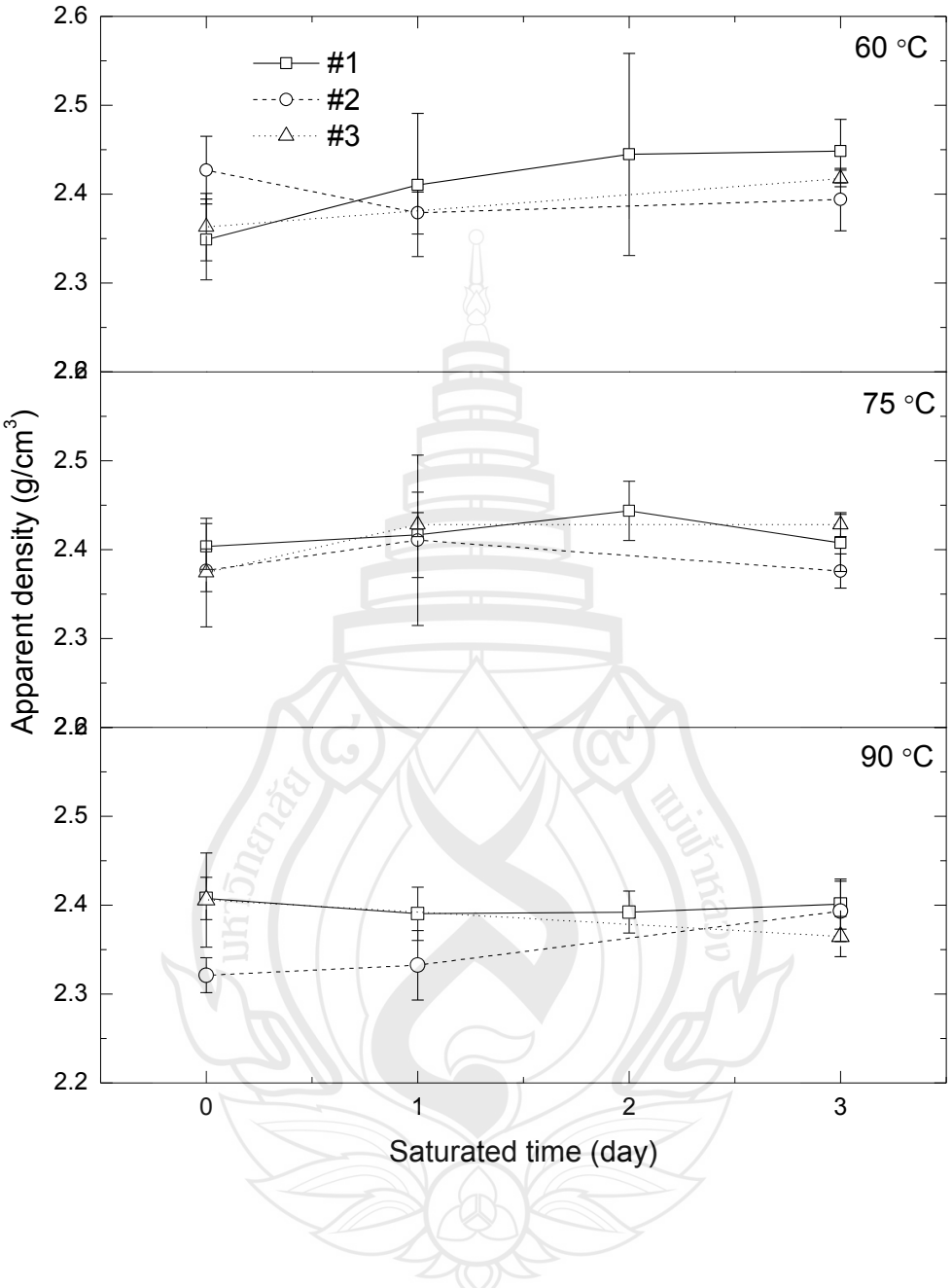

Figure 4.5 Effect of Open and Saturated Condition on Apparent Density of Fly Ash-Based Geopolymer

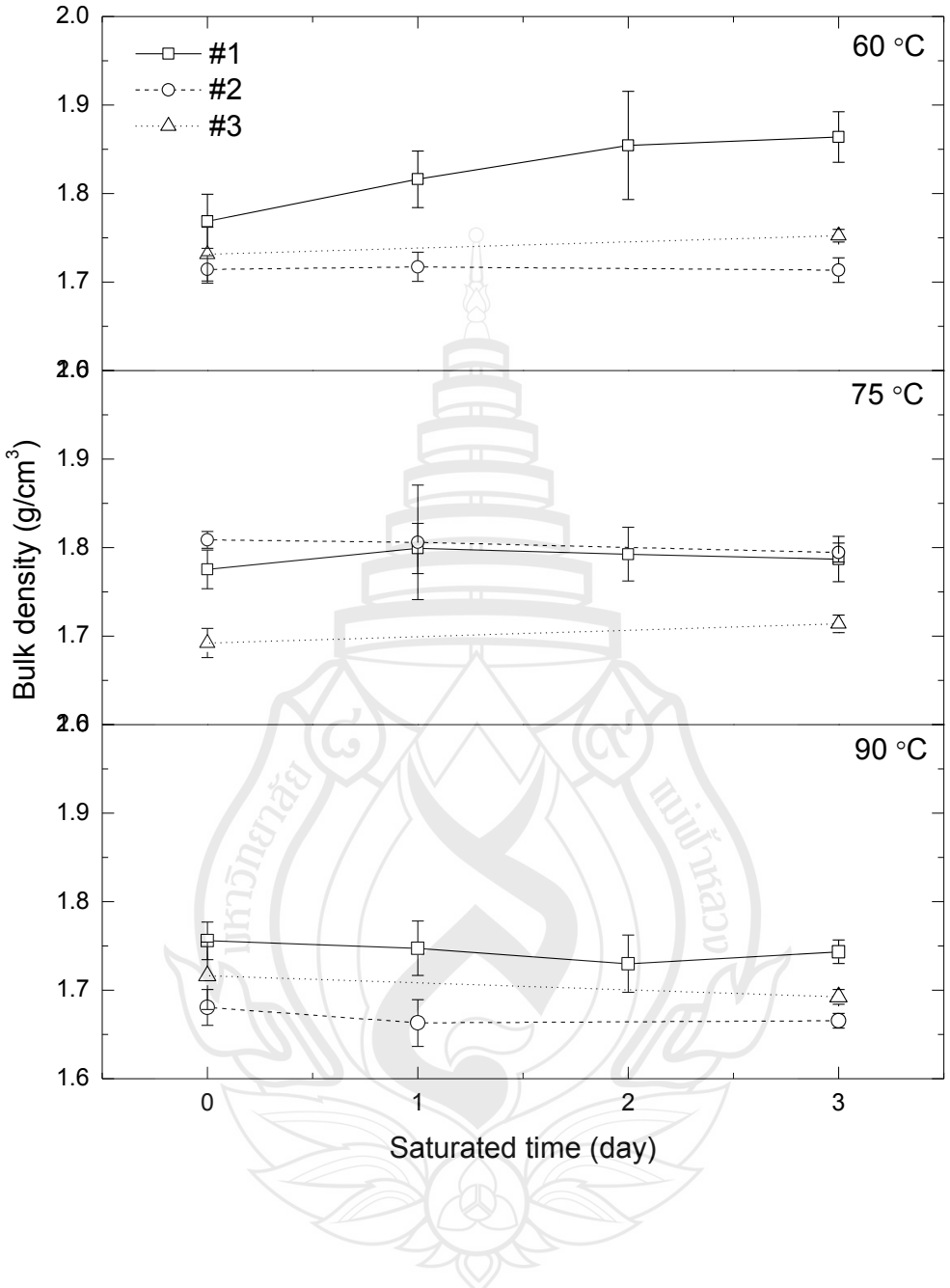

Figure 4.6 Effect of Open and Saturated Condition on Bulk Density of Fly Ash-Based Geopolymer

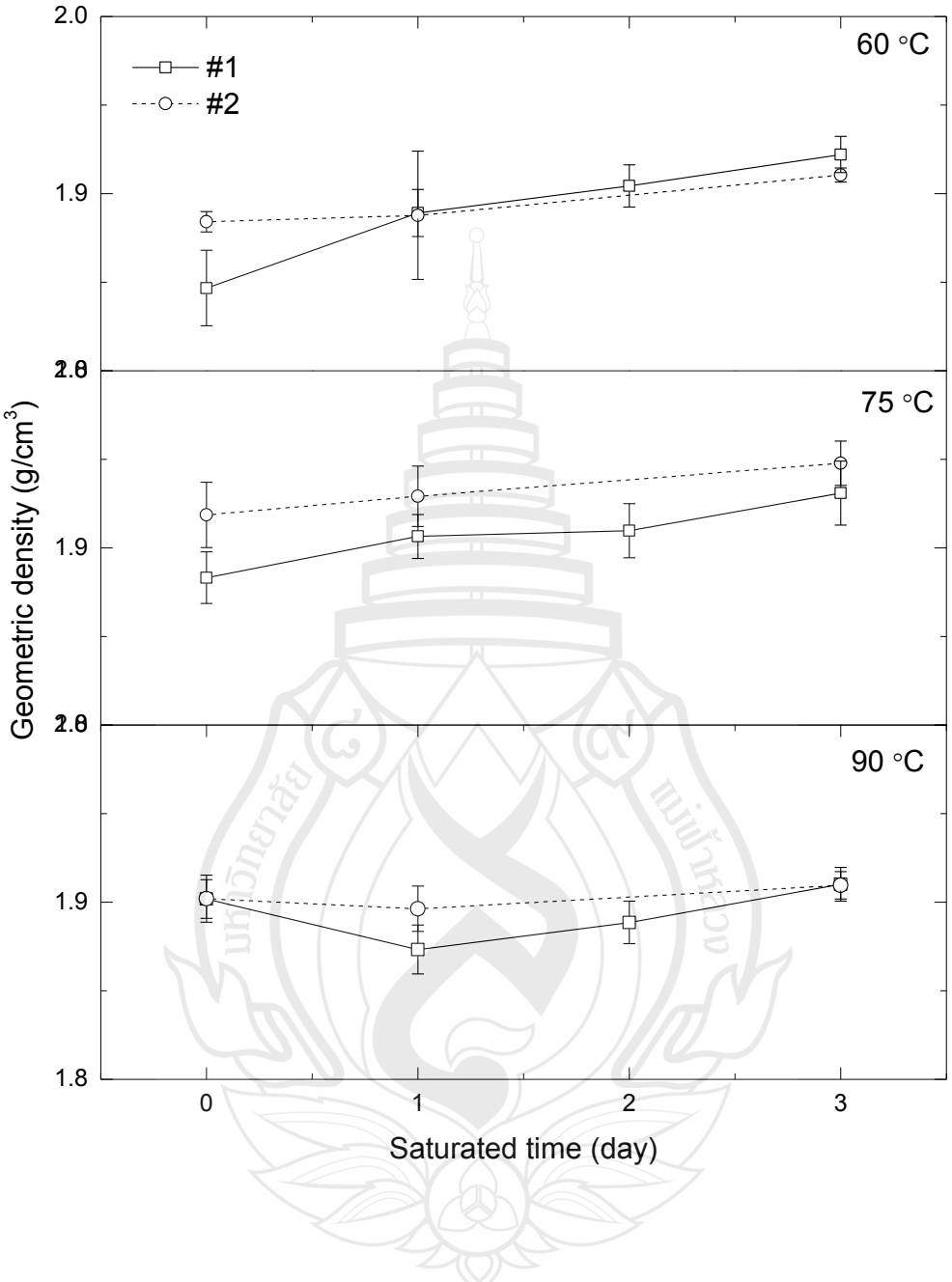

Figure 4.7 Effect of Open and Saturated Condition on Geometric Density of Fly Ash-Based Geopolymer

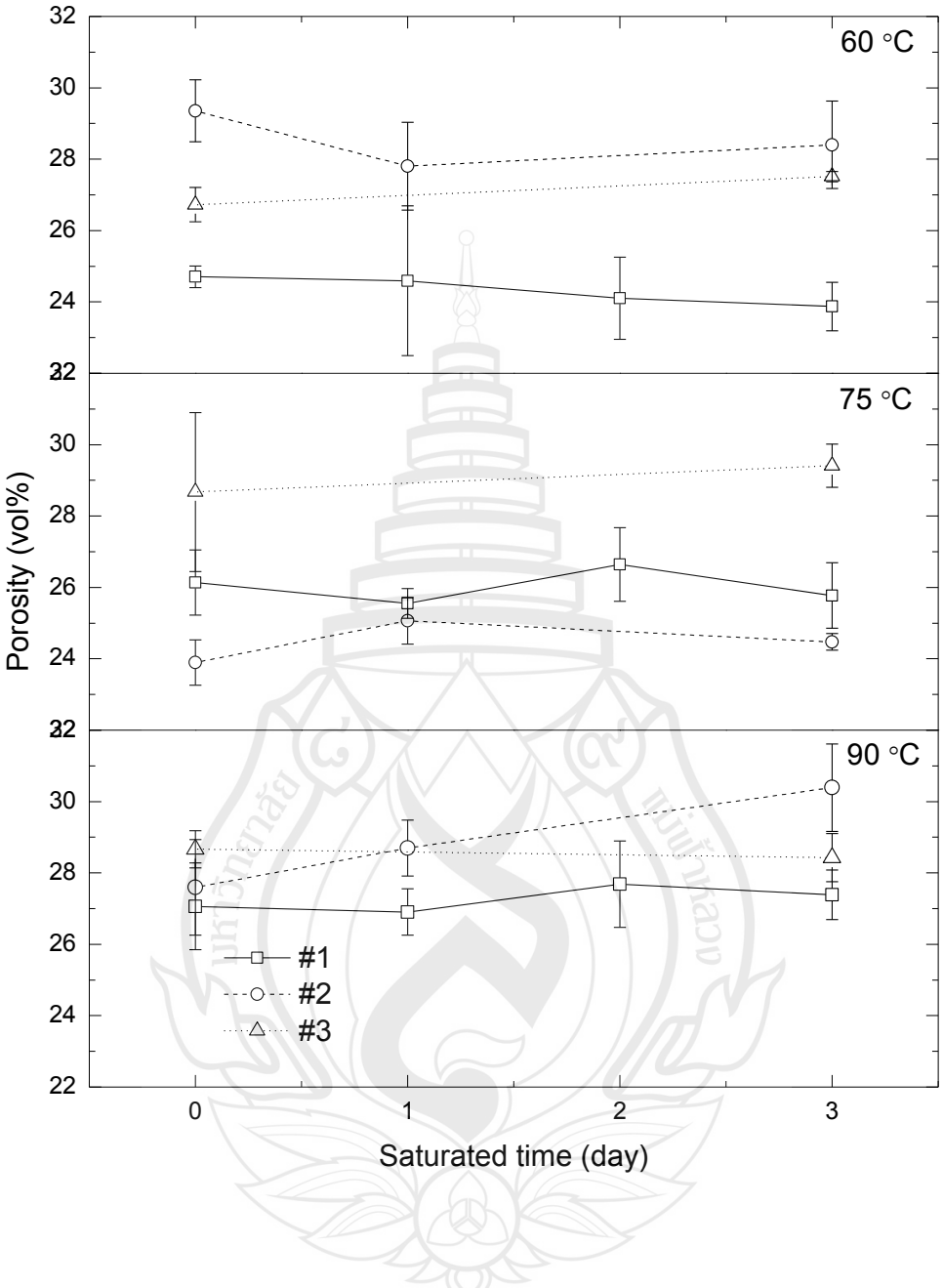

Figure 4.8 Effect of Open and Saturated Condition on Porosity of Fly Ash-Based Geopolymer

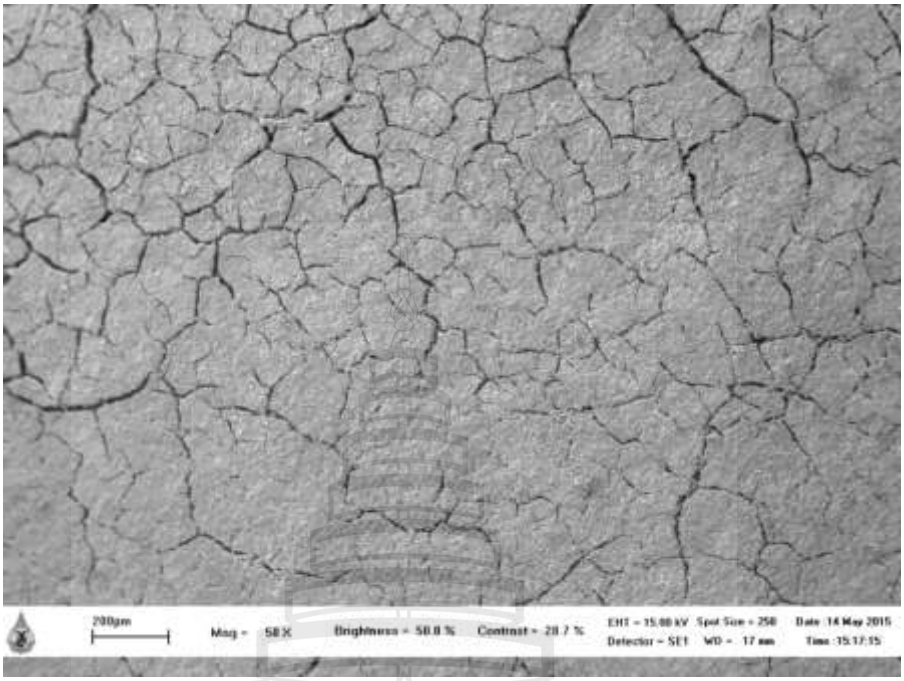

(a)

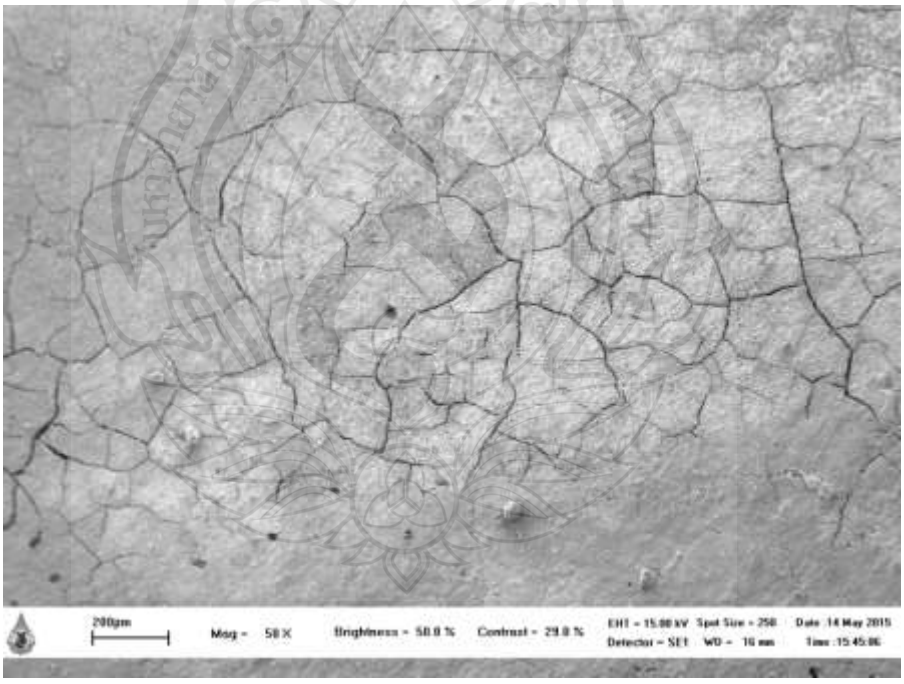

(b)

Figure 4.9 SEM Image with Magnification of 50X on Hardened Surface of Fly Ash-Based Geopolymer with Initial Water Content of 29 wt% Cured under (a) Open Condition, and (b) Saturated Condition Activated at 60 ℃

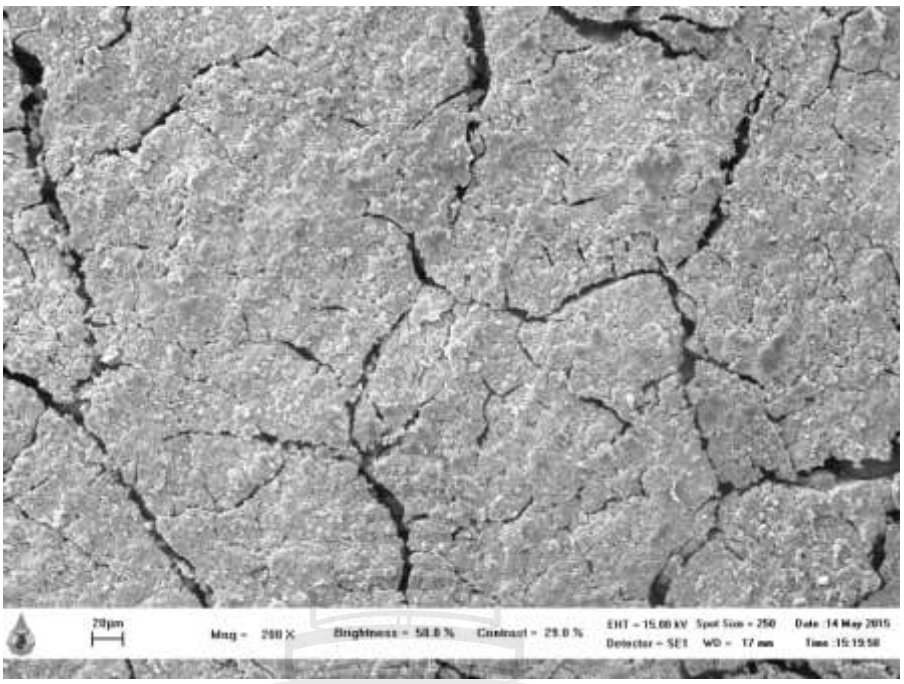

(a)

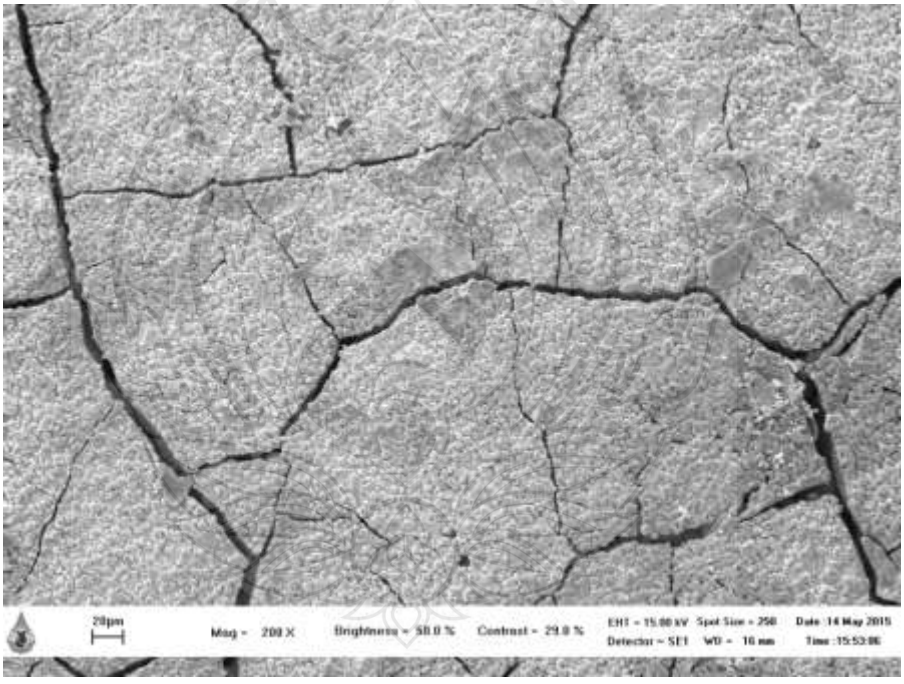

(b)

Figure 4.10 SEM Image with Magnification of 200X on Hardened Surface of Fly Ash-Based Geopolymer with Initial Water Content of 29 wt% Cured under (a) Open Condition, and (b) Saturated Condition Activated at 60 ℃

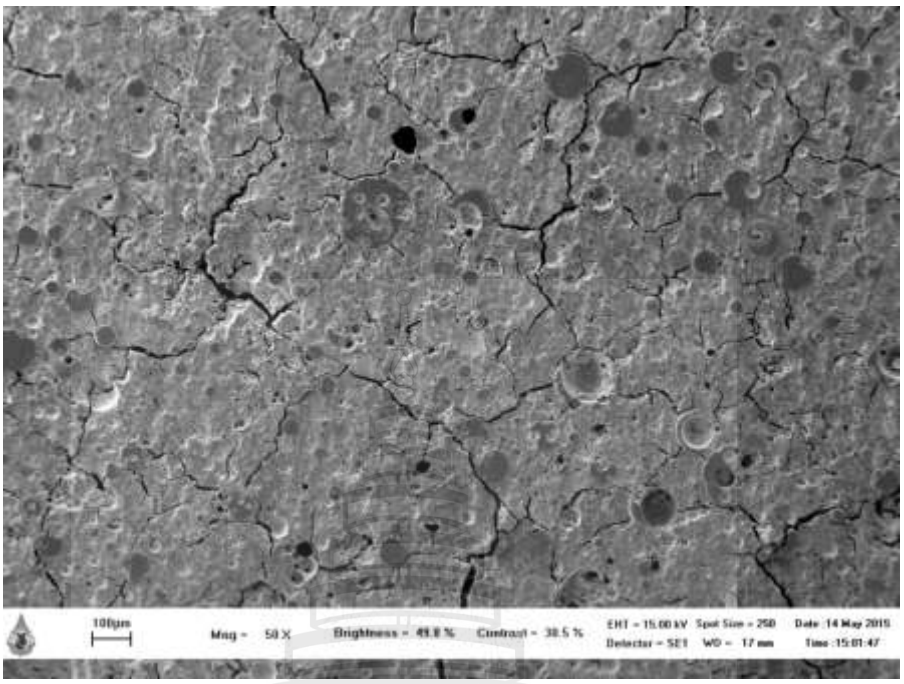

(a)

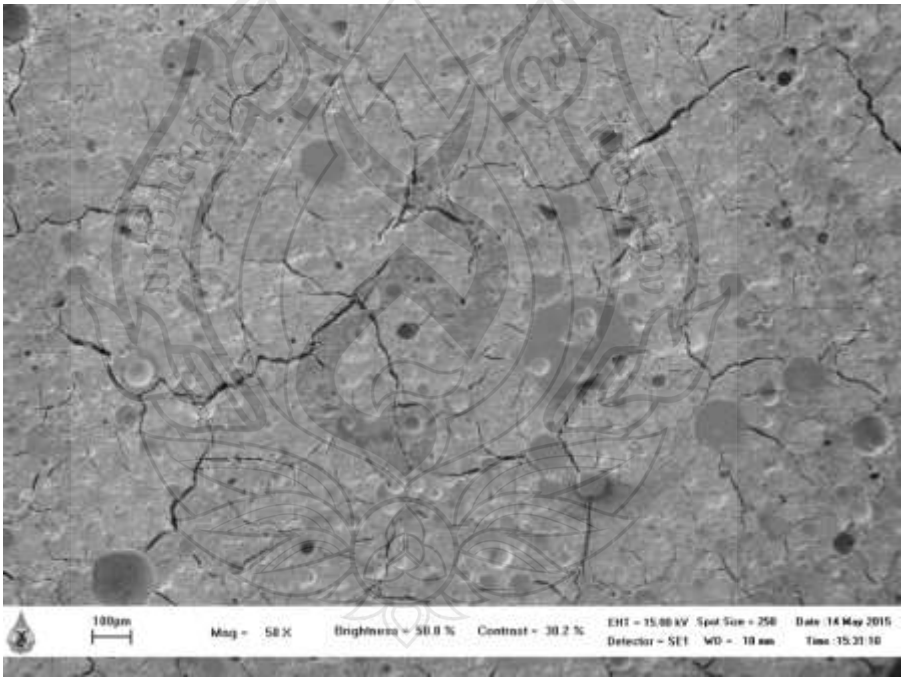

(b)

Figure 4.11 SEM Image with Magnification of 50X on Polished Surface of Fly Ash-Based Geopolymer with Initial Water Content of 29 wt% Cured under (a) Open Condition, and (b) Saturated Condition Activated at 60 ℃

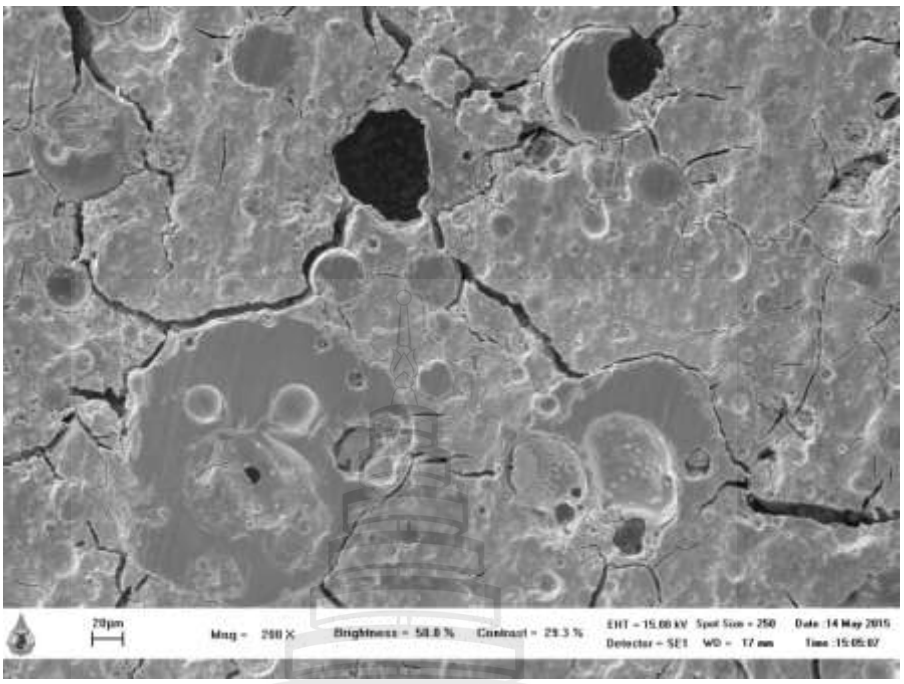

(a)

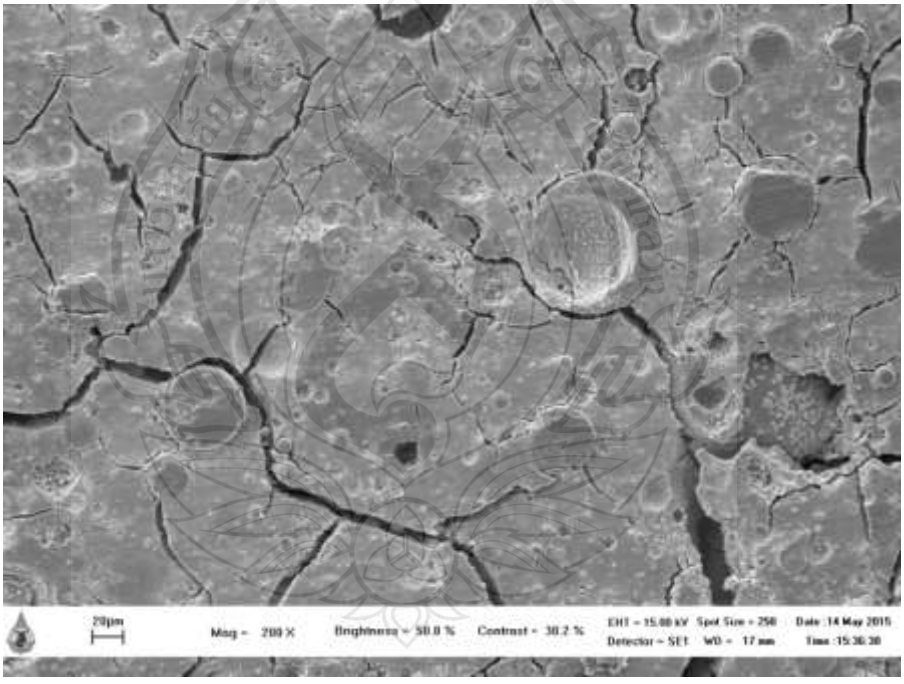

(b)

Figure 4.12 SEM Image with Magnification of 200X on Polished Surface of Fly Ash-Based Geopolymer with Initial Water Content of 29 wt% Cured under (a) Open Condition, and (b) Saturated Condition Activated at 60 ℃

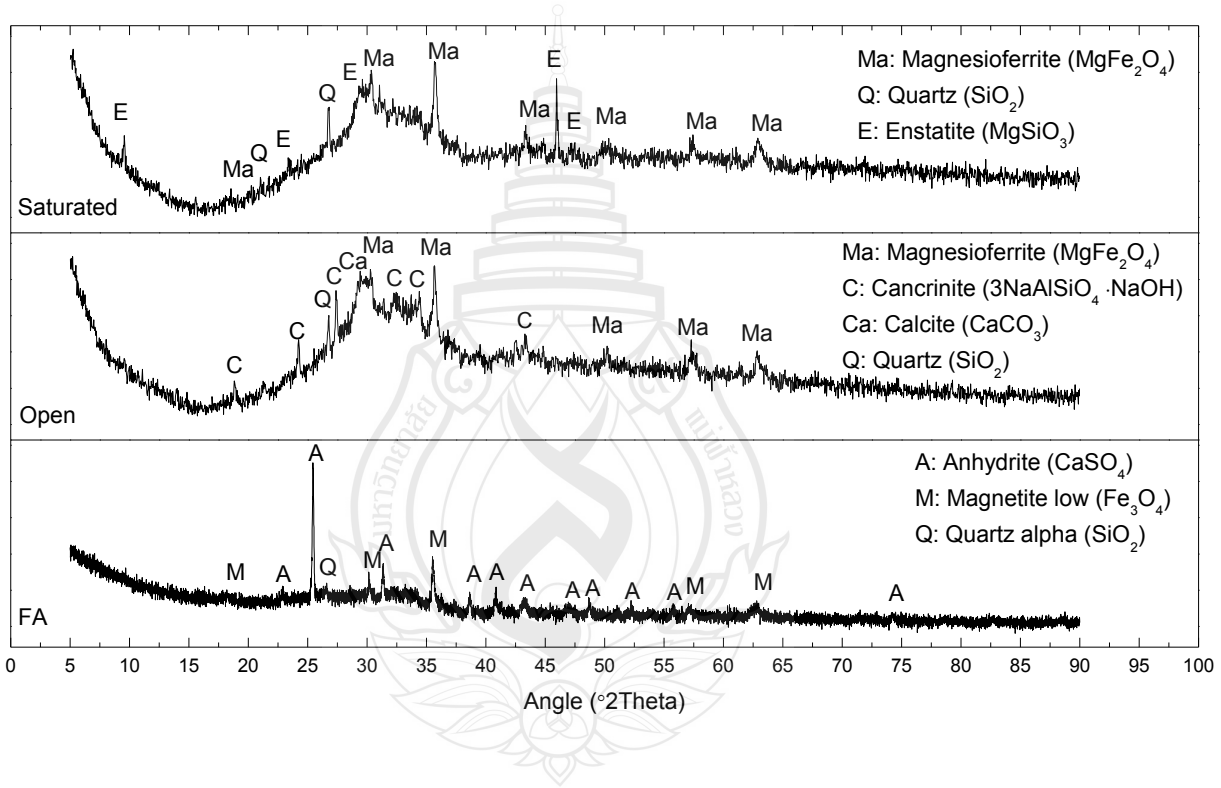

Figure 4.13 X-ray Diffraction Analysis on Hardened Fly Ash-Based Geopolymer with Initial Water Content of 29 wt% Cured under Open Condition and Saturated Condition Activated at 60 ℃

CHAPTER 5

THE EFFECT OF ACTIVATION TEMPERATURE ON PHYSICAL PROPERTIES AND COMPRESSIVE STRENGTH OF FLY ASH-BASED GEOPOLYMER

5.1 Abstract

This work has been done to study the effect of activation temperature on physical properties and compressive strength of fly ash-based geopolymer. Some samples were activated at 60, 75 or 90 ℃ for 24 h under saturated condition and then cured at 40 ℃ under open condition for 6 days. Other samples were activated at the similar conditions under saturated condition and then cured at 40 ℃ under saturated condition for 1, 2 and 3 days, finally cured at 40 ℃ under open condition for 5, 4 and 3 days, respectively. Physical properties, such as apparent density, bulk density, geometric density and porosity were tested. Compressive strength was tested using universal testing machine (UTM). To observe the microstructure of samples, scanning electron microscope (SEM) was used. X-ray diffraction (XRD) was used to characterize the phase of hardened fly ash-based geopolymer. It was concluded that compressive strength of fly ash-based geopolymer was highest for samples activated at 75 ℃. Such trend was well agreed with the microstructural evidences and the measured physical properties of the samples. Apparent density, bulk density and geometric density were increased as activation temperature was increased from 60 ℃ to 75 ℃ and decreased at 90 ℃.

5.2 Introduction

From literature review (section 2.2.6), activation temperature was one of the most important factor which affected the compressive strength of fly ash-based geopolymer. Figure 2.8 showed that the compressive strength was increased with increasing activation temperature at the range from 30 to 100 ℃. It was worth noting that the compressive strength increased from 15 MPa to 70 MPa with increasing activation temperature from 20 to 70 ℃. However, the different result was obtained from Figure 2.7 which was that the compressive strength was increasing and then decreasing with increasing activation temperature at the range from 30 to 100 ℃. The contradicting results may account for different processing system. In order to obtain the optimum activation temperature for this work's processing system and to understand the role of activation temperature in the synthesis of fly ash-based geopolymer, a series of temperature from 60, 75 or 90 ℃ has been selected.

5.3 Experiment

5.3.1 Preparation of Fly Ash-Based Geopolymer

All steps followed section 4.3.2.

5.3.2 Characterization

Physical properties, compressive strength, microstructure and phase composition of fly ash-based geopolymer were performed following section 4.3.3.2-4.3.3.5.

5.4 Results and discussion

For compressive strength, the value was increasing from 60 to 75 ℃ and then decreasing from 75 to 90 ℃ in most cases, such as for open condition (#2 and #3), for 1 day saturation (#1 and #2) and for 3 day saturation (#1 and #2). Increasing compressive strength with increasing activation temperature from 60 to 90 ℃

occurred in the case of open condition (#1). Decreasing compressive strength occurred in 2 day saturation (#1). Furthermore, activation temperature of 75 ℃ generally contributed to highest compressive strength which was slightly greater than that obtained from activation temperature of 60 ℃. However, raising the activation temperature to 90 ℃ resulted in lowest compressive strength (Figure 5.1). The results showed the same trend as reported in section 2.2.6.1.

Apparent density was increased when the activation temperature was changed from 60 to 75 ℃ and then decreased at 90 ℃ in most cases, such as for open condition (#1), for 1 day saturation (#1 and #2), for 2 day saturation (#1) and for 3 day saturation (#2). The increased apparent density from 60 to 90 ℃ occurred in the case of open condition (#3). Decreased apparent density occurred for open condition (#2). Apparent density was decreased and then increased in the various temperatures was observed for 3 day saturation (#1). Therefore, generally activation temperature of 75 ℃ contributed to the highest apparent density which was slightly greater than that obtained from activation temperature of 60 ℃. However, it was clear that activation temperature of 90 ℃ resulted in lowest apparent density which was almost similar to the relationship between compressive strength and activation temperature (Figure 5.2).

Bulk density was increased from 60 to 75 ℃ and then decreased from 75 to 90 ℃ in most cases, such as for open condition (#1 and #2), for 1 day saturation (#2) and for 3 day saturation (#1). Decreased bulk density occurred from 60 to 90 ℃ for open condition, for example, for 1 day saturation (#1), for 2 day saturation (#1) and for 3 day saturation (#2). Bulk density was decreased and then increased in the various temperatures was observed for open condition (#3). Therefore, generally activation temperature of 75 ℃ contributed to the highest bulk density which was slightly greater than or almost similar to that obtained from activation temperature of 60 ℃. However, it was clear that activation temperature of 90 ℃ resulted in the lowest bulk density which was almost similar to the relationship between compressive strength and activation temperature (Figure 5.3).

Geometric density was increased from 60 to 75 ℃ and then decreased from 75 to 90 ℃ in most cases, such as for open condition (#2), for 1 day saturation (#1 and #2), for 2 day saturation (#1) and for 3 day saturation (#1). Geometric density was increased in the various temperatures was observed for open condition (#1). Therefore,

activation temperature of 75 ℃ contributed to the highest geometric density which was greater than that obtained from activation temperature of both 60 ℃ and 90 ℃ which was almost similar to the relationship between compressive strength and activation temperature (Figure 5.4).

Porosity was decreased from 60 to 75 ℃ and then increased from 75 to 90 ℃, such as for open condition (#2), for 1 day saturation (#2) and for 3 day saturation (#1). Porosity was increased from 60 to 90 ℃, such as for open condition (#1), for 1 day saturation (#1) and for 2 day saturation (#1). Increased and then decreased porosity occurred in some cases, for example, for open condition (#3) and for 3 day saturation (#2). Therefore, generally activation temperature of 75 ℃ contributed to the lowest porosity which was less than or slightly greater than that from activation temperature of 60 ℃. However, it was clear that activation temperature of 90 ℃ resulted in the highest porosity which had a reverse trend to the relationship between compressive strength and activation temperature (Figure 5.5).

Activation temperature was very important for geopolymerization because it always affected the dissolution of raw materials. The lower activation temperature with a slow dissolution rate contributed to low concentration of monomer and low condensation rate, taking activation temperature of 60 ℃ for example. The higher activation temperature was definitely contributed to higher dissolution and condensation rate. Furthermore, the dissolution and condensation occurred at the same time. Therefore, after condensation, some undissolved parts cannot be further dissolved easily which resulted in a lower reaction level and lower compressive strength, taking activation temperature of 90 ℃ which was well agreed with the work (Jiménez et al., 2005). Therefore, both 60 ℃ and 90 ℃ resulted in the lower compressive strength. From all above, it was believed that a proper activation temperature, 75 ℃, was good for geopolymerization and compressive strength.

Scanning electron microscopy has been used for observing the microstructure of hardened fly ash-based geopolymer. The fly ash particle was larger for activation temperature of 60 ℃ (Figure 5.6(a)) than that for activation temperature of 75 ℃ and 90 ℃ (Figure 5.6(b) and (c)). It was believed that higher activation temperature was good for dissolving fly ash particles and continued increasing activation temperature did not affect the dissolving. The crack was larger for activation temperature of 60 ℃

and 90 ℃ (Figure 5.7(a) and (c)) than that for activation temperature of 75 ℃ (Figure 5.7(b)). It seemed that higher activation temperature resulted in crack because the water evaporation rate was faster. The cracks were more frequently observed near the interfacial area between fly ash particle and matrix for activation temperature of 60 ℃ (Figure 5.8(a)), while the microstructure of the area above was similar for activation temperature of both 75 ℃ and 90 ℃ (Figure 5.8(b) and (c)). We believed that the activation temperature of 90 ℃ was good for dissolving fly ash particles and condensation between matrix and fly ash particles.

X-ray diffraction analysis was used for analyzing the crystallinity and phase. There was no obvious peak being observed from Figure 5.9. It meant that the phase content was mainly amorphous rather than crystalline. For activation temperature of 60 ℃, magnesioferrite ($MgFe_2O_4$), quartz low (SiO_2) and latiumite ($K_{0.85}Ca_{3(}Si_{2.15}Al_{2.85})O_{11}(SO_4)_{0.7}(CO_3)_{0.3}$) were observed. For activation temperature of 75 ℃, magnesioferrite ($MgFe_2O_4$), calcite ($CaCO_3$), quartz (SiO_2) and lazurite ($Na_{8.16}(Al_6Si_6O_{24})(SO_4)_{1.14}S_{0.86}$) were observed. For the activation temperature of 90 ℃, magnesioferrite ($MgFe_2O_4$), quartz low (SiO_2), lazurite ($Na_{8.16}(Al_6Si_6O_{24})(SO_4)_{1.14}S_{0.86}$) and latiumite ($K_{0.85}Ca_{3(}Si_{2.15}Al_{2.85})O_{11}(SO_4)_{0.7}(CO_3)_{0.3}$ were observed. Compared with activation temperature of 60 ℃, 75 ℃ and 90 ℃, magnesioferrite existed for all conditions.

5.5 Conclusions

Compressive strength of fly ash-based geopolymer was higher for samples activated at 75 ℃ and that was lower for samples activated at 60 and 90 ℃. Apparent density, bulk density and geometric density were increasing from 60 to 75 ℃ and decreasing from 75 to 90 ℃. However, the porosity decreased from 60 to 75 ℃ and then increased from 75 to 90 ℃. SEM images showed that the crack was larger for activation temperature of 60 ℃ and 90 ℃ than that for activation temperature of 75 ℃.

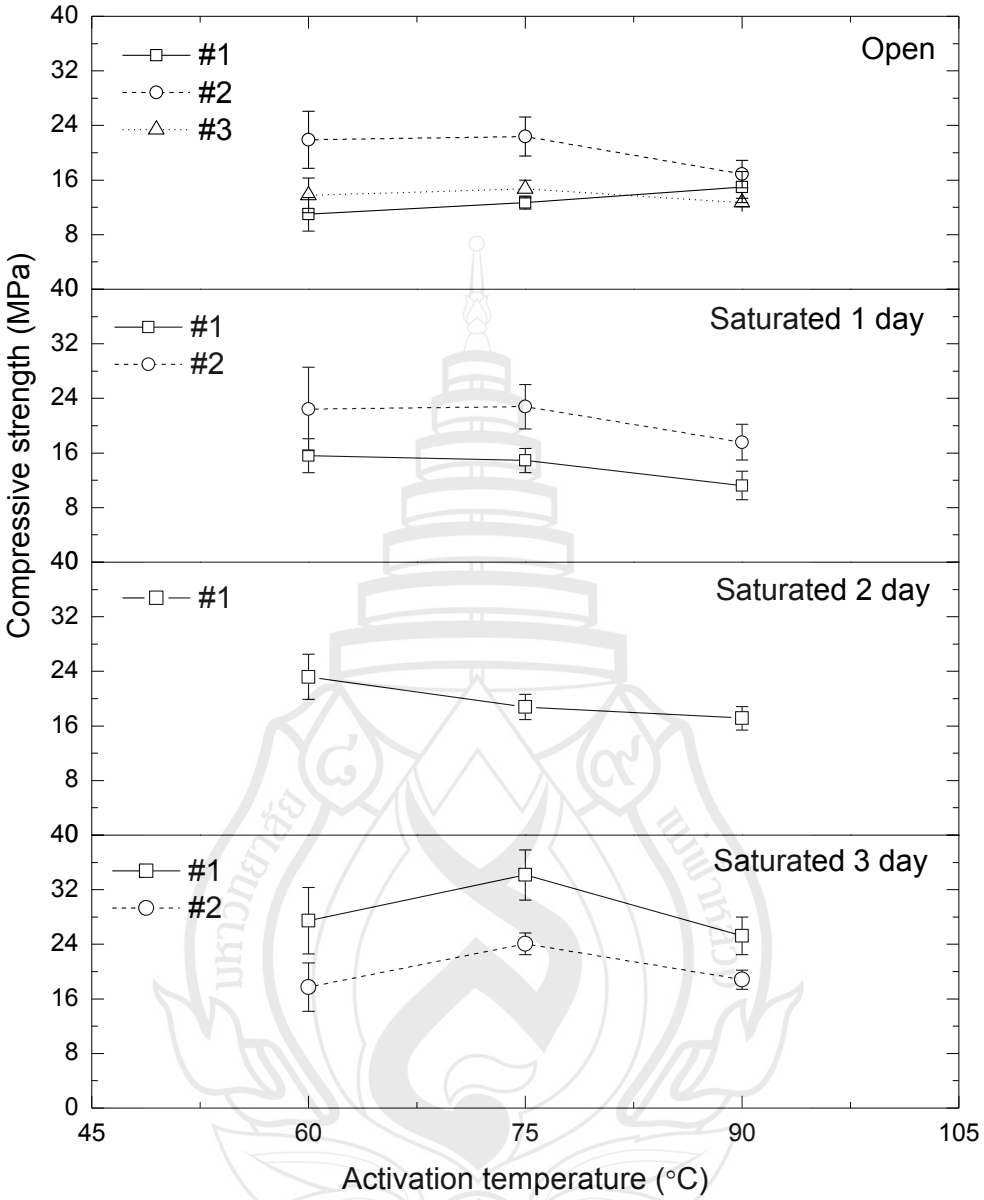

Figure 5.1 Effect of Activation Temperature on Compressive Strength of Fly Ash-Based Geopolymer

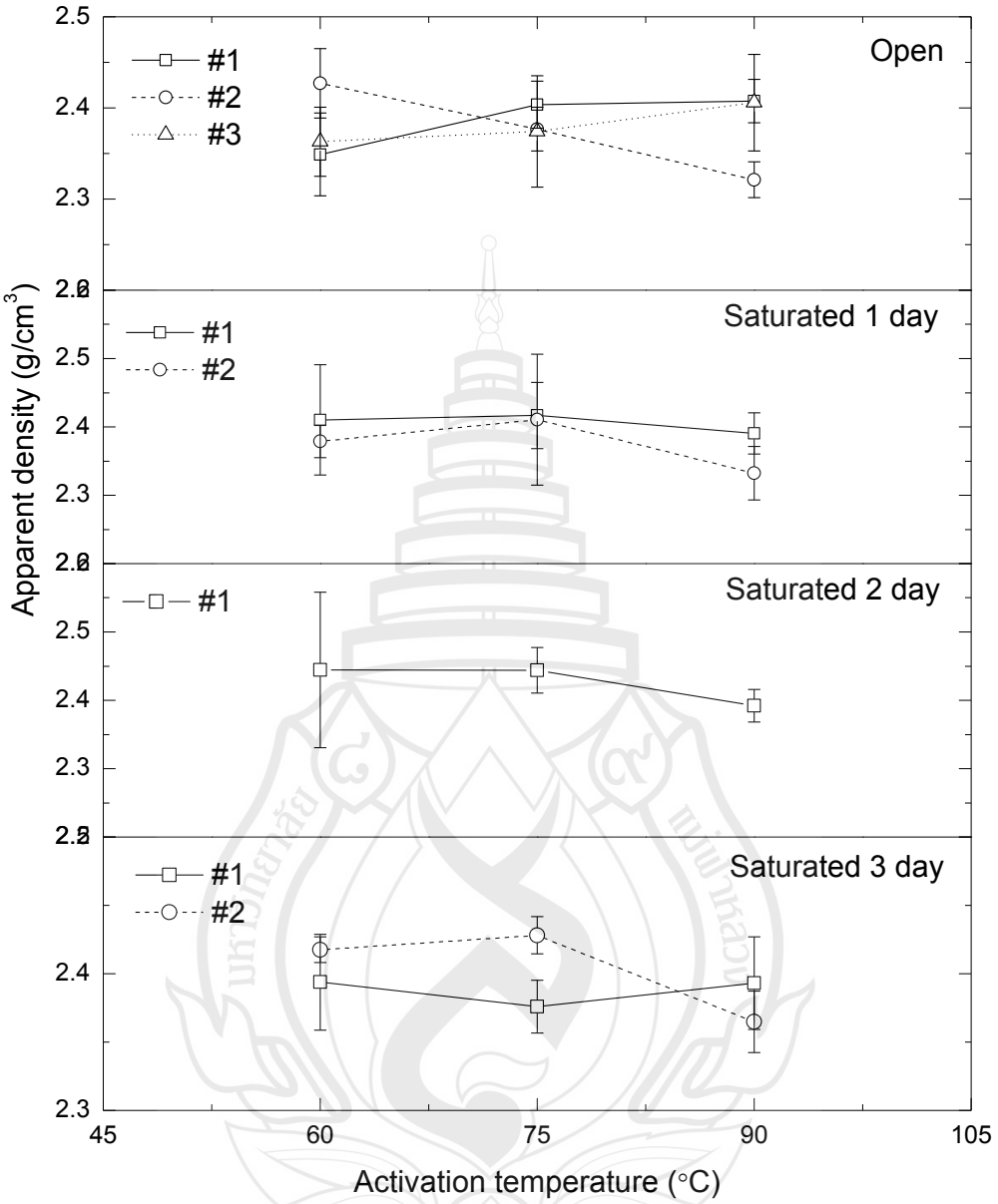

Figure 5.2 Effect of Activation Temperature on Apparent Density of Fly Ash-Based Geopolymer

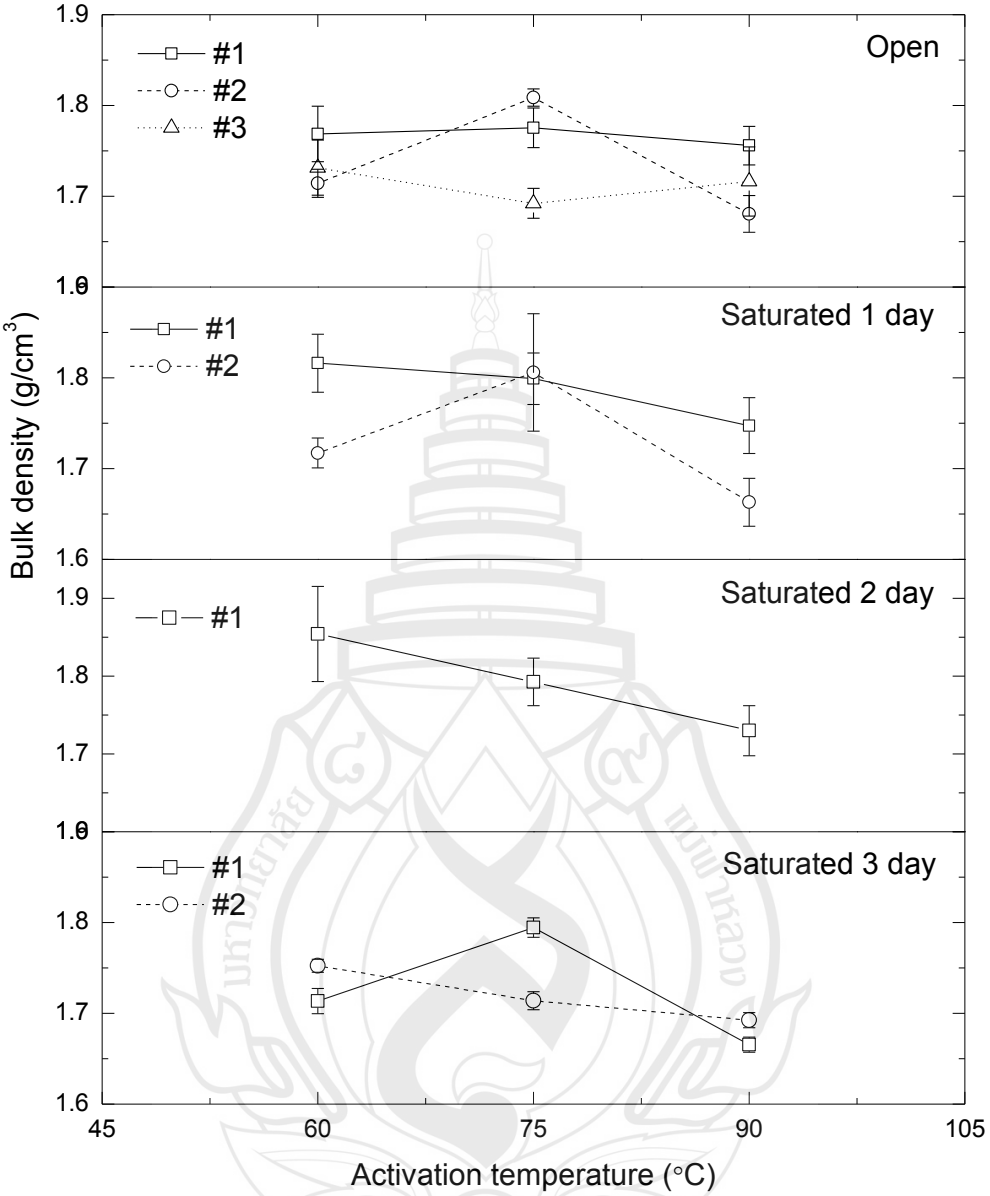

Figure 5.3 Effect of Activation Temperature on Bulk Density of Fly Ash-Based Geopolymer

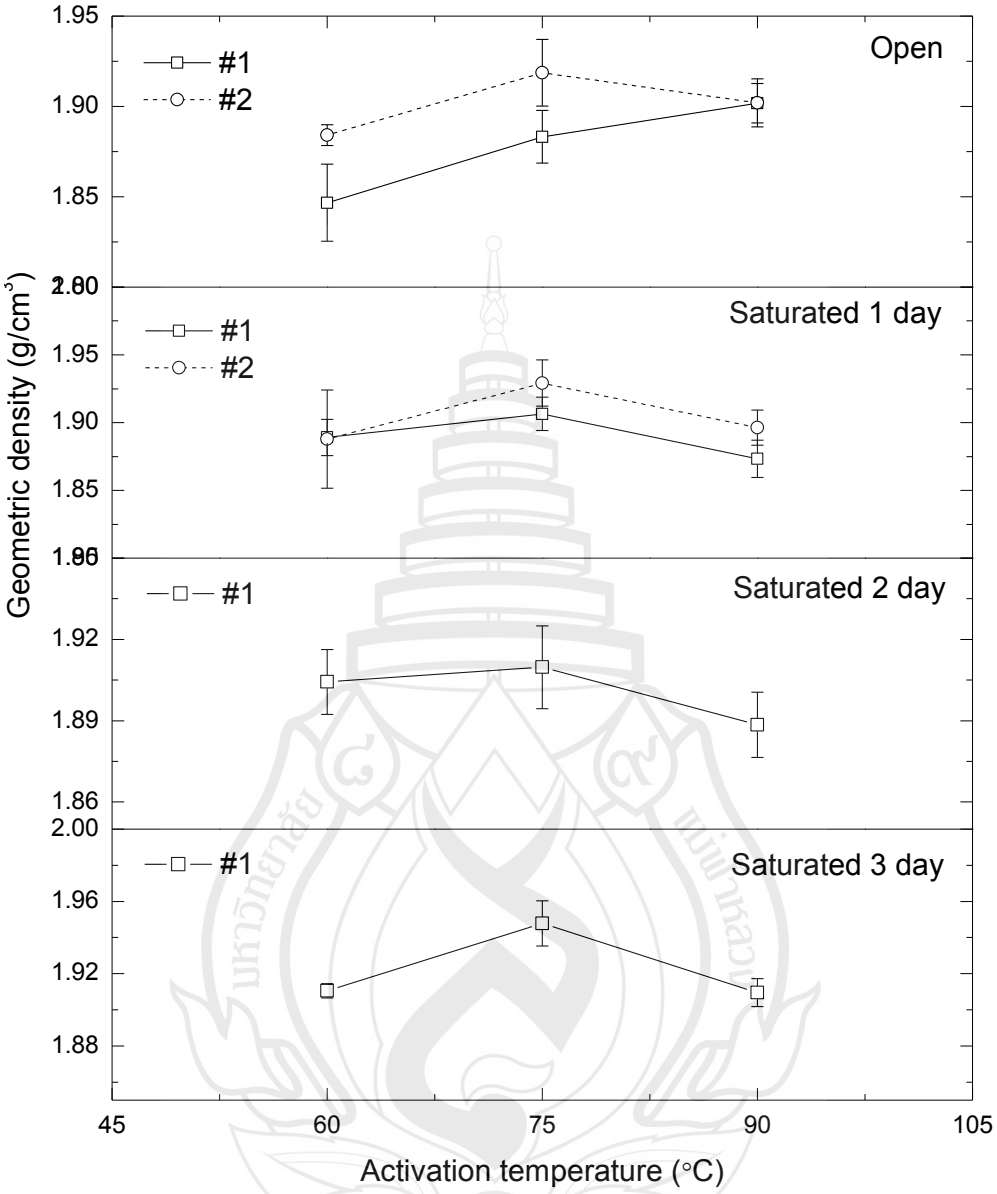

Figure 5.4 Effect of Activation Temperature on Geometric Density of Fly Ash-Based Geopolymer

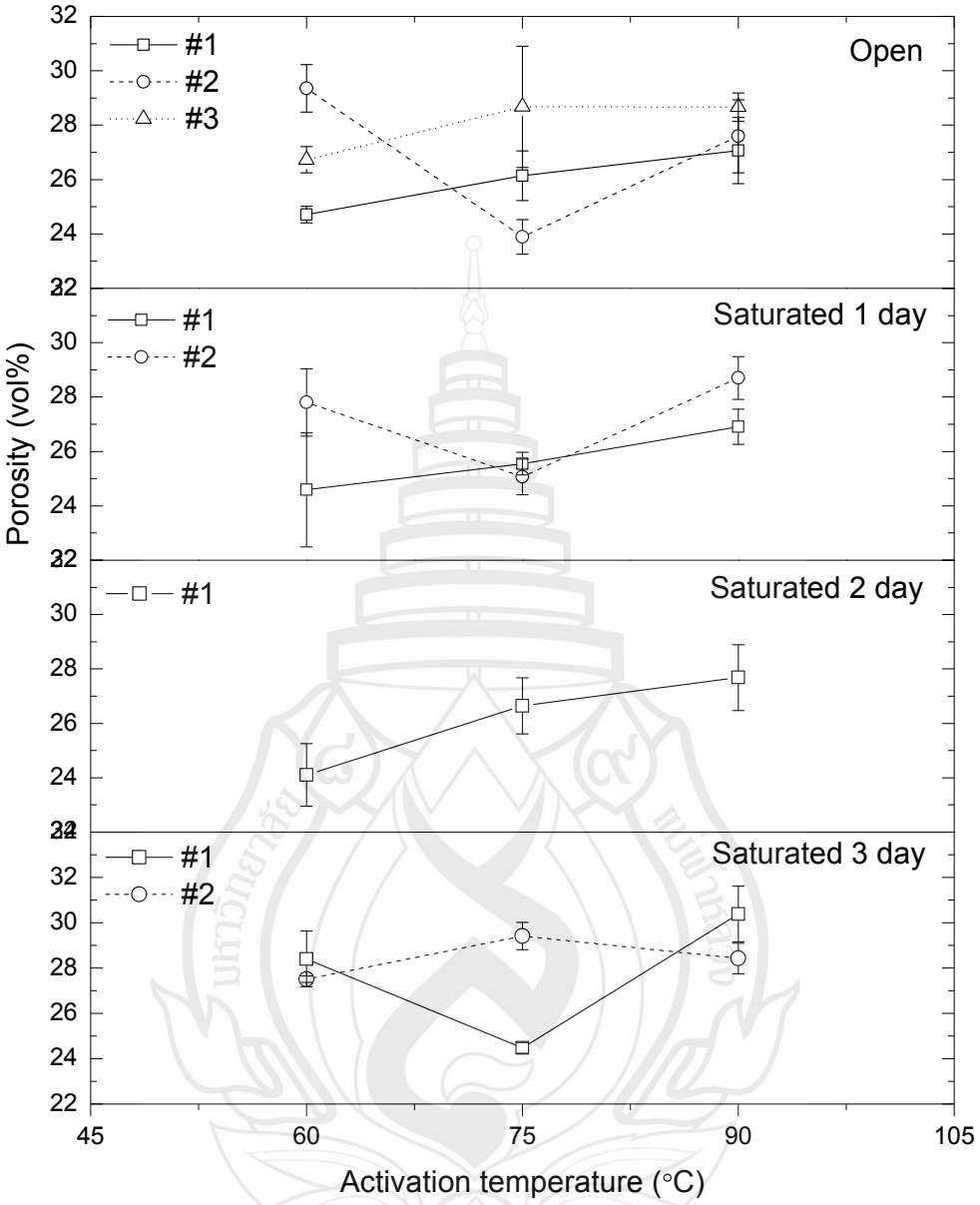

Figure 5.5 Effect of Activation Temperature on Porosity of Fly Ash-Based Geopolymer

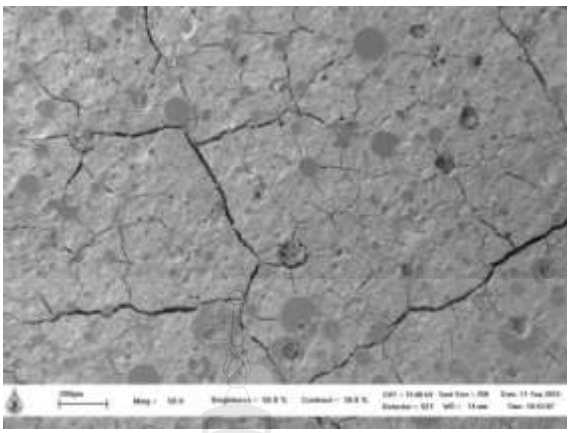

(a)

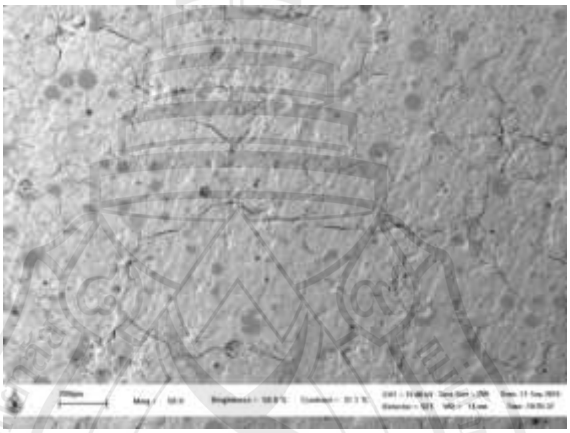

(b)

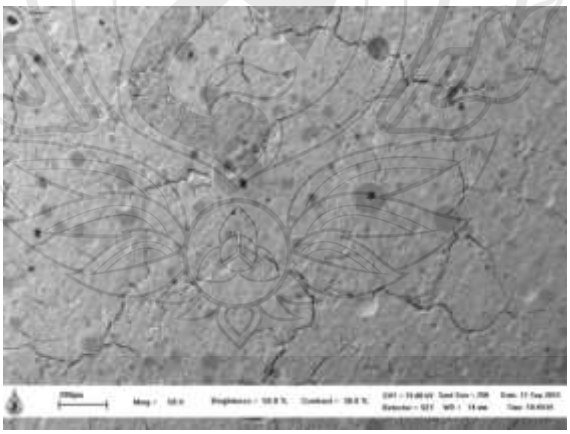

(c)

Figure 5.6 SEM Image with Magnification of 50X on Polished Surface of Fly Ash-Based Geopolymer Activated at (a) 60 ℃, (b) 75 ℃, and (c) 90 ℃ under Saturated Condition with Initial Water Content of 29 wt%

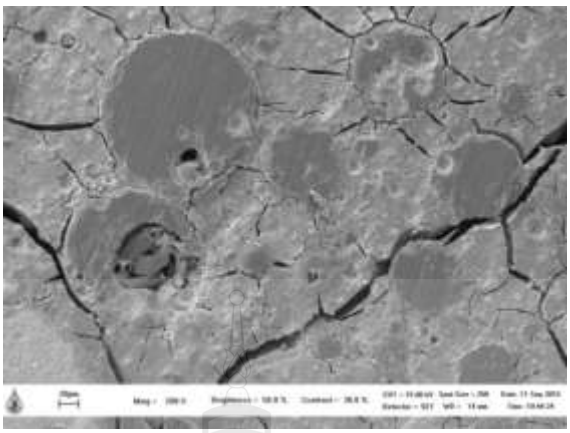

(a)

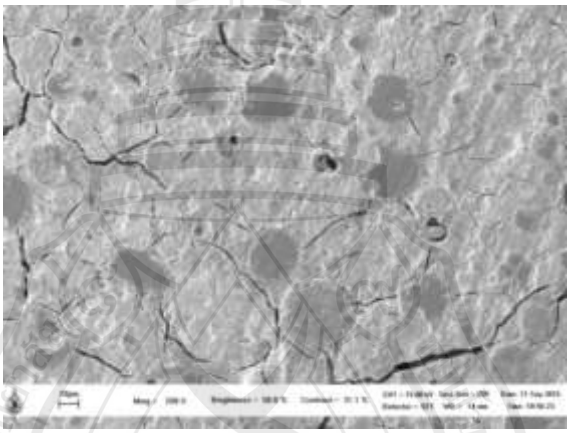

(b)

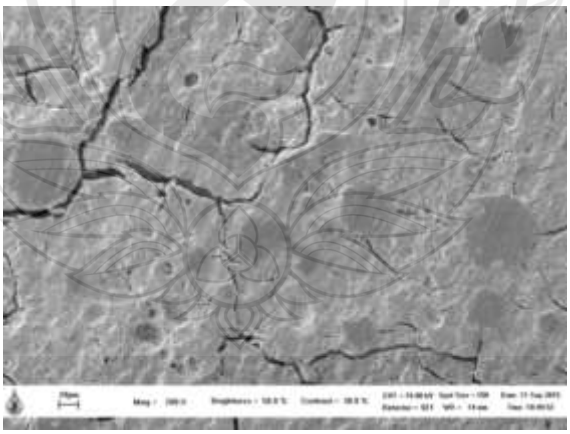

(c)

Figure 5.7 SEM Image with Magnification of 200X on Polished Surface of Fly Ash-Based Geopolymer Activated at (a) 60 ℃, (b) 75 ℃, and (c) 90 ℃ under Saturated Condition with Initial Water Content of 29 wt%

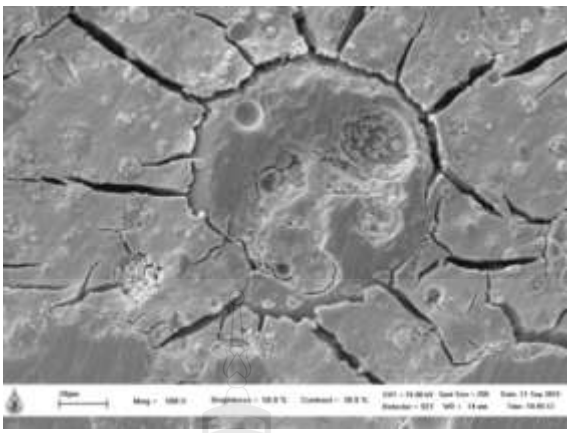

(a)

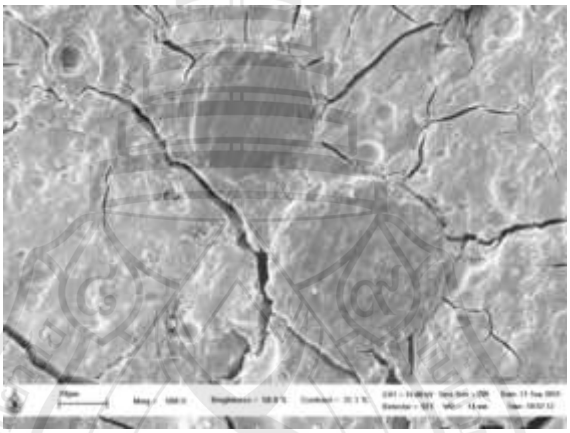

(b)

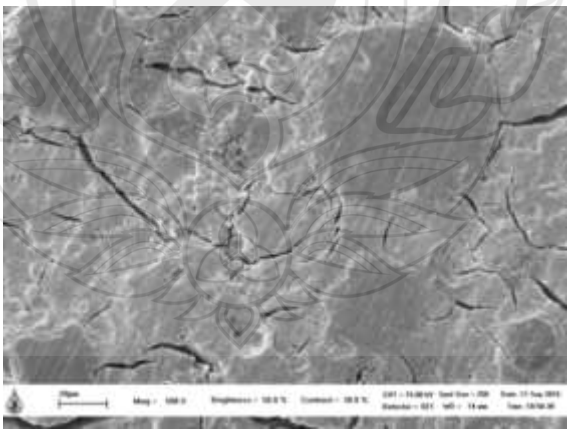

(c)

Figure 5.8 SEM Image with Magnification of 500X on Polished Surface of Fly Ash-Based Geopolymer Activated at (a) 60 ℃, (b) 75 ℃, and (c) 90 ℃ under Saturated Condition with Initial Water Content of 29 wt%

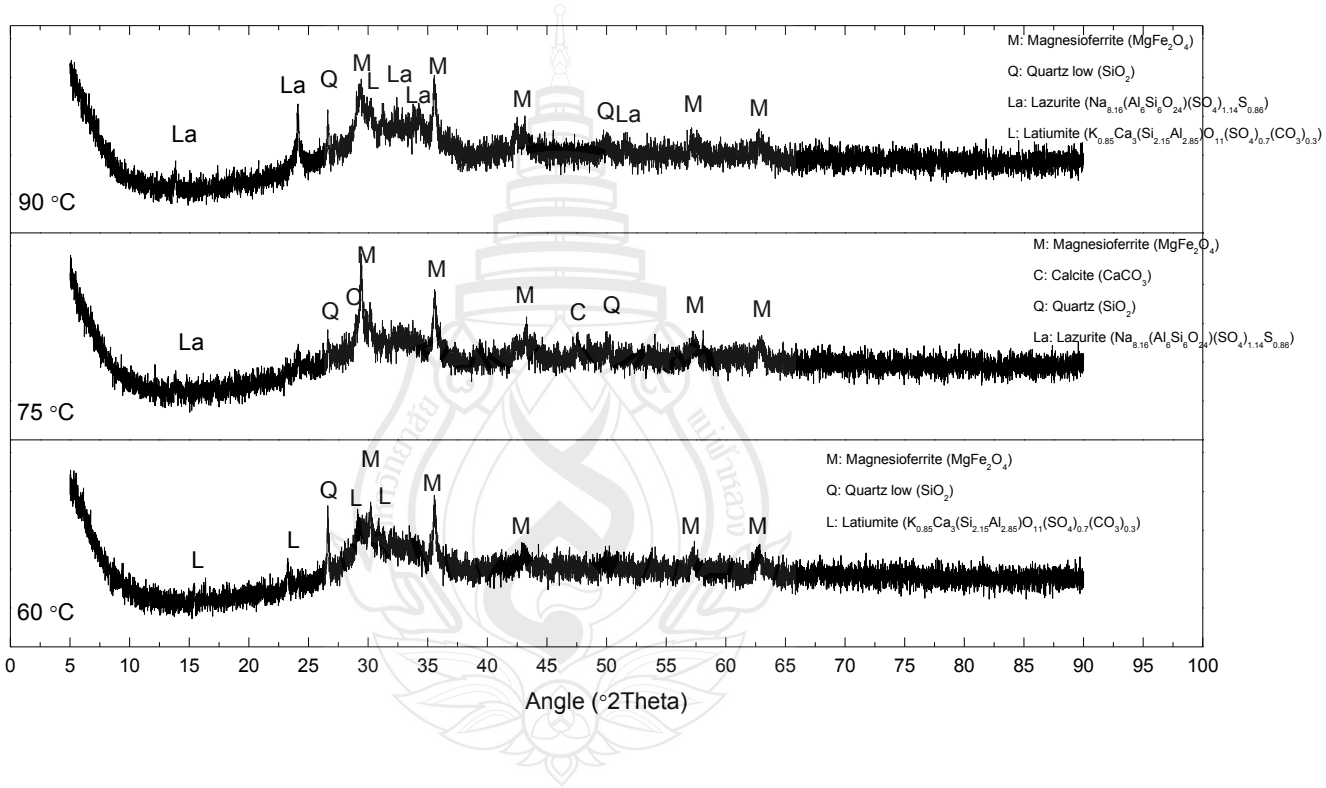

Figure 5.9 X-ray Diffraction Analysis on Hardened Fly Ash-Based Geopolymer Activated at 60 ℃, 75 ℃, or 90 ℃ under Saturated Condition with Initial Water Content of 29 wt%

CHAPTER 6

THE EFFECT OF INITIAL WATER CONTENT ON PHYSICAL PROPERTIES AND COMPRESSIVE STRENGTH OF FLY ASH-BASED GEOPOLYMER

6.1 Abstract

This study presents the effect of initial water content on physical properties and compressive strength of fly ash-based geopolymer. Samples with initial water content of 29, 34 or 44 wt% were activated at 60, 75 or 90 ℃ for 24 h under saturated condition and then cured at 40 ℃ under open condition for 6 days. Setting time of the mixtures was also determined using Vicat Tester. Furthermore, to determine the lower practice limit of initial water content, samples with initial water content of 24, 26 or 29 wt% were prepared and activated at 75 ℃ for 24 h under saturated condition and then cured at 40 ℃ under saturated condition for 3 days, finally cured at 40 ℃ under open condition for another 3 days. Physical properties, such as apparent density, bulk density, geometric density and porosity of hardened fly ash-based geopolymer were tested. Compressive strength was tested using universal testing machine (UTM). To observe the microstructure of the samples, scanning electron microscope (SEM) was used. X-ray diffraction (XRD) was a method to characterize the phase of hardened fly ash-based geopolymer. It was concluded that compressive strength of fly ash-based geopolymer was higher with lower initial water content. However, the lower limit of initial water content was 24 wt% in this study, because the mixture did not flow when initial water content was less than 24 wt%. Apparent density was almost constant with increasing initial water content. Bulk density and geometric density decreased, which had a reverse changing direction with porosity, with increasing initial water content. SEM images showed that more cracks existed and the surface crack size was larger for the initial water content of 44 wt% than that of the 29 wt%.

6.2 Introduction

It was clear that water was the reaction medium for ions transportation in the geopolymerization process (Davidovits, 2008). In geopolymerization, some water was a part of the network while the excess water was expelled from three dimensional networks (Figure 6.1). One work reported that metahalloysite based geopolymer with initial water to metahalloysite ratio of 8 wt% showed the compressive strength of 76 MPa after geopolymerization using pressure compaction method (Zivica et al., 2014). However, the operation did not suit large-scale production. To solve the problem, initial water content would be reduced until it reached the lower workability limit at which the mixture would not flow with gravity.

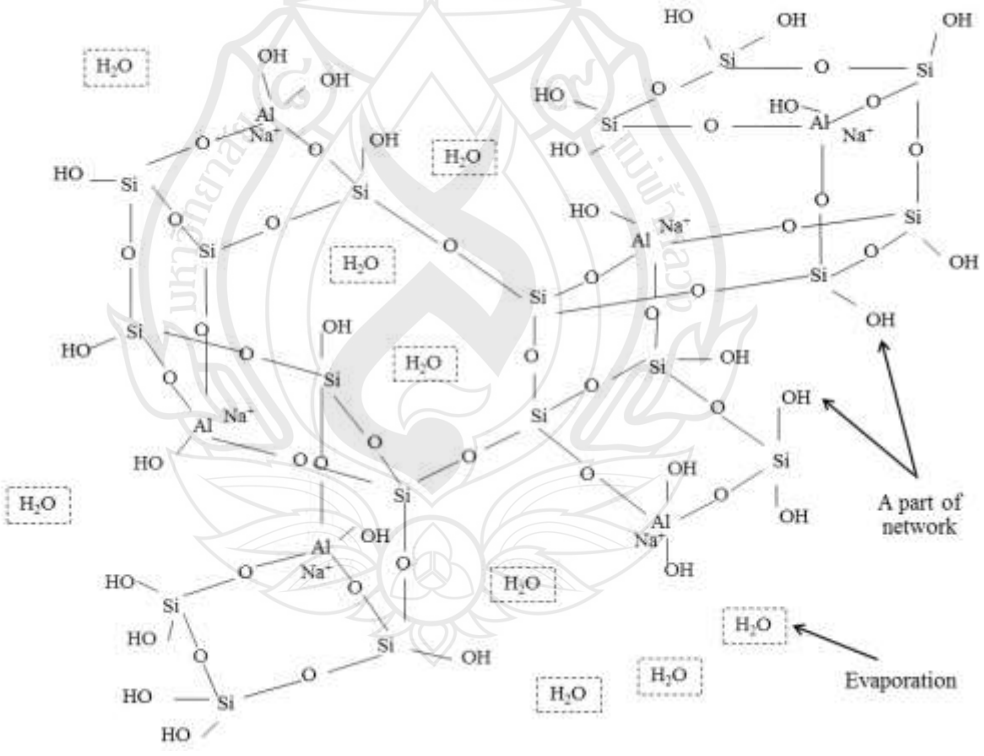

Figure 6.1 Diagram of Three Dimensional Networks of Fly Ash-Based Geopolymer Taking Na-poly(sialate-disiloxo) for Example

6.3 Experiment

6.3.1 Materials

Fly ash (source: Mae Moh, Lampang, Thailand) has been selected as the raw material to produce geopolymer. Sodium hydroxide solutions with various concentrations of 10 Mol/L (10M NaOH), 15 Mol/L (15M NaOH) or 18 Mol/L (18M NaOH) were mixed with sodium silicate solution (Na_2SiO_3) to obtained alkaline activating liquid.

6.3.2 Preparation of Samples with Various Initial Water Content of 29, 34 and 44 wt%

10M NaOH and Na_2SiO_3 were mixed at the weight ratio of 1 and stirred by stirring bar for 3 min. To prepare samples with initial water content of 29 wt%, fly ash powders were added into activating solution following the solution to fly ash weight ratio of 3:5 (Table 6.1). For samples with initial water content of 34 and 44 wt%, fly ash powders were added into activated solution following the solution to fly ash to extra water weight ratio of 3:5:0.32 and 3:5:0.96, respectively. The mixture was stirred for 30 s until no obvious agglomerate was observed. Then it was poured into a cylindrical shape plastic mold with 11.6 mm diameter and 29 mm height. The mold continued to be kept in a sealed container with water saturated atmosphere by supplying 160 mL extra water. The container was kept in the oven and activated at 60, 75 or 90 ℃ for 24 h with saturated atmospheric water. And then all samples were cured at 40 ℃ under open condition for 6 days. Finally, the samples were removed from mold for characterization (Figure 6.2).

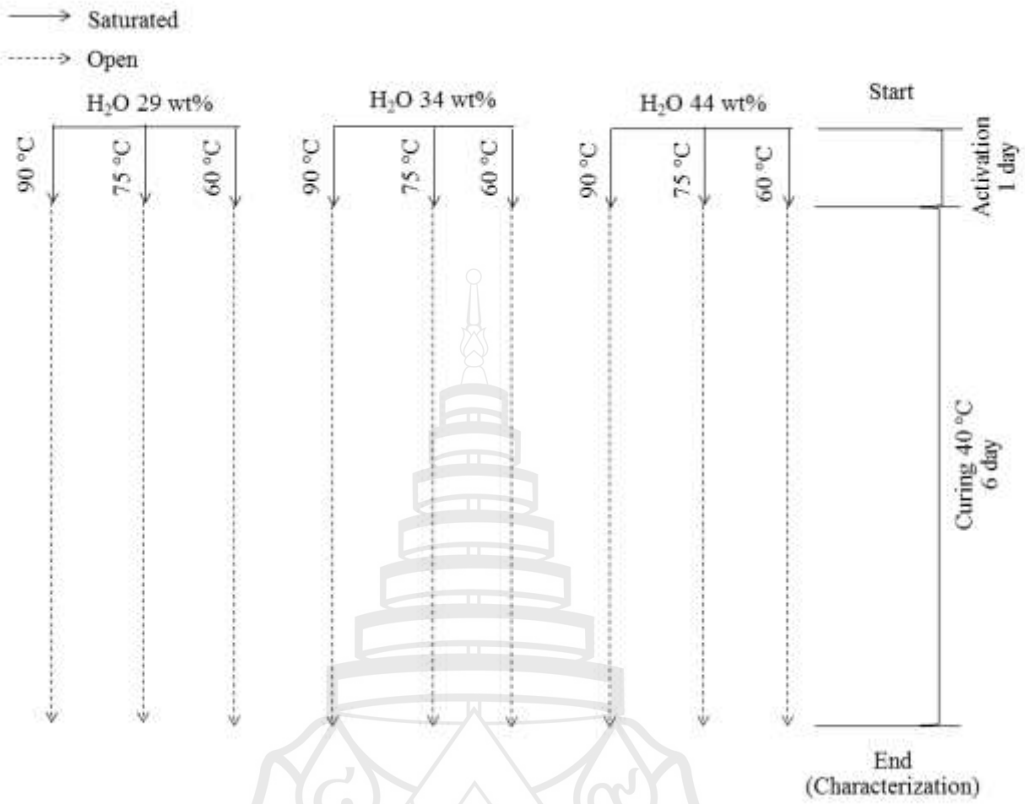

Figure 6.2 Diagram of Preparation of Fly Ash-Based Geopolymer with Initial Water Content of 29, 34 and 44 wt%

6.3.3 Preparation of Samples with Various Initial Water Content of 24, 26 and 29 wt%

To prepare samples with initial water content of 29 wt%, 10M NaOH and Na_2SiO_3 were mixed following the weight ratio of 1 and stirred by stirring bar for 3 min. Fly ash powders were added into activated solution following the solution to fly ash weight ratio of 3:5. Since the molar ratios of elements were very important to properties of fly ash-based geopolymer, the molar ratios Si:Al:Na must be 2.46:1:1.38 (Table 6.1). For preparation of samples with initial water content of 24 wt%, 15M NaOH and Na_2SiO_3 were mixed following the weight ratio of 0.22:0.30 and stirred by stirring bar for 3 min. Fly ash powders were added into activated solution following the solution to fly ash to extra water weight ratio of 2.58:5:1.24. For preparation of samples with initial water content of 26 wt%, 18M NaOH and Na_2SiO_3 were mixed

following the weight ratio of 0.19:0.30 and stirred by stirring bar for 3 min. Fly ash powders were added into activated solution following the solution to fly ash to extra water weight ratio of 2.44:5:0.39. The mixture was stirred for 30 s until no obvious agglomerate was observed. Then it was poured into a plastic mold with 11.6 mm diameter and 29 mm height cylindrical shape. The mold continued to be kept in a sealed container with water saturated atmosphere by supplying 160 mL extra water. The container was kept in the oven and activated at 75 ℃ for 24 h with saturated atmospheric water since the samples with higher compressive strength were obtained at activation temperature of 75 ℃ (Chapter 5). Then all samples were cured at 40 ℃ under saturated condition for 3 days and continued to be cured at 40 ℃ under open condition for another 3 days since saturated curing condition contributed to the higher compressive strength (Chapter 4). Finally, the samples were removed from mold for characterization (Figure 6.3).

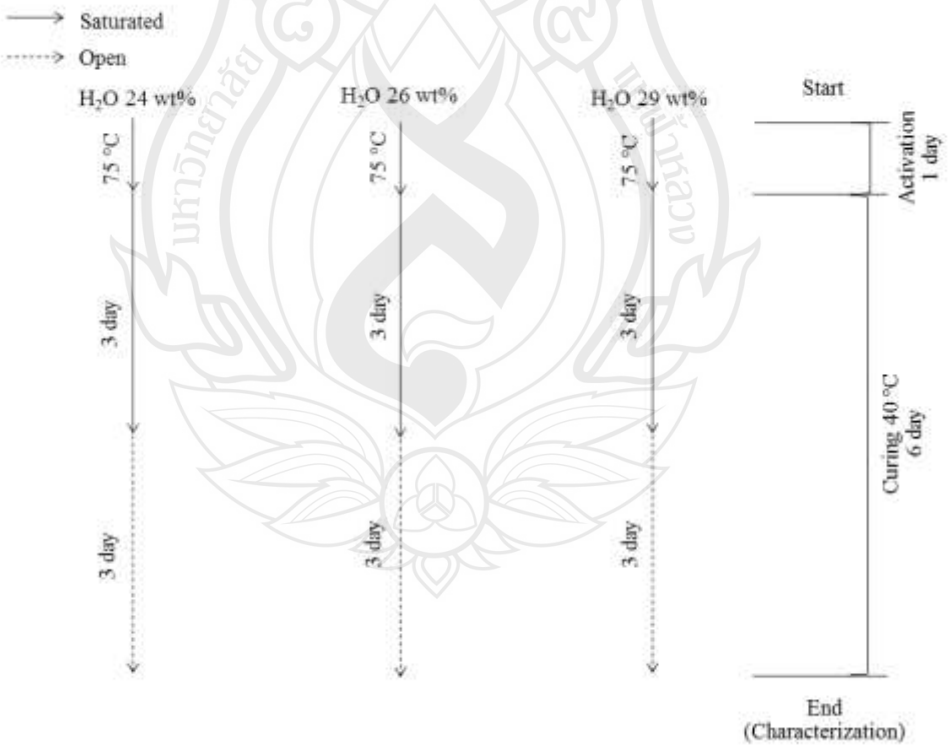

Figure 6.3 Diagram of Preparation of Fly Ash-Based Geopolymer with Initial Water Content of 24, 26 and 29 wt%

Table 6.1 Composition of Mixture

FA (g)	Na_2SiO_3 (g)	NaOH (g)			Extra H_2O (g)	Total H_2O/Total Solid (wt%)	Molar Ratio Si:Al:Na
		10M	15M	18M			
100	30	30	-	-	19.2	44	2.46:1:1.38
100	30	30	-	-	6.4	34	2.46:1:1.38
100	30	30	-	-	-	29	2.46:1:1.38
100	30	-	-	18.81	7.8	26	2.46:1:1.38
100	30	-	21.66	-	2.47	24	2.46:1:1.38

6.3.4 Characterization

6.3.4.1 Setting Time

To measure the initial setting time and final setting time, the Vicat Tester (Humboldt Mfg. Co. USA) has been used. The preparation of mixture for setting time test followed preparation of samples with initial water content of 29, 34 and 44 wt% as described in section 6.3.2. The received mixture was poured into a conical ring. The penetration test was performed by lowering the needle until it rested on the surface of the geopolymer paste. The set screw was tightened and the indicator was set at the upper end of the scale. After 1 to 2 s, the rod quickly was released by releasing the set screw. The penetration of needle was determined every 30 min or less until a penetration of 4±1 mm was obtained from the bottom. The time between the initial contact of fly ash and solution and the penetration of 4±1 mm was initial setting time. After initial setting time determination, the conical ring was kept upside down immediately. The penetration of needle was determined every 15 min until a penetration of 0.5 mm was obtained from the top. The time between the initial contact of fly ash and solution and the penetration of 0.5 mm was the finial setting time (Ministry of Housing and Urban-Rural Development of the People's Republic of China, 2010).

6.3.4.2 Geopolymer Testing

Physical properties, compressive strength, microstructure and phase composition of fly ash-based geopolymer were performed following section 4.3.3.2-4.3.3.5.

6.4 Results and discussion

6.4.1 Setting time

Figure 6.4 showed that both initial and finial setting time were prolonged with increasing initial water content. The initial setting times were 86, 90 and 124 min for initial water content of 29, 34 and 44 wt%, respectively. Following the same order, the final setting time were 172, 179 and 217 min. According to the fact that short setting time can stand for high reaction rate, more initial water may have a disadvantage of dissolution and condensation in the early age. It was also observed that the difference between initial and finial setting time was similar, about 90 min. From all above, it was supposed that at room temperature, more initial water may result in low rate of dissolution while it may not significantly affect the condensation in the early age.

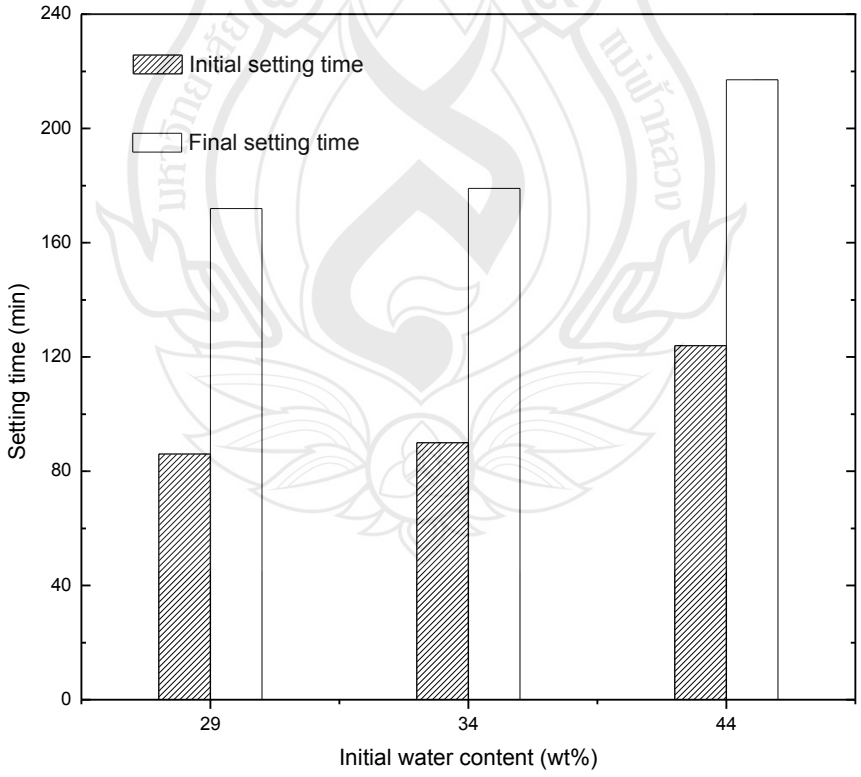

Figure 6.4 Effect of Initial Water Content on Setting Time

6.4.2 Initial water content of 29, 34 and 44 wt%

Compressive strength decreased significantly with increasing initial water content from 29 to 44 wt% for the activation temperature of 60, 75 or 90 ℃ (Figure 6.5). The results showed the same trend to section 2.2.4.

Apparent density values were almost unchanged for increasing initial water content from 29 to 34 wt% and then decreased slightly by less than 3%, for that from 34 to 44 wt% in the case of activation temperature of 60 ℃ and 75 ℃. For the activation temperature of 90 ℃, apparent density tended to decrease slightly from various initial water contents. However, it was believed that the apparent density was almost unchanged due to the high standard deviation (Figure 6.6).

Bulk density decreased sharply with increasing initial water content for all various activation temperatures which was almost similar to the relationship between compressive strength and initial water contents (Figure 6.7).

Geometric density also decreased significantly with increasing initial water content for all various activation temperatures which had a same changing direction with bulk density (Figure 6.8).

Porosity increased significantly with increasing initial water content for the activation temperature of 60, 75 or 90 ℃, which had a reverse trend to the relationship between compressive strength and initial water contents (Figure 6.9).

Therefore, the compressive strength was really related to bulk density and porosity in this study. Bulk density had an inverse relationship with porosity since lower bulk density contributed to higher porosity. Compressive strength hardly had a relationship with apparent density, since apparent density stood for the density of reacted parts. However, an almost constant apparent density was found in case of using different initial water content.

From the SEM image, Figure 6.10 showed that more cracks existed and the surface crack size was larger when samples contain higher initial water content. The same phenomenon was also observed at a higher magnification, as shown in Figure 6.11. It was believed that the extra water would evaporate from the inside and result in the cracks during the stage of condensation. More water evaporation contributed to the more and bigger cracks. Therefore, following the same mechanism, more and bigger cracks were observed inside fly ash-based geopolymer with initial water

content of 44 wt%, as shown in Figure 6.12 (b) in the magnification of 50X. Another phenomenon, from Figure 6.12 and Figure 6.13, was that more fly ash particles existed and more cracks occurred between unreacted fly ash particles and matrix in case of 44 wt% initial water content. It was believed that more initial water resulted in lower concentration of NaOH and fly ash particles could not be dissolved completely.

X-ray diffraction analysis was used for analyzing the crystallinity and phase of hardened fly ash-based geopolymer. For initial water content of 29 wt%, magnesioferrite ($MgFe_2O_4$), quartz (SiO_2) and enstatite ($MgSiO_3$) were observed. For initial water content of 44wt%, magnesioferrite ($MgFe_2O_4$), calcite ($CaCO_3$) and quartz low (SiO_2) were obtained from Figure 6.12. It was observed that magnesioferrite existed predominantly in both initial water content of 29 wt% and 44 wt%. However, quartz existed dominantly in initial water content of 29 wt% while calcite took the second place in that of 44 wt%.

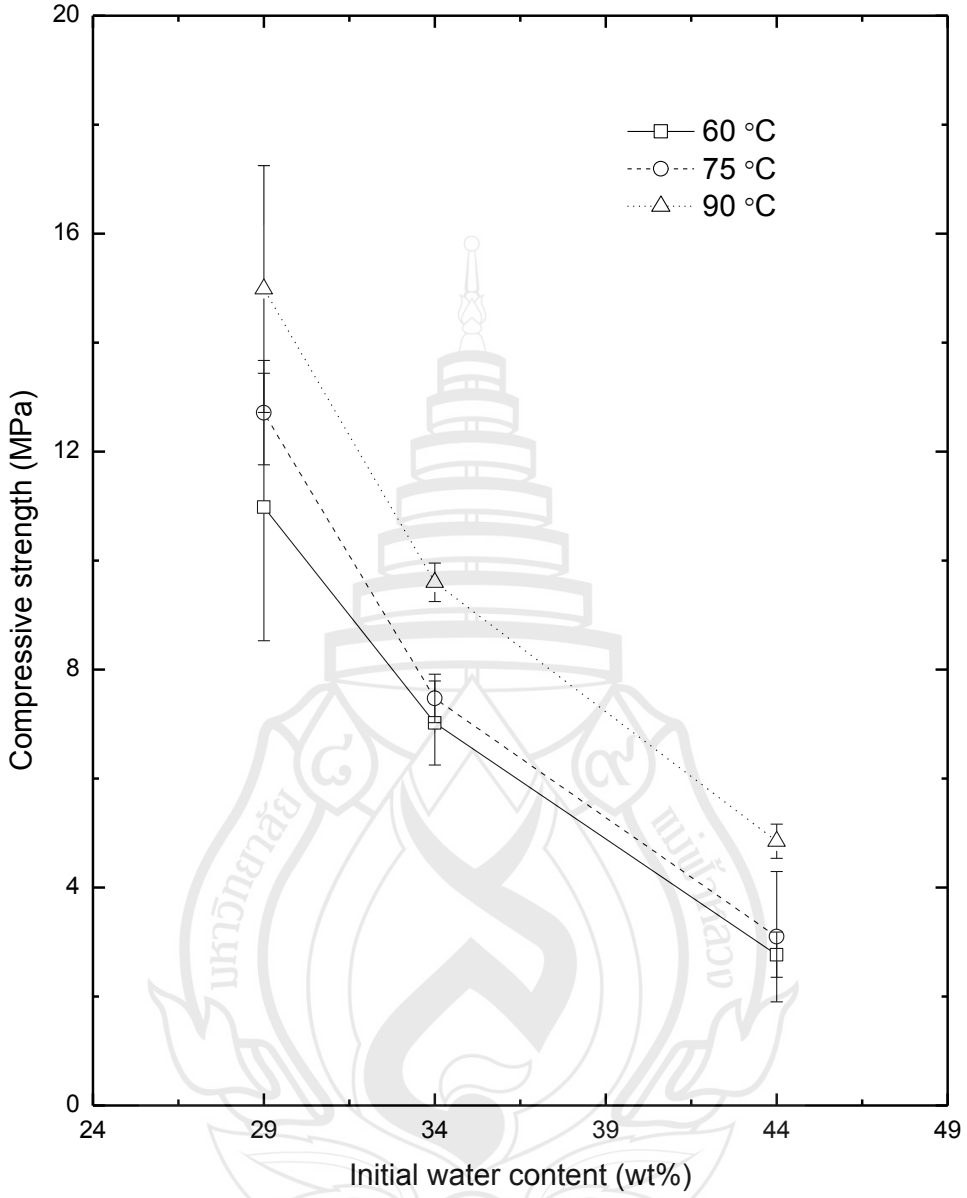

Figure 6.5 Effect of Initial Water Content on Compressive Strength of Fly Ash-Based Geopolymer

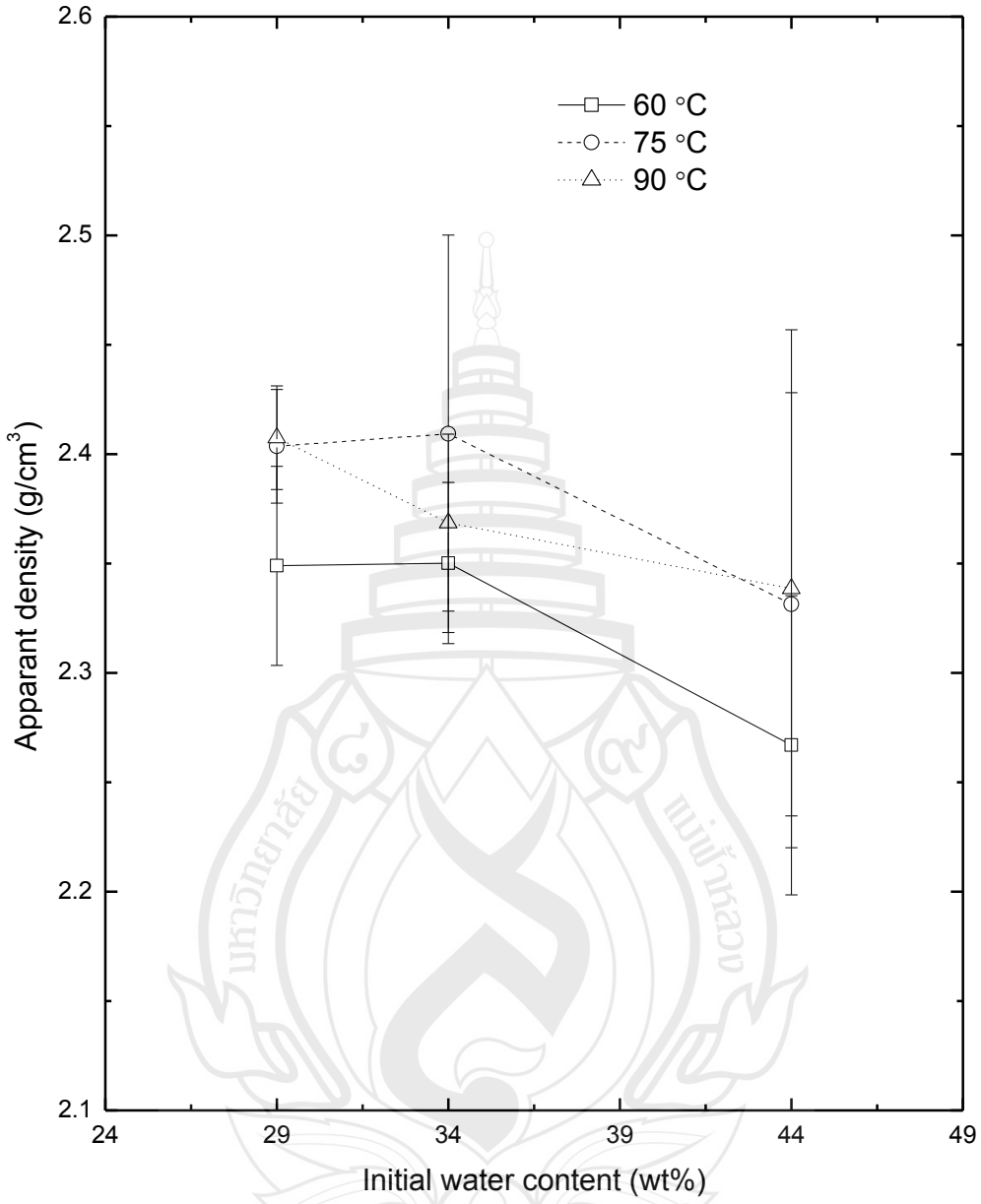

Figure 6.6 Effect of Initial Water Content on Apparent Density of Fly Ash-Based Geopolymer

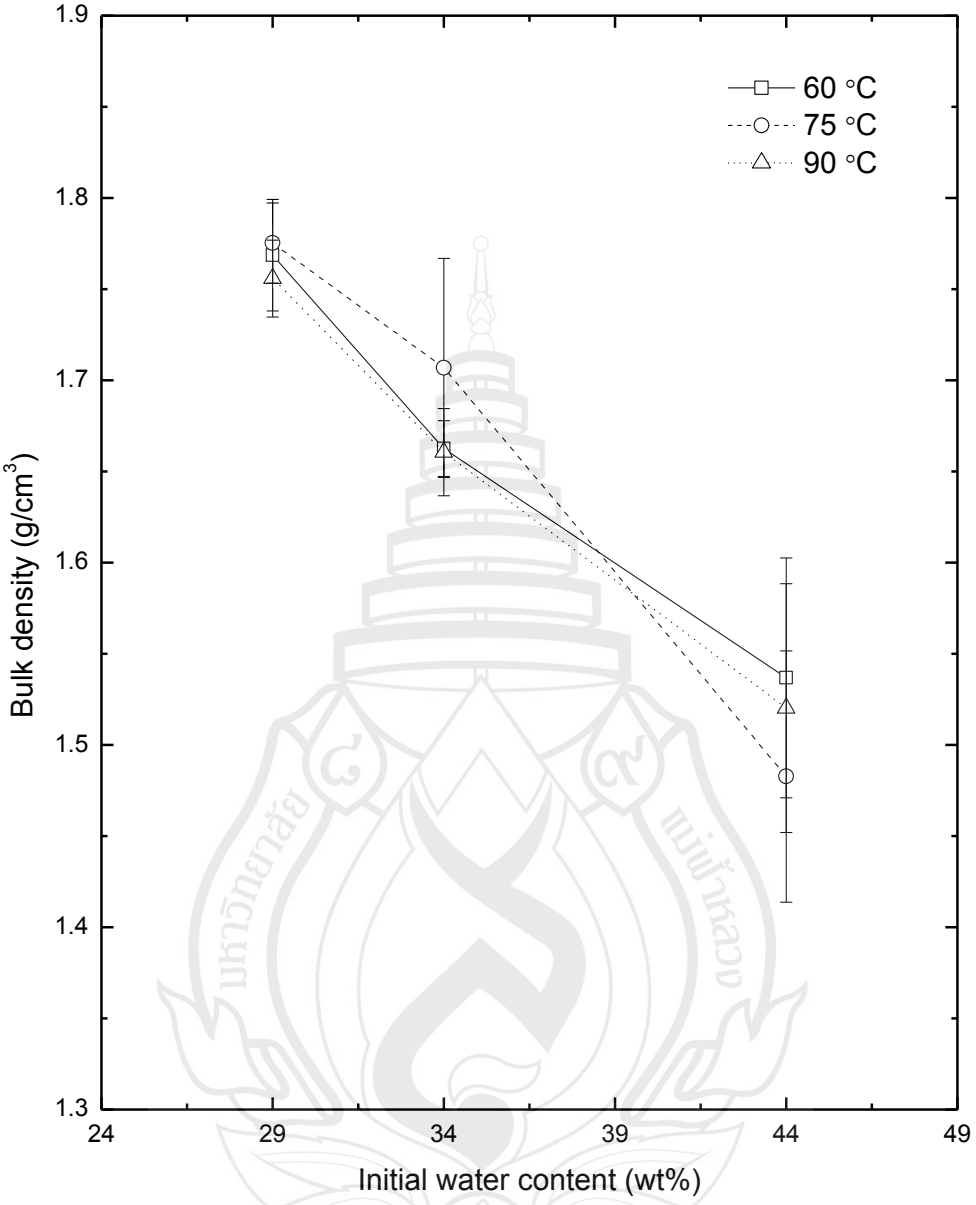

Figure 6.7 Effect of Initial Water Content on Bulk Density of Fly Ash-Based Geopolymer

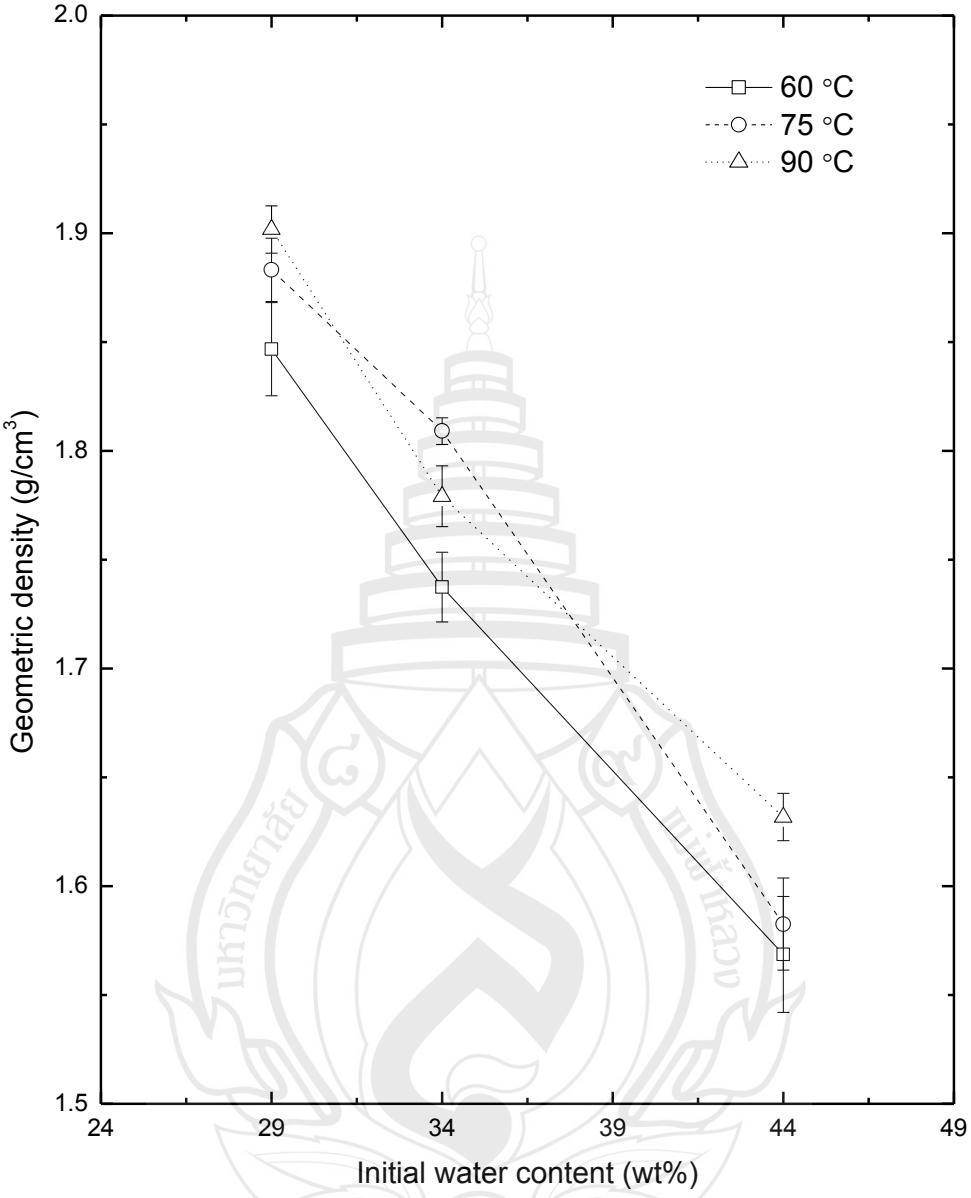

Figure 6.8 Effect of Initial Water Content on Geometric Density of Fly Ash-Based Geopolymer

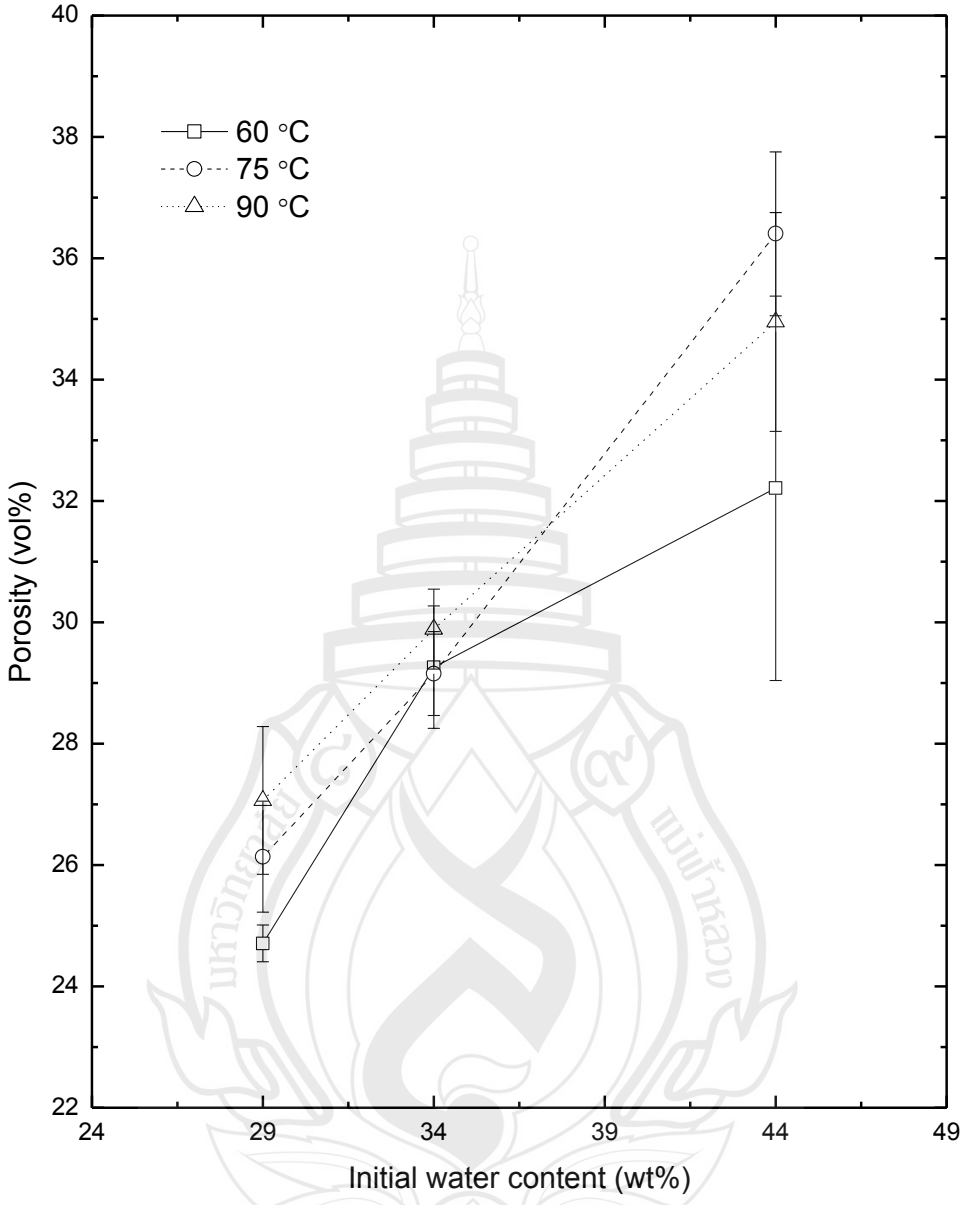

Figure 6.9 Effect of Initial Water Content on Porosity of Fly Ash-Based Geopolymer

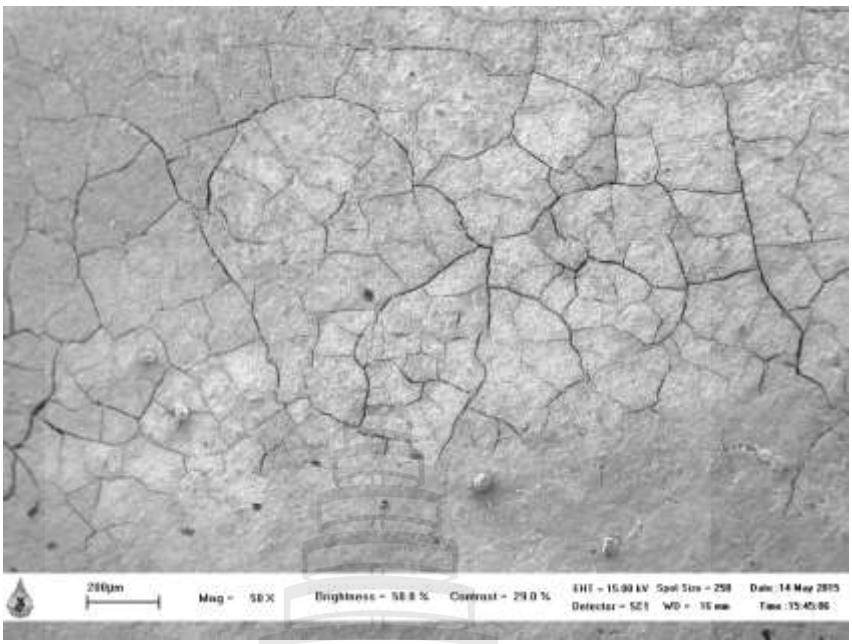

(a)

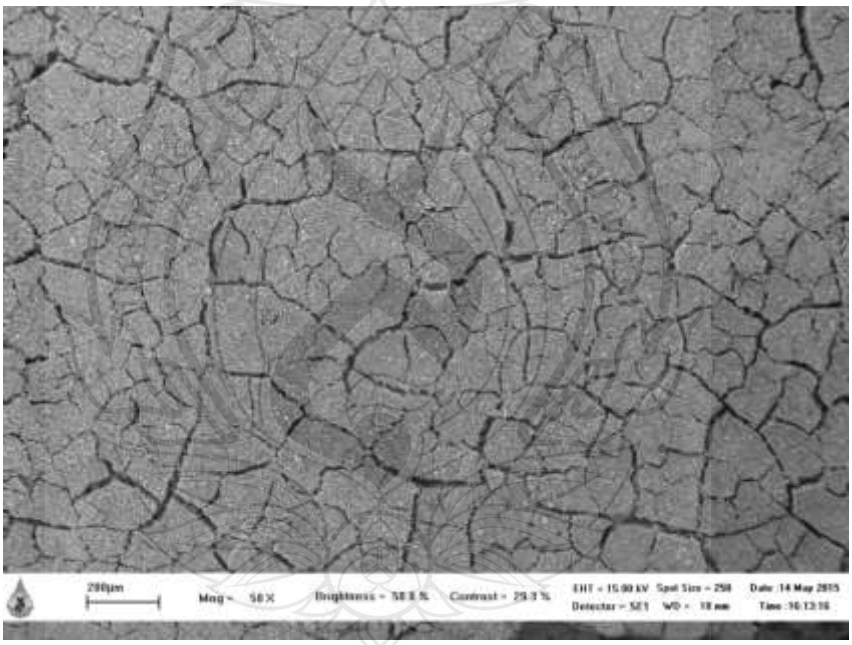

(b)

Figure 6.10 SEM Image with Magnification of 50X on Surface of Fly Ash-Based Geopolymer with Initial Water Content of (a) 29 wt%, and (b) 44 wt% under Saturated Curing Condition Activated at 60 ℃

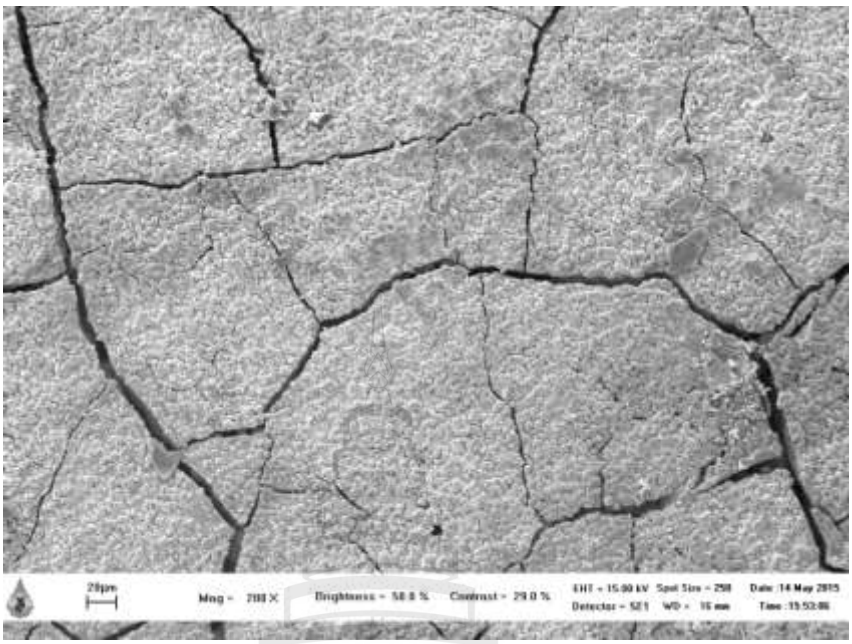

(a)

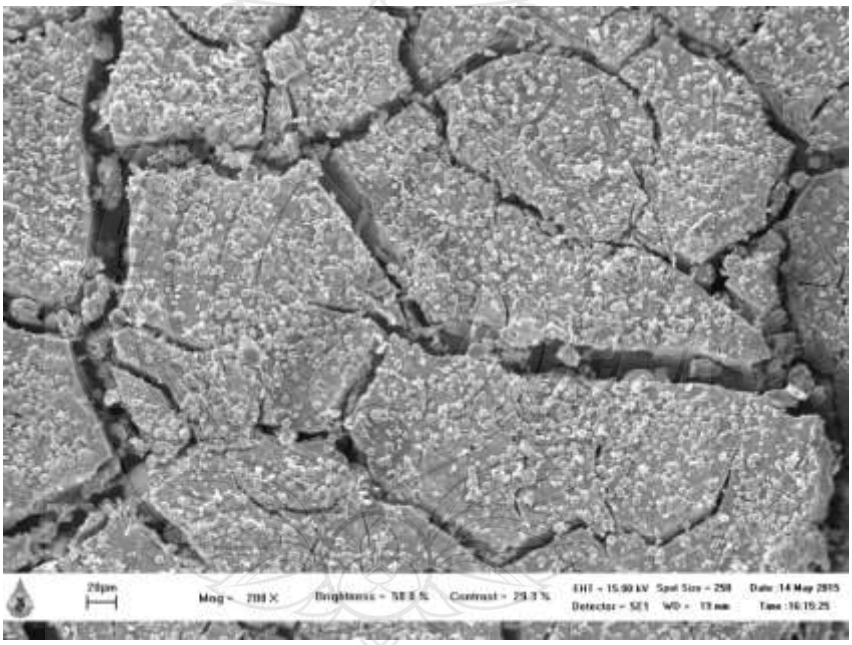

(b)

Figure 6.11 SEM Image with Magnification of 200X on Surface of Fly Ash-Based Geopolymer with Initial Water Content of (a) 29 wt%, and (b) 44 wt% under Saturated Curing Condition Activated at 60 ℃

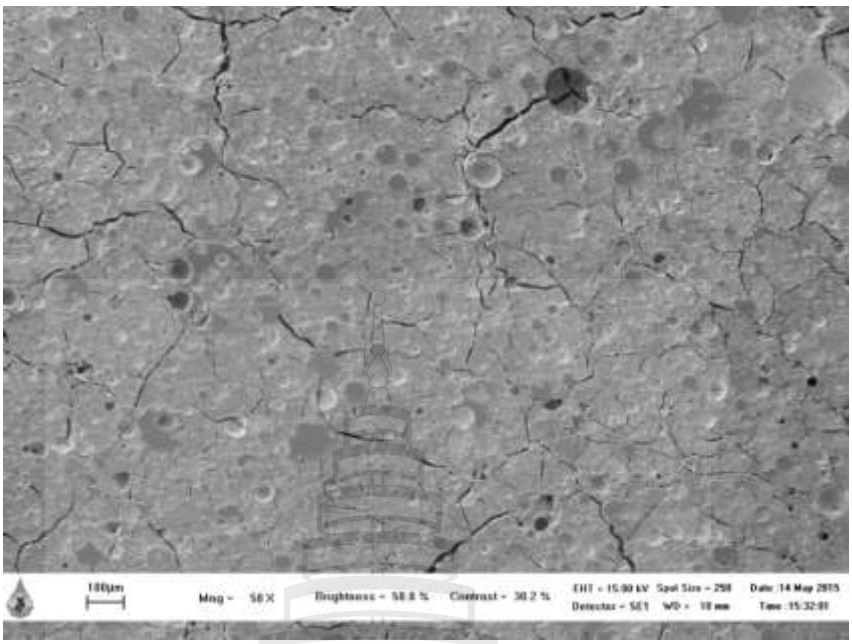

(a)

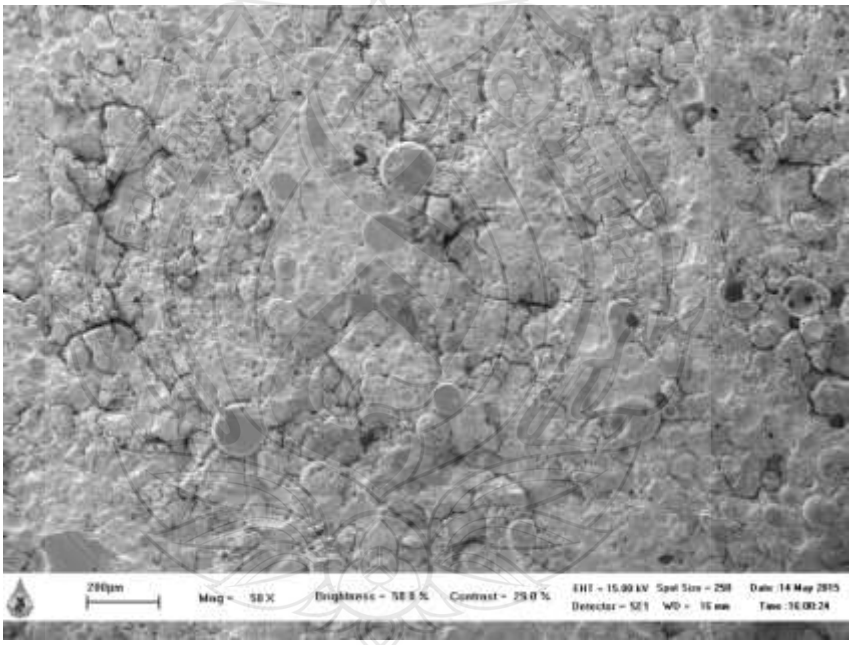

(b)

Figure 6.12 SEM Image with Magnification of 50X on Polished Surface of Fly Ash-Based Geopolymer with Initial Water Content of (a) 29 wt%, and (b) 44 wt% under Saturated Curing Condition Activated at 60 ℃

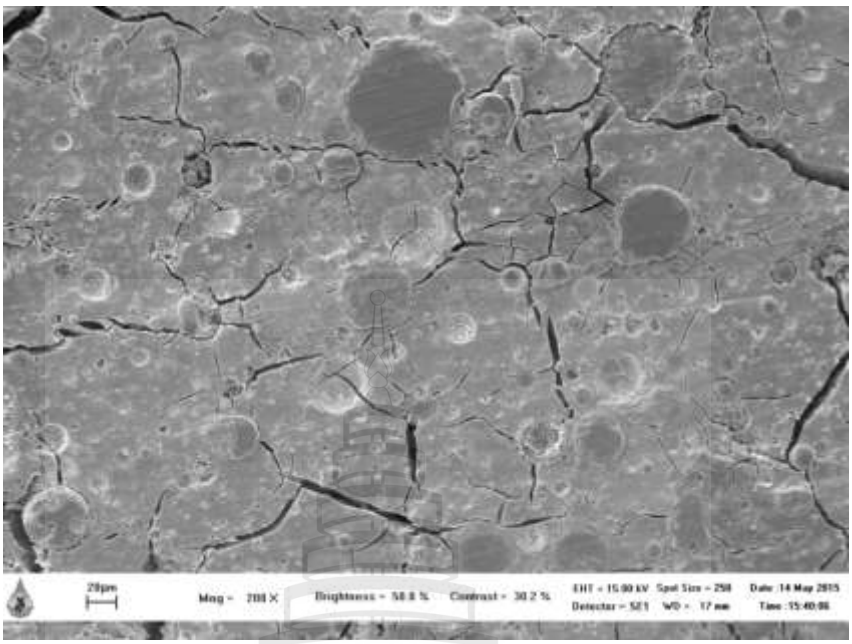

(a)

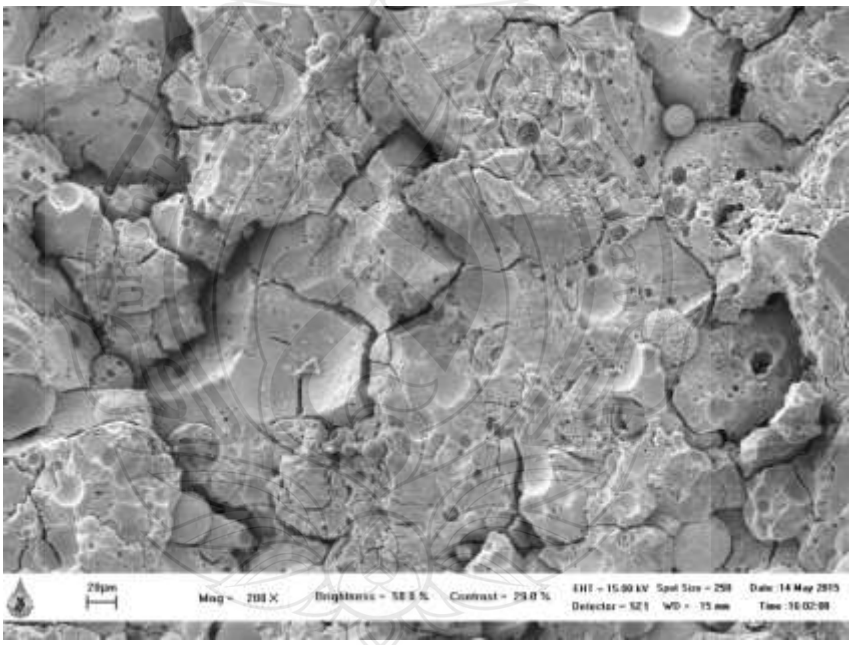

(b)

Figure 6.13 SEM Image with Magnification of 200X on Polished Surface of Fly Ash-Based Geopolymer with Initial Water Content of (a) 29 wt%, and (b) 44 wt% under Saturated Curing Condition Activated at 60 ℃

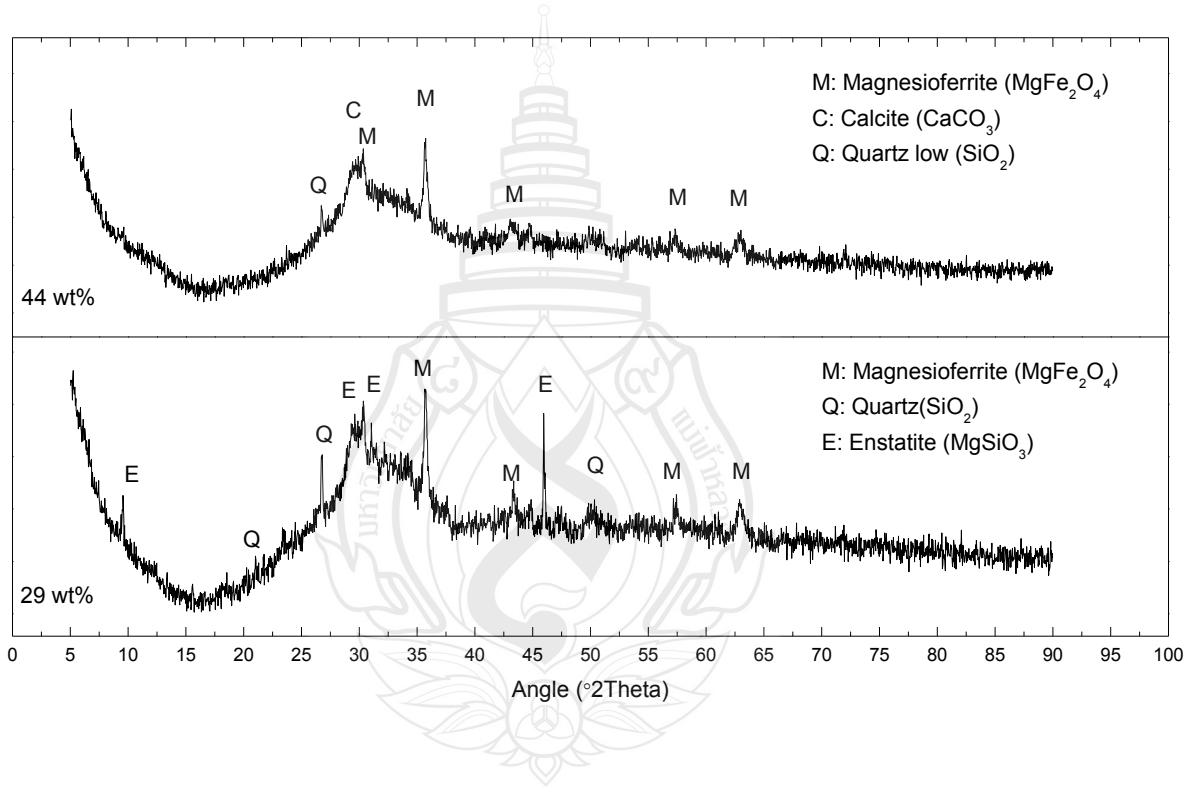

Figure 6.14 X-ray Diffraction Analysis on Hardened Fly Ash-Based Geopolymer with Initial Water Content of 29 wt% and 44 wt% under Saturated Curing Condition Activated at 60 ℃

6.4.3 Initial water content of 24, 26 and 29 wt%

Effect of initial water content on compressive strength was clear according to previous work. Figure 6.5 showed that the compressive strength increased with decreasing initial water content from 44, 34 to 29 wt% for activation temperature of 60, 75 or 90 ℃. However, the workability of the paste is poor if the initial water content reaches a certain level, resulting in poor mold filling and hence the compressive strength. In order to find the practical lower limit of initial water content, samples with initial water content of 24, 26 and 29 wt% were activated at 75 ℃ for 24 h and then cured at 40 ℃ under saturated condition for 3 days. Finally, the samples were cured at 40 ℃ under open condition for another 3 days.

The compressive strength of 28.07 ± 5.37, 28.52 ± 3.02 and 22.53 ± 1.53 MPa were obtained for initial water content of 24, 26 and 29 wt%, respectively. Figure 6.15 showed clearly the compressive strength had a decreased trend with increasing initial water content. The apparent density of 2.35 ± 0.02, 2.35 ± 0.01 and 2.36 ± 0.02 g/cm^3 and the bulk density of 1.81 ± 0.01, 1.77 ± 0.01 and 1.70 ± 0.01 g/cm^3 were obtained for initial water content of 24, 26 and 29 wt%, respectively. The figure also showed apparent density kept an almost constant value with changing initial water content. Bulk density decreased obviously with increasing initial water content. The porosity of 22.77 ± 0.93, 24.63 ± 0.20 and 28.01 ± 0.69 vol% were obtained for initial water content of 24, 26 and 29 wt%, respectively. The porosity decreased with increasing initial water content. It was reasonable that porosity had a positive relationship with initial water content which had an inverse relationship with bulk density, and apparent density had no obvious relationship with initial water content. The results were well agreed with previous work as showed in Figure 6.5, Figure 6.6, Figure 6.7 and Figure 6.9.

According to Figure 6.15, the initial water limitation reached 24 wt% considering balance between workability and compressive strength. When the initial water content was less than 24 wt%, prepared fly ash mixture could not flow. The strength of 28.07 ± 5.37 MPa was obtained with the value of 24 wt% initial water content. The high standard deviation of 5.37 MPa demonstrated inhomogeneous phase inside samples.

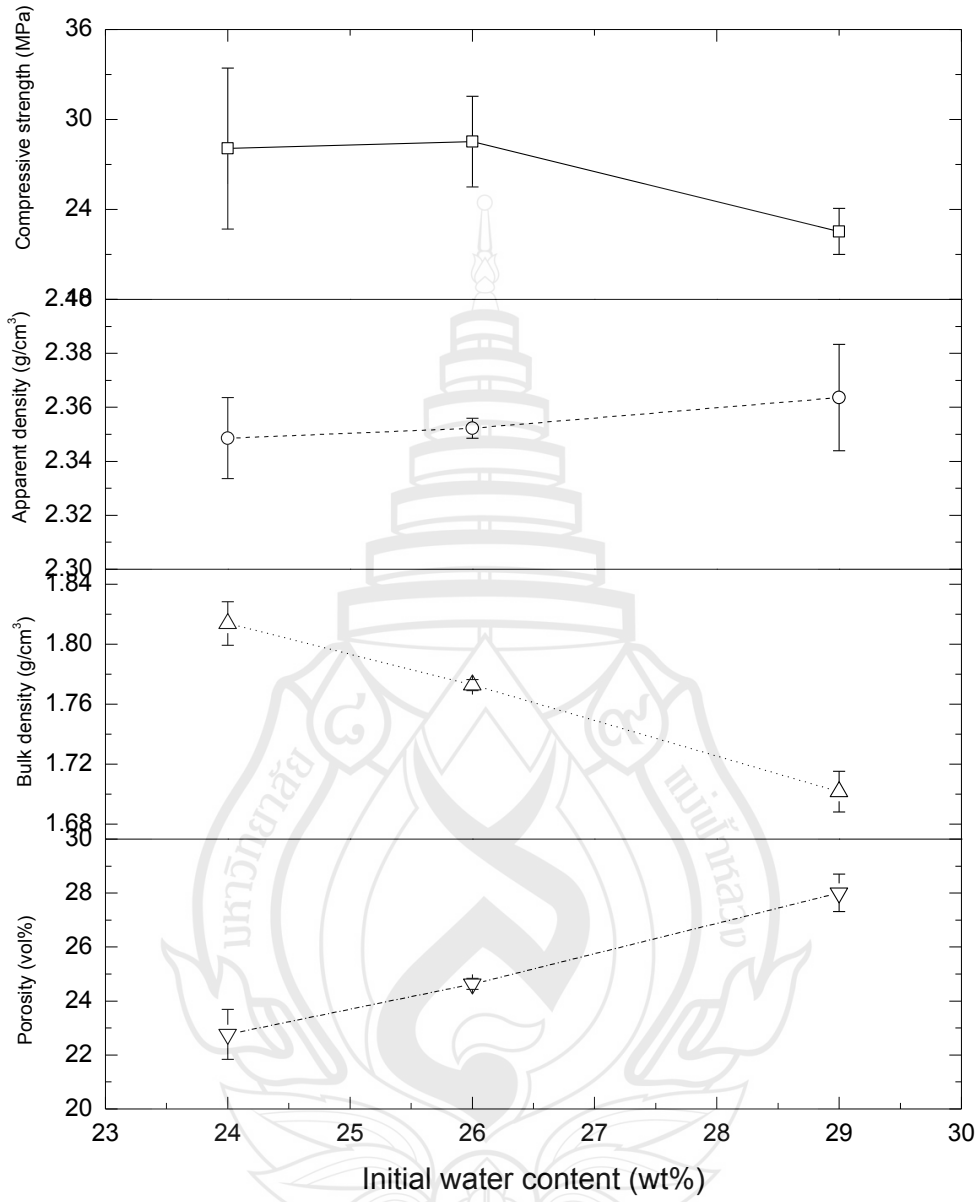

Figure 6.15 Effect of Initial Water Content on Compressive Strength, Apparent Density, Bulk Density and Porosity of Fly Ash-Based Geopolymer Activated at 75 ℃

6.5 Conclusions

Compressive strength of fly ash-based geopolymer was significantly higher, 14.98±2.26 MPa, with lower initial water content of 29 wt%. However, the lower limit of initial water content was 24 wt% in this study due to workability. Apparent density was almost constant with increasing initial water content. Bulk density and geometric density decreased with increasing initial water content, which had a reverse trend with porosity. SEM images showed that more cracks existed and the surface crack size was larger for the initial water content of 44 wt% than that of the 29 wt%.

CHAPTER 7

THE EFFECT OF PARTICLE SIZE ON PHYSICAL PROPERTIES AND COMPRESSIVE STRENGTH OF FLY ASH-BASED GEOPOLYMER

7.1 Abstract

In this chapter, the work has been presented in two parts. The first part focused on effect of milling time on particle size distribution and morphology of fly ash. Fly ash without milling was used as control group, while the fly ash milled for 10, 20, 30 and 40 min were used as experimental group. Particle size analyzer (PSA) was used to characterize the particle size distribution of fly ash particles. In the second part, physical properties and compressive strength of geopolymers made from fly ash with various average particle sizes (milling time) and activated at 60 or 75 ℃ and cured under various conditions were reported. Microstructure as well as phase content of harden geopolymer samples were characterized and their correlation with compressive strength and physical properties were discussed. It was concluded that compressive strength of fly ash-based geopolymer was higher with finer average particle size of fly ash. Apparent density, bulk density and geometric density increased with finer particle size of fly ash which had a reverse changing trend with porosity. SEM images showed more undissolved fly ash particles and larger cracks inside hardened fly ash-based geopolymer prepared coarse fly ash particles.

7.2 Introduction

According to literature review (section 2.2.1), there was a clear relationship between compressive strength and particle size distribution. Finer fly ash particles gave rise to a higher compressive strength. This was because finer fly ash particles had a larger specific surface area allowing them to be easily dissolved in the activation solution because of larger contact area. However, there were many ways to receive finer particles which depend on each milling system. In order to choose the appropriated milling condition for our milling system, the effect of milling time on particle size distribution has been characterized. The fly ash will be grand under the selected condition to be used further in preparation of geopolymers.

7.3 Experiment

7.3.1 Preparation of Fly Ash

A plastic bottle of 125 ml was used as milling bottle. High-purity Y_2O_3-stabilized ZrO_2 with density of 6.0 g/cm^3 was used as milling ball. There are two types of milling ball. The large ball with average diameter of 10.19 mm and the small ball with that of 5.06 mm were selected. Milling balls with large size of 80 g and with small size of 80 g were filled into the 125 ml milling bottle. Fly ash was filled into the bottle with the weight of 32 g. The bottle was kept in rapid milling system (vibratory mill) for 10, 20, 30 or 40 min. Finally, the milled fly ash was obtained.

7.3.2 Preparation of Geopolymers

Fly ash (FA) and fly ash with milling time of 10 min (FA10) were chosen for the experiment. 10M NaOH and Na_2SiO_3 were mixed following the weight ratio of 1 and stirred by magnetic stirrer for 3 min. Fly ash powders and extra water was added into activated solution following the solution to fly ash weight ratio of 0.6 and stirred for 30 s. Then it was poured into cylindrical shape plastic mold with 11.6 mm diameter and 29 mm height. Some samples were cured at 60 ℃ for the first 24 h in saturated atmosphere, then cured continuously at 40 ℃ under saturated condition for

3, 6 or 9 days and at 40 ℃ for another 3, 7 and 4 days, respectively. The compressive strength of samples cured for 3 days has been tested on the 7th day and samples cured for 6 and 9 days has been tested on the 14th day. Other samples were activated at 75 ℃ under saturated condition for 24 h and then cured at 40 ℃ under saturated condition for 3 days and finally cured at 40 ℃ under open condition for another 3 days. The compressive strength of samples has been tested on the 7th day (Figure 7.1).

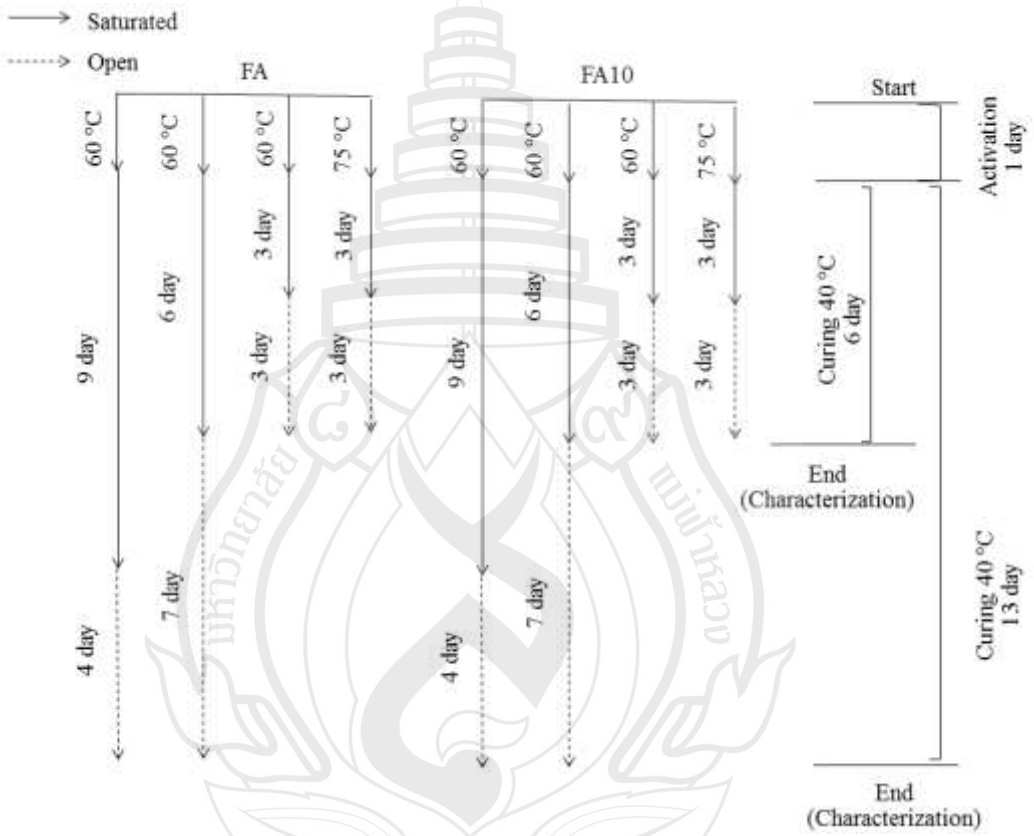

Figure 7.1 Diagram of Preparation of Fly Ash-Based Geopolymer Using FA or FA10

7.3.3 Characterization

7.3.3.1 Particle Size Distribution

Particle size analyzer (Malvern, Mastersizer 2000, Hydro 2000MU) has been used to characterize fly ash particle size distribution. Fly ash powders were added into distilled water and stirred by automatic stir bar with ultrasonic cleaner.

7.3.3.2 Geopolymer Testing

Physical properties, compressive strength, microstructure and phase composition of fly ash-based geopolymer were performed following section 4.3.3.2-4.3.3.5.

7.4 Results and Discussion

7.4.1 Fly Ash Particle Size

According to Figure 7.2 and 7.3, the average size of fly ash particle decreased rapidly with milling time of 10 min, then decreased slowly with prolong. SEM images as Figure 7.4 showed that the amount of broken fly ash particles was produced with increasing milling time. A very different morphology was distinguished between FA and FA10 which was well agreed with Table 7.1 and Figure 7.3 by numbers.

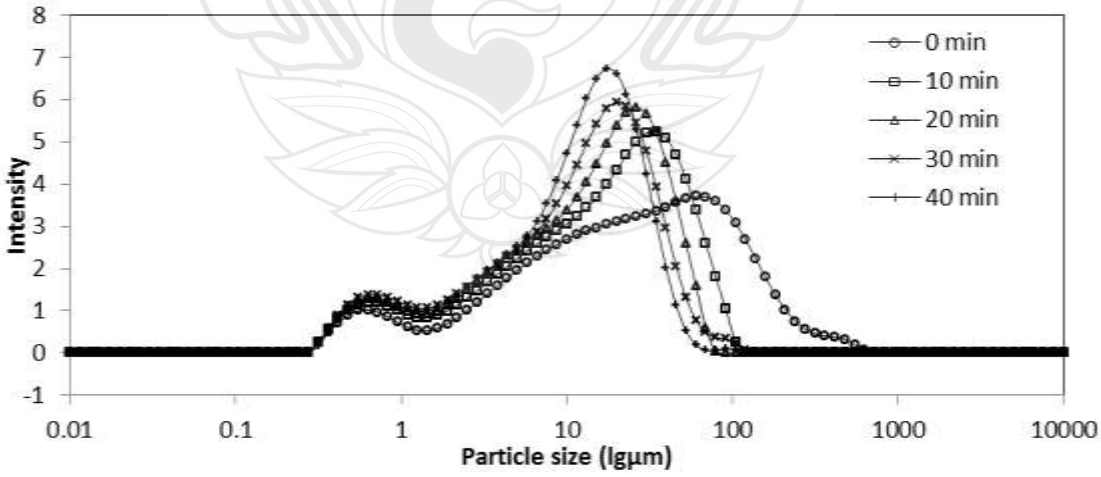

Figure 7.2 Particle Size Distribution of Fly Ash in Logarithm with Base 10

Table 7.1 Particle Size Distribution of Fly Ash with Milling Time

	D10 (μm)	D50 (μm)	D90 (μm)	Average (μm)	Milling time (min)
FA	2	27	135	55	0
FA10	1	18	58	25	10
FA20	1	15	43	19	20
FA30	1	13	38	17	30
FA40	1	13	32	15	40

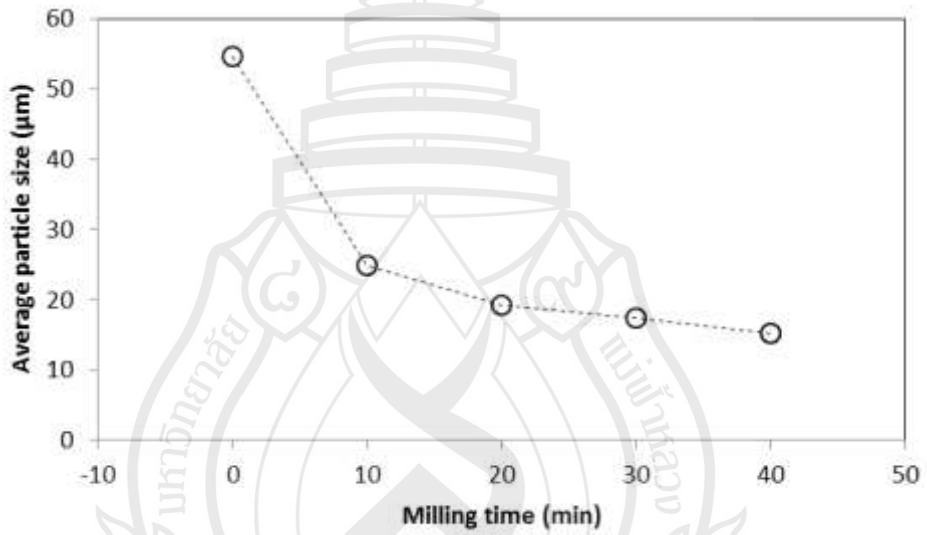

Figure 7.3 Relationship between Average Particle Size of Fly Ash and Rapid Milling Time

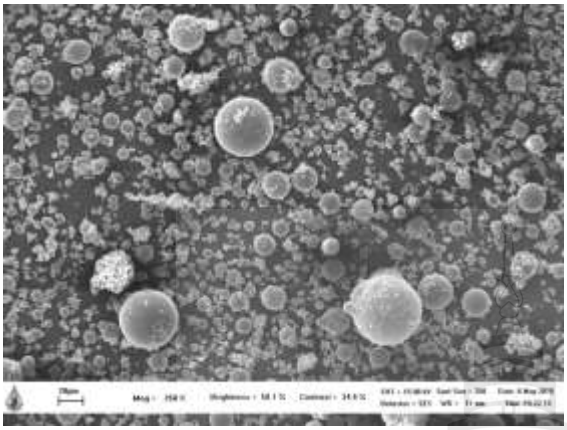

(FA: no milling)

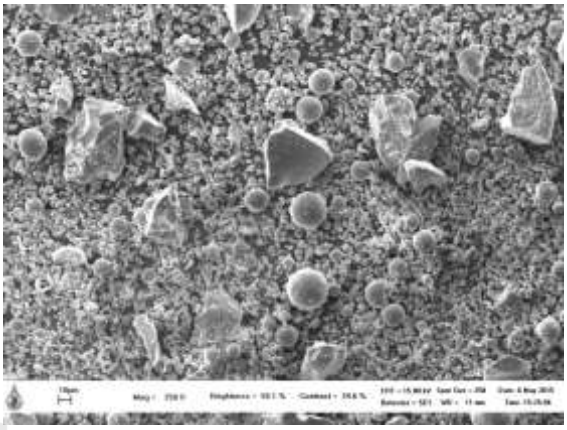

(FA10: milling for 10 min)

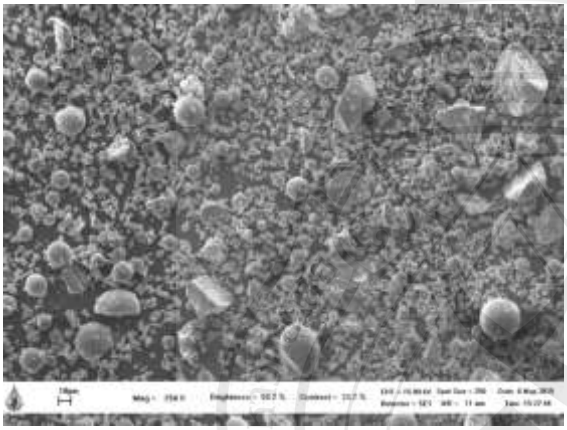

(FA20: milling for 20 min)

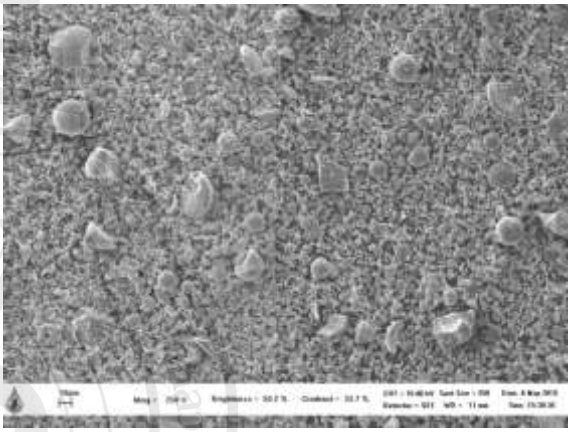

(FA30: milling for 30 min)

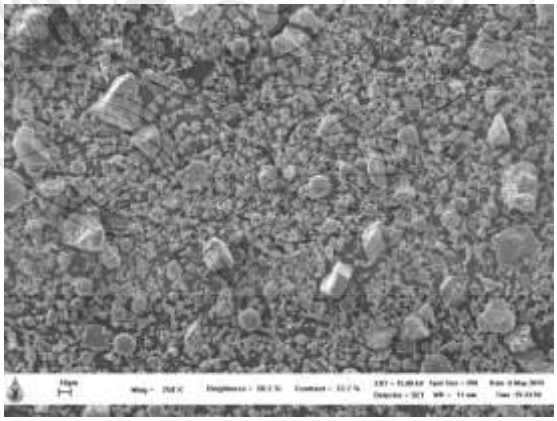

(FA40: milling for 40 min)

Figure 7.4 Morphology of Milled Fly Ash by Scanning Electron Microscope

7.4.2 Fly Ash Particle Size on Properties of Geopolymers

Compressive strength increased significantly with decreasing average particle size of fly ash from 55 to 25 μm for every curing condition. The value even increased from 22.24±2.06 to 64.15±21.69 MPa in the case of activation temperature of 75 ℃ for curing time of 3 day under saturated condition (Figure 7.5). This was because finer fly ash particles had larger surface area which contributed the faster reaction between particles and alkaline solution. The results showed very similar trend to section 2.2.2.

Apparent density increased with decreasing average particle size of fly ash in most cases, such as activation temperature of 75 ℃ for curing time of 3 day, 60 ℃ for that of 6 day and 60 ℃ for that of 9 day. For the activation temperature of 60 ℃ for curing time of 3 day, apparent density tended to decrease slightly from various average particle size (Figure 7.6). It meant that more fly ash particles reacted with alkaline solution, so the matrix density was higher.

Bulk density increased sharply with decreasing average particle size of fly ash in all cases which had a same changing direction with compressive strength (Figure 7.7).

Geometric density also increased significantly with decreasing average particle size of fly ash for all various activation temperatures and saturated time which had a same changing trend with compressive strength and bulk density (Figure 7.8).

Porosity decreased significantly with decreasing average particle size of fly ash for activation temperature of 75 ℃ for curing time of 3 day and for 60 ℃ for saturated time of 3 or 9 day. Porosity increased slightly in the case of 60 ℃ for 6 day. In general, porosity tended to increase with particle size, in turn, lower the compressive strength (Figure 7.9).

Scanning electron microscopy was used for observing the microstructure of hardened fly ash-based geopolymer. More fly ash residues and larger cracks were observed, as shown in Figure 7.10(a) with a magnification of 50X. The same phenomenon was observed in a higher magnification (Figure 7.11). From Figure 7.12(a) with a magnification of 500X, it was clear that more unreacted fly ash particles and more cracks were observed when fly ash was used without milling. Small irregular shape fly ash particles were observed in a higher magnification, from Figure 7.12(b). Therefore, compressive strength, apparent density, bulk density, and

geometric density increased with decreasing average particle size of fly ash was supported by SEM images. Porosity decreased was also supported by the SEM images.

X-ray diffraction analysis was used for analyzing the crystallinity and phase. From Figure 7.13, magnesiferrite ($MgFe_2O_4$), faujasite-Na ($Na_{14}Al_{12}Si_{13}O_{51}\cdot 6H_2O$) and wollastonite 1A ($CaSiO_3$) were detected for geopolymer made from fly ash without milling. Magnesioferrite ($MgFe_2O_4$), calcite ($CaCO_3$), and quartz low (SiO_2) were detected for average particle size of 25 μm. Magnesiofferrite existed in geopolymer made from both fly ash (55 μm) and fly ash (25 μm) with milling time of 10 min.

7.5 Conclusions

Compressive strength of fly ash-based geopolymer was higher with finer average particle size of fly ash. Apparent density, bulk density and geometric density increased with finer particle size of fly ash which had a reverse changing trend with porosity. SEM images showed that more fly ash particles and more and larger cracks occurred inside hardened fly ash-based geopolymer for coarse fly ash particles compared to fine particles.

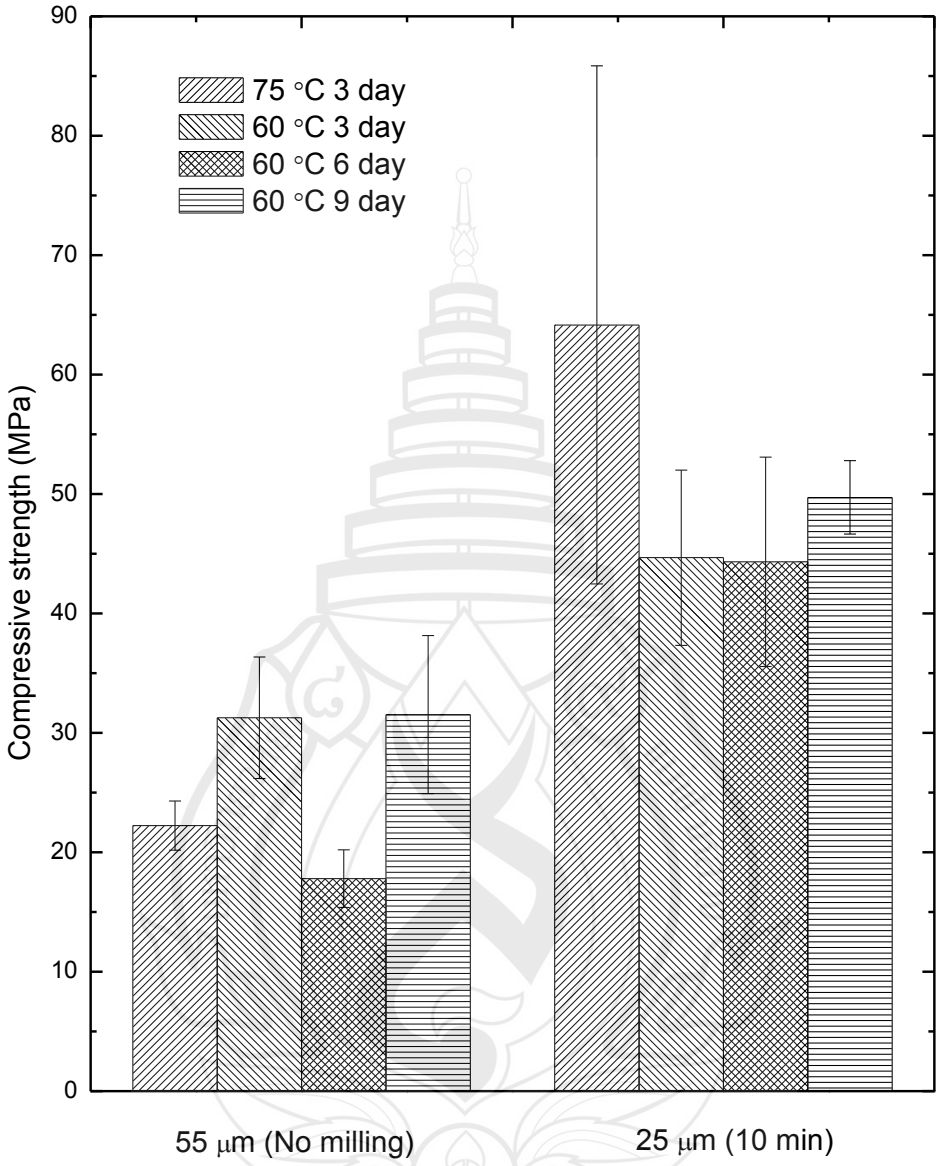

Figure 7.5 Effect of Particle Size on Compressive Strength of Fly Ash-Based Geopolymer

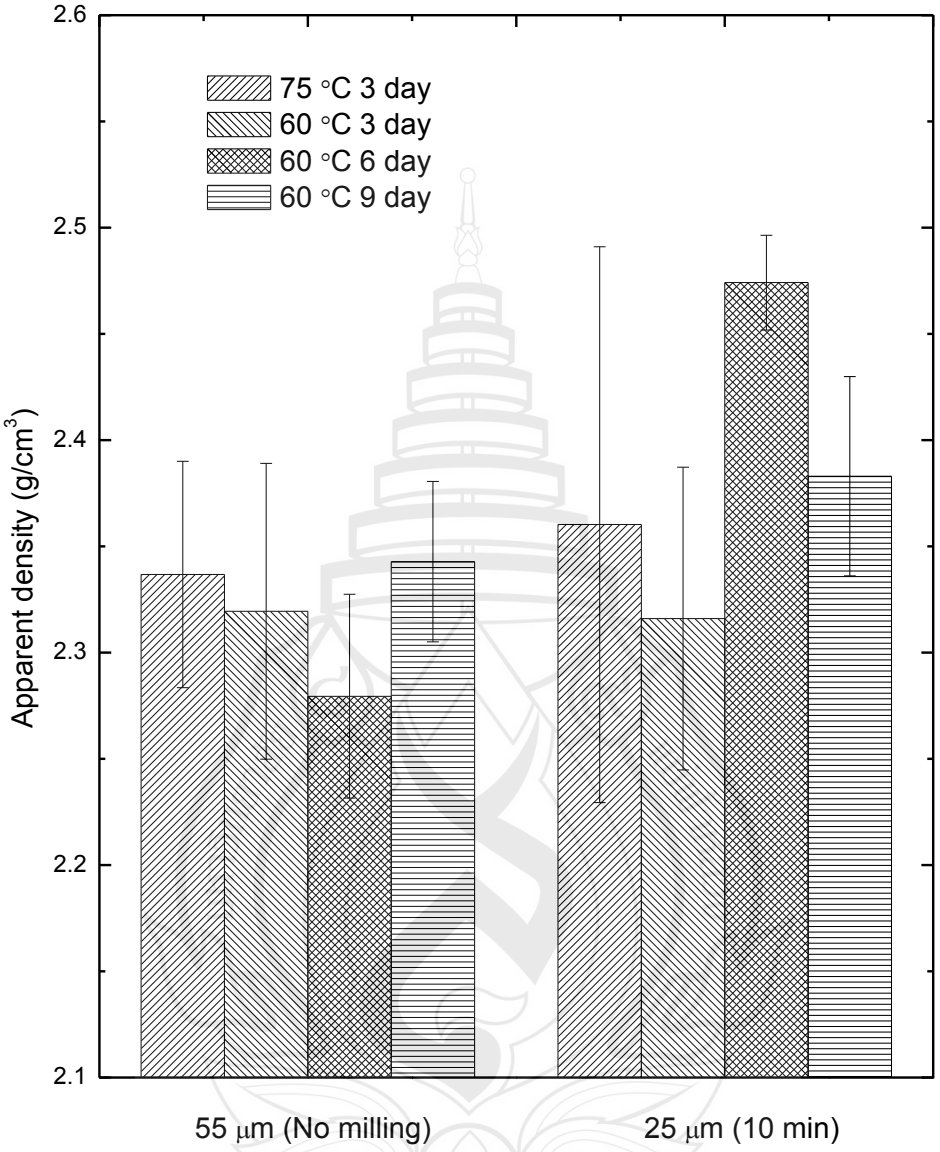

Figure 7.6 Effect of Particle Size on Apparent Density of Fly Ash-Based Geopolymer

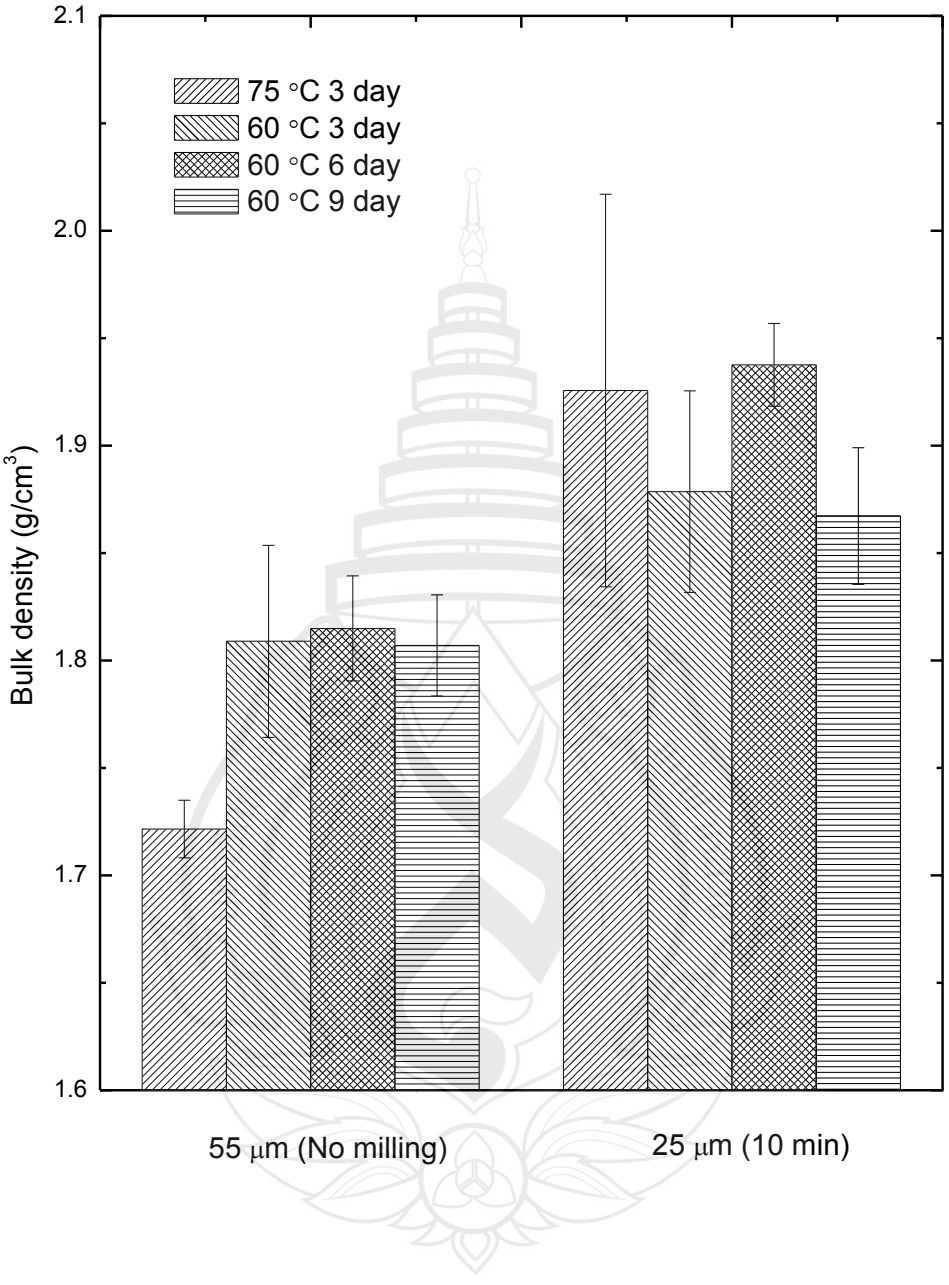

Figure 7.7 Effect of Particle Size on Bulk Density of Fly Ash-Based Geopolymer

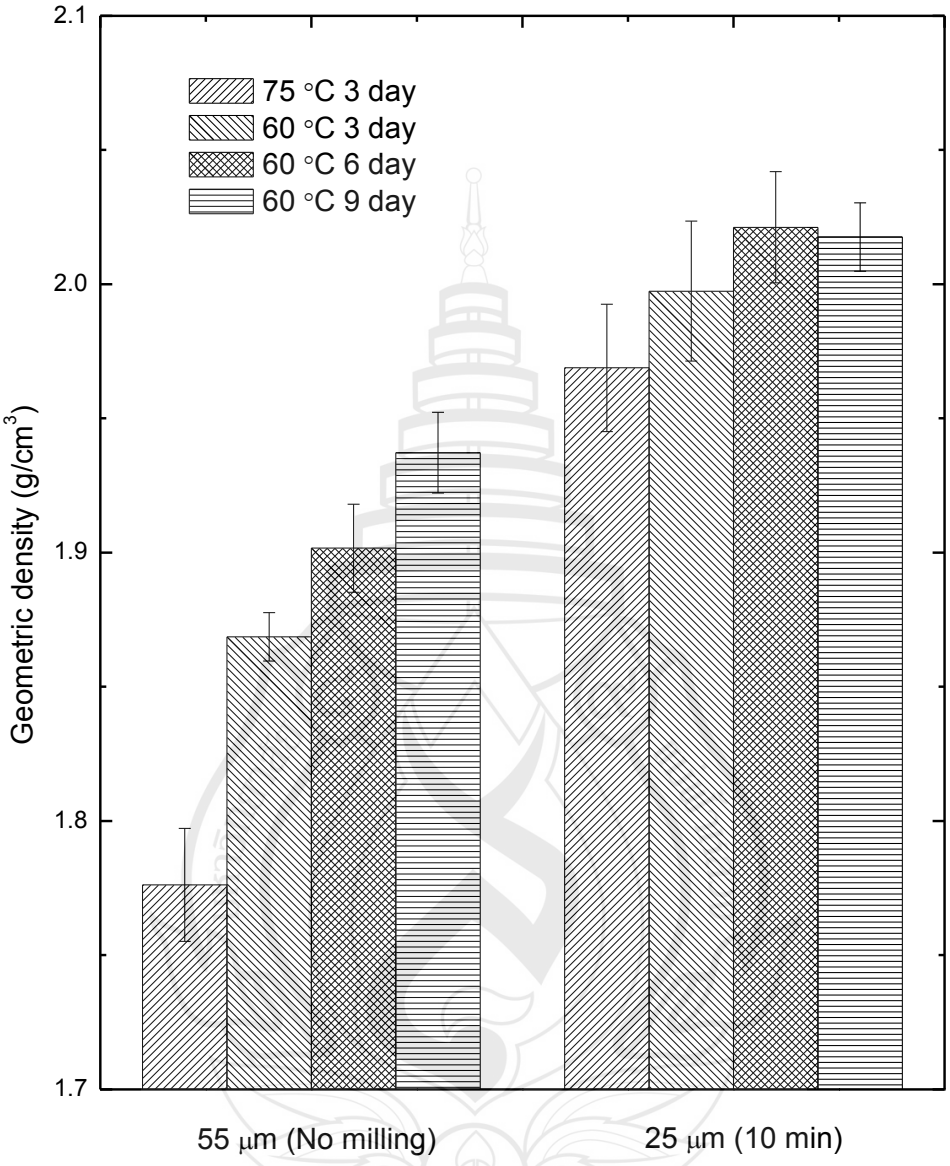

Figure 7.8 Effect of Particle Size on Geometric Density of Fly Ash-Based Geopolymer

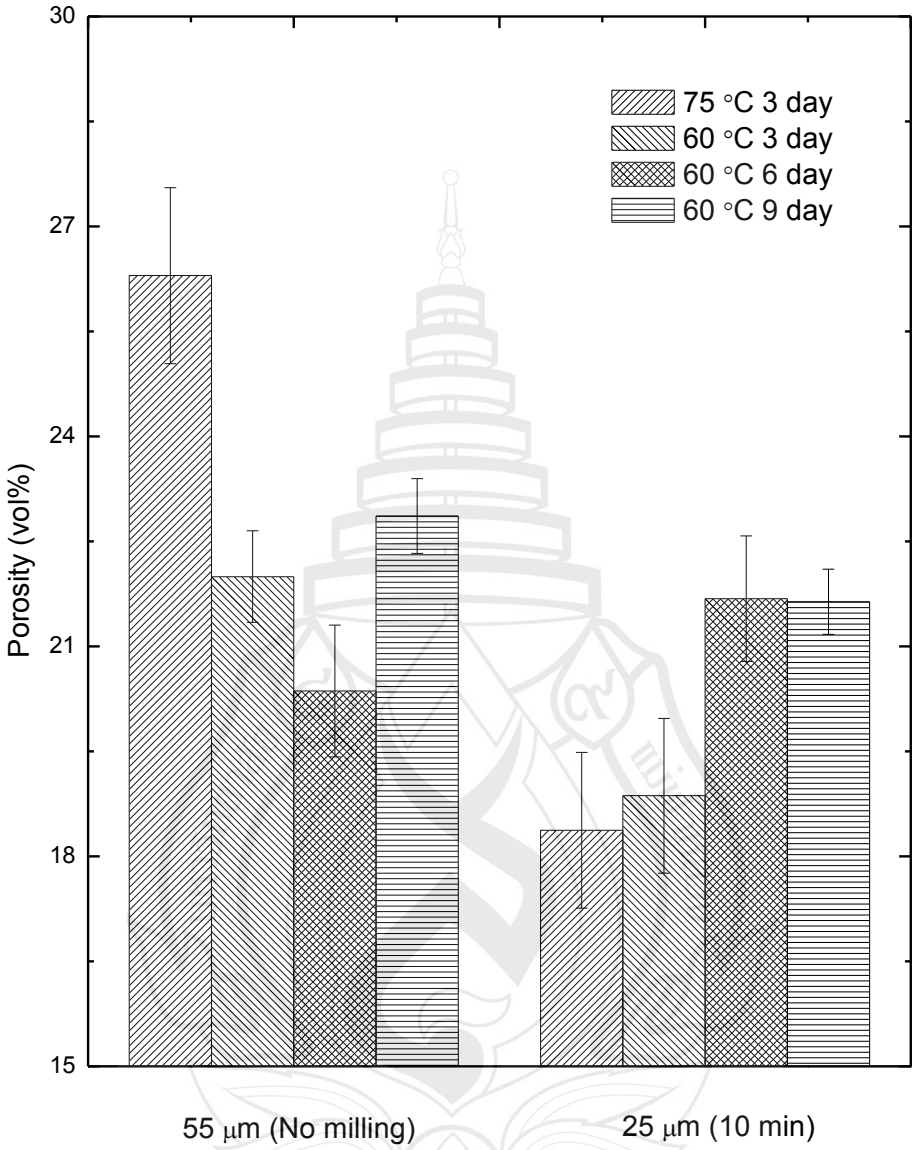

Figure 7.9 Effect of Particle Size on Porosity of Fly Ash-Based Geopolymer

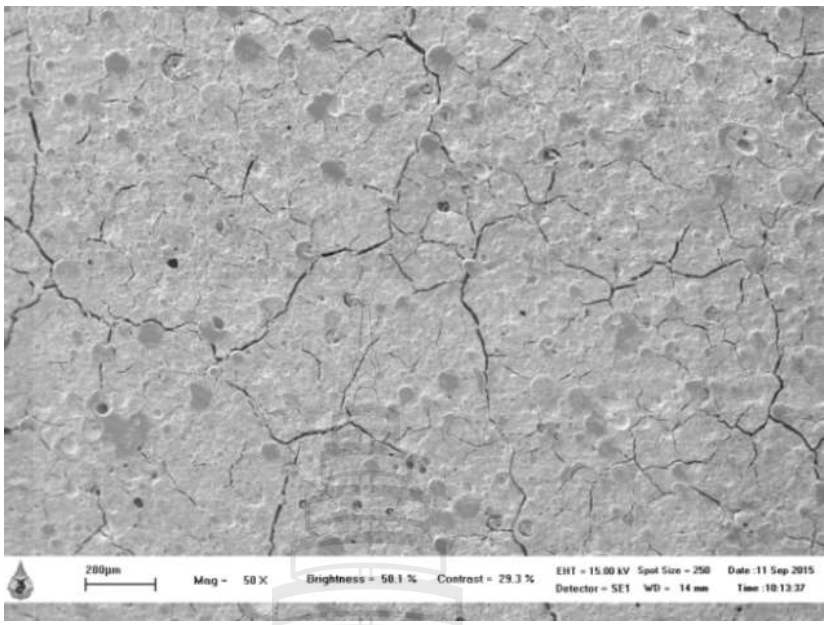

(a)

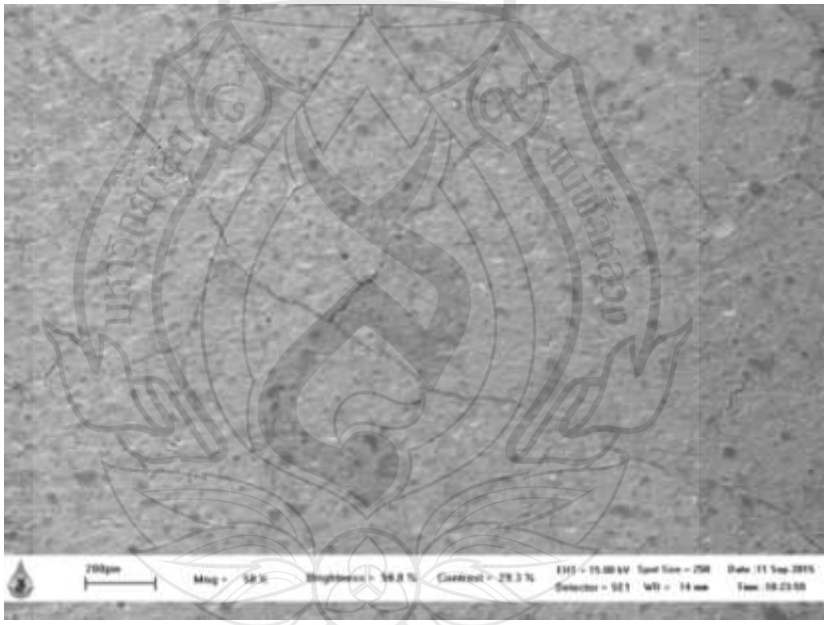

(b)

Figure 7.10 SEM Image with Magnification of 50X on Polished Surface of Geopolymer Made from Fly Ash with Average Particle Size of (a) 55 µm (no milling) and (b) 25 µm (milling 10 min) Activated at 60 ℃ under Saturated Condition with Initial Water Content of 29 wt%

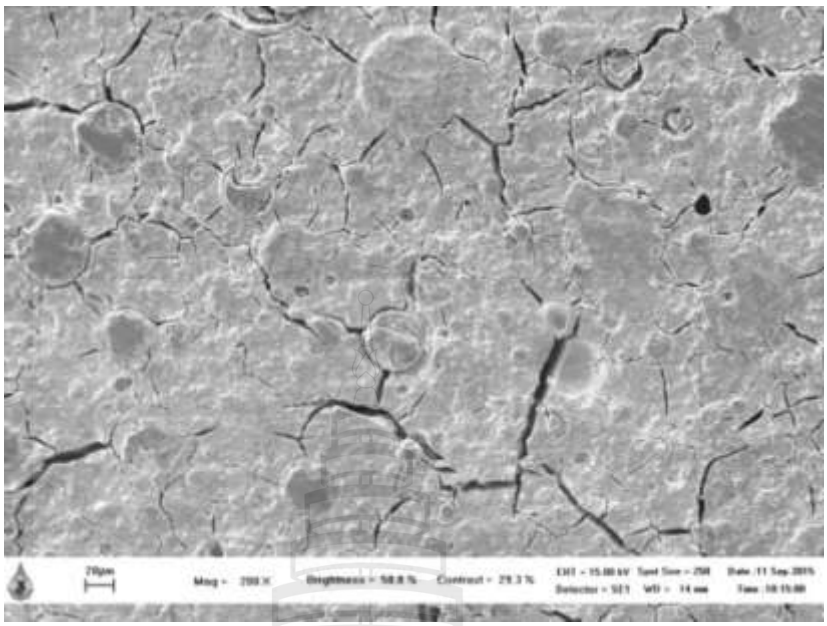

(a)

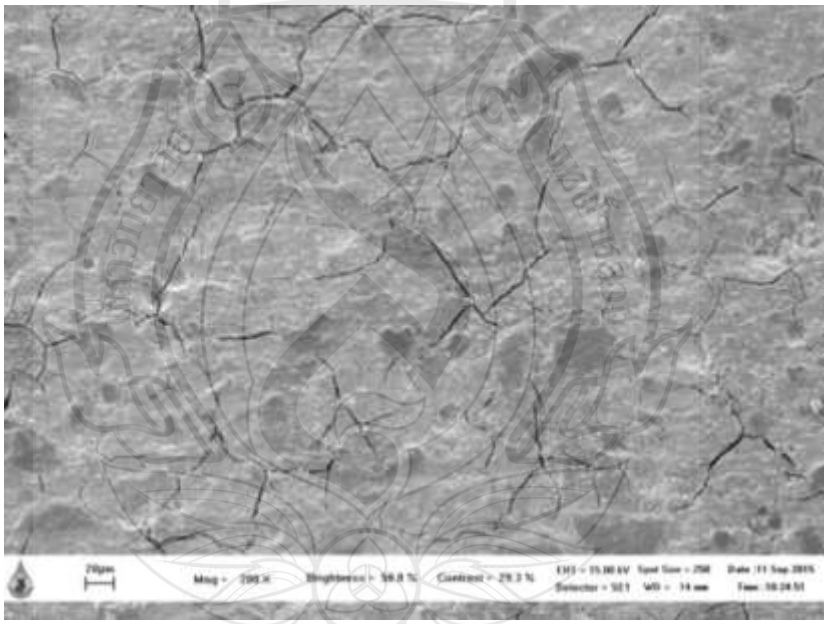

(b)

Figure 7.11 SEM Image with Magnification of 200X on Polished Surface of Geopolymer Made from Fly Ash with Average Particle Size of (a) 55 μm (no milling) and (b) 25 μm (milling 10 min) Activated at 60 ℃ under Saturated Condition with Initial Water Content of 29 wt%

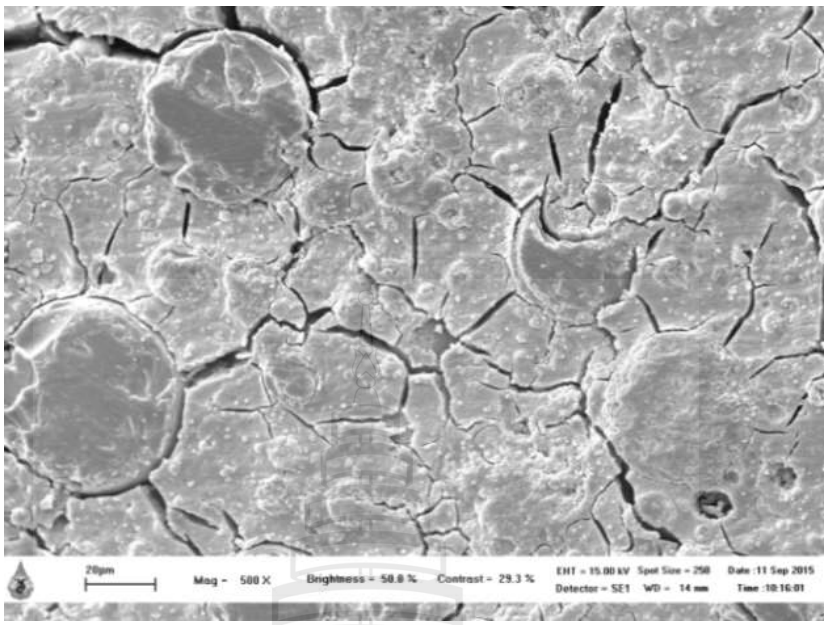

(a)

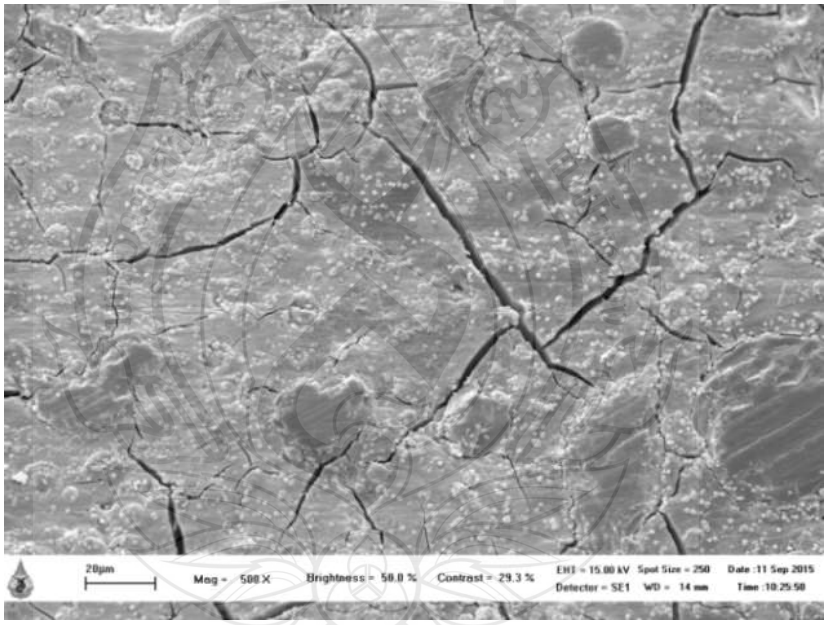

(b)

Figure 7.12 SEM Image with Magnification of 500X on Polished Surface of Geopolymer Made from Fly Ash with Average Particle Size of (a) 55 µm (no milling) and (b) 25 µm (milling 10 min) Activated at 60 ℃ under Saturated Condition with Initial Water Content of 29 wt%

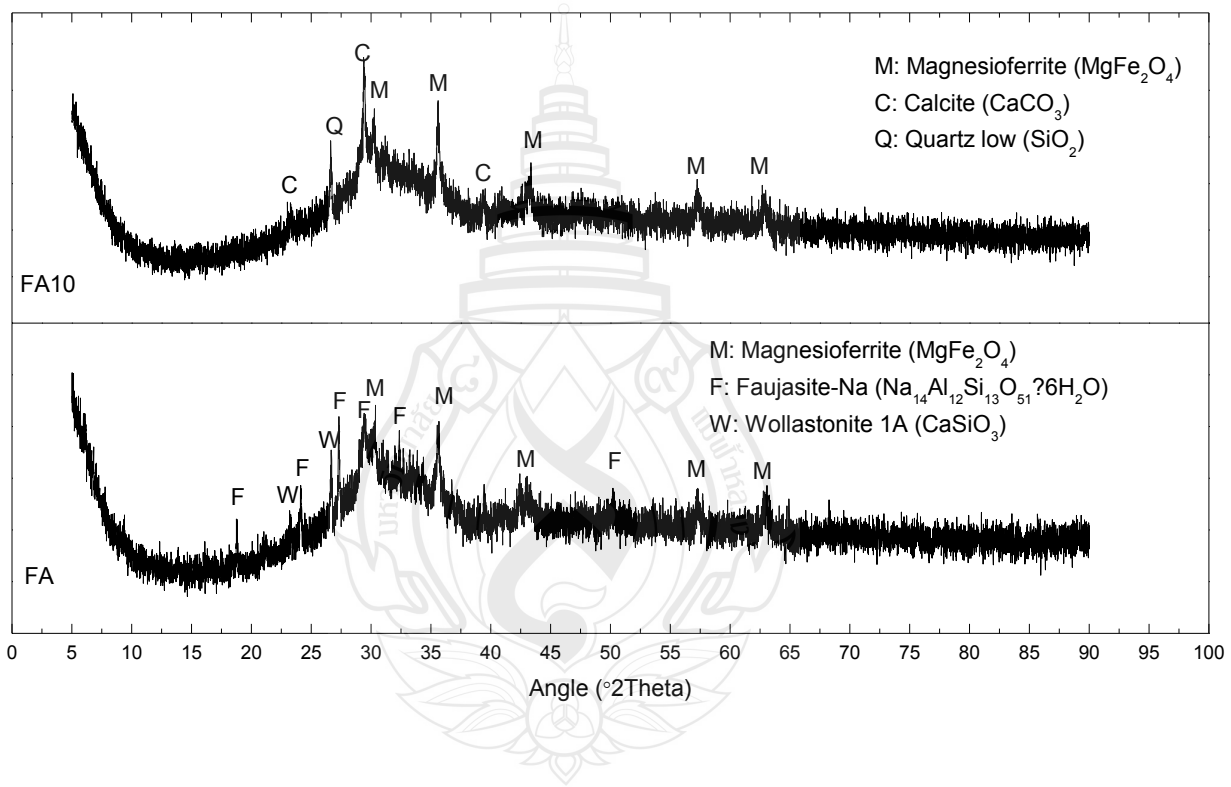

Figure 7.13 X-ray Diffraction Analysis on Geopolymer Made from Fly Ash with Average Particle Size of (a) 55 μm (no milling) and (b) 25 μm (milling 10 min) Activated at 60 ℃ under Saturated Condition with Initial Water Content of 29 wt%

CHAPTER 8

SUMMARY

In this research, factors affecting physical and mechanical properties, such as apparent, bulk, geometric density, porosity and compressive strength of fly ash-based geopolymer have been studied. The work was divided into four parts which were related to four factors. The first part was trying to improve compressive strength of fly ash-based geopolymer using saturated curing condition. The results showed that saturated curing condition was an effective method to increase significantly compressive strength compared to open condition. However, the activation temperature played an important role in geopolymerization as did the curing atmospheric condition. Therefore, the second part focused on activation temperature. The results showed that activation temperature of 75 ℃ gave a higher compressive strength compared to the 60 and 90 ℃ conditions. In addition to the curing atmospheric condition and activation temperature, another important factor, initial water content, was studied in part three. It was found that compressive strength was always increased when initial water content decreased. However, the lowest initial water content was limited to 24 wt% due to the poor workability of the paste. In the final part, particle size of fly ash as a key factor was studied. A significant increasing compressive strength was observed for the samples made from fly ash with average particle size of 25 μm. Nevertheless, the difference of compressive strength values as well as other physical properties among samples from the same batch was very large due to its poor workability. From all above, it could be concluded that the highest compressive strength was obtained at the activation temperature of 75 ℃ compared to 60 ℃ and 90 ℃, under saturated condition, using finer fly ash and with lower initial water content. Finally, fly ash-based geopolymer in this work was expected to be used as pavement materials or for small road construction since geopolymer with a compressive strength of 64.15±21.69 MPa was obtained.

REFERENCES

REFERENCES

Alvarez-Ayuso, E., Querol, X., Plana, F., Alastuey, A., Moreno, N., Izquierdo, M., Font, O., Moreno, T., Diez, S., Vazquez, E. & Bzrra, M. (2008). Environmental, physical and structural characterization of geopolymer matrixes synthesized from coal (co-)combustion fly ashes. *Journal of Hazardous Materials*, *154*, 175-183.

Arioz, E., Arioz, O. & Kockar, O. M. (2012). An experimental study on the mechanical and microstructural properties of geopolymers. *Procedia Engineering*, *42*, 100-105.

Arioz, E., Arioz, O. & Kockar, O. M. (2012). Leaching of F-type fly ash based geopolymers. *Procedia Engineering*, *42*, 1114-1120.

Armstrong, T. (2013). An overview of global cement sector trends. Retrieved November 8, 2015, from http://www.ficem.org/boletines/ct-2013/presentaciones2013/1-EXPERTOS/2_THOMAS-ARMSTRONG/ICR-FICEM-Presentation-Handout-30Aug13.pdf

Bakri, A. M. M. A., Kamarudin, H., Hussain, M. B., Nizar, I. K., Zarina, Y. & Rafiza, A. R. (2011). The Effect of Curing Temperature on Physical and Chemical Properties of Geopolymers. *Physics Procedia*, *22*, 286-291.

Bohlooli, H., Nazari, A., Khalaj, G., Kaykha, M. M. & Riahi, S. (2012). Experimental investigations and fuzzy logic modeling of compressive strength of geopolymers with seeded fly ash and rice husk bark ash. *Composites: Part B, 43*, 1293-1301.

Chanh, N. V., Trung, B. D. & Tuan, D. V. (2008). Recent research geopolymer concrete. *The 3rd ACF International Conference-ACF/VCA 2008 A.*18.

Chi, M. & Huang, R. (2013). Binding mechanism and properties of alkali-activated fly ash/slag mortars. *Construction and Building Materials*, *40*, 291-298.

Chindaprasirt, P., Chareerat, T. & Sirivivatnanon, V. (2007). Workability and strength of coarse high calcium fly ash geopolymer. *Cement & Concrete Composites*, *29*, 224-229.

Chindaprasirt, P., Jaturapitakkul, C., Challe, W. & Rattanasak, U. (2009). Comparative study on the characteristics of fly ash and bottom ash geopolymers. *Waste Management*, *29*, 539-543.

Criado, M., Jiménez, A. F. & Palomo, A. (2010). Effect of sodium sulfate on the alkali activation of fly ash. *Cement & Concrete Composites*, *32*, 589-594.

Davidovits, J. (2008, April 2). Chemical structure and applications. *Geopolymer Institute*. Retrieved November 8, 2015, from http://www.geopolymer.org/science/chemical-structure-and-applications/

Davidovits, J. (2011). Geopolymer Chemistry & Applications (3rd ed.). France: Institut Géopolymère.

Davidovits, J. (2008, May 25). H_2O, SiO_2 and Al_2O_3 ratios. *Geopolymer Institute*. Retrieved November 8, 2015, from http://www.geopolymer.org/faq/h2o-sio2-and-al2o3-ratios/

Ferone, C., Colangelo, F., Cioffi, R., Montagnaro, F. & Santoro, L. (2011). Mechanical performances of weathered coal fly ash based geopolymer bricks. *Procedia Engineering*, *21*, 745-752.

Görhan, G. & Kürklü, G. (2014). The influence of the NaOH solution on the properties of the fly ash-based geopolymer mortar cured at different temperatures. *Composites:Part B*, *58*, 371-377.

Guo, X., Shi, H. & Dick, W. A. (2010). Compressive strength and microstructural characteristics of class C fly ash geopolymer. *Cement & Concrete Composites*, *32*, 142-147.

Izquierdo, M., Querol, X., Phillipart, C., Antenucci, D. & Towler, M. (2010). The role of open and closed curing conditions on the leaching properties of fly ash-slag-based geopolymes. *Journal of Hazardous Materials*, *176*, 623-628.

Jaarsveld, J. G. S. V., Deventer, J. S. J. & Lukey, G. C. (2002). The effect of composition and temperature on the properties of fly ash- and kaolinite-based geopolymers. *Chemical Engineering Journal*, *89*, 63-73.

Jiménez, A. F., Palomo, A. & Criado, M. (2005). Microstructure development of alkali-activated fly ash cement: a descriptive model. *Cement and Concrete Research*, *35*, 1204-1209.

Joseph, B. & Mathew, G. (2012). Influence of aggregate content on the behavior of fly ash based geopolymer concrete. *Scientia Iranica A*, *19*(5), 1188-1194.

Kumar, S. & Kumar, R. (2011). Mechanical activation of fly ash: Effect on reaction, structure and properties of resulting geopolymer. *Ceramics International*, *37*, 533-541.

Lee, N. K. & Lee, H. K. (2013). Setting and mechanical properties of alkali-activated fly ash/slag concrete manufactured at room temperature. *Construction and Building Materials*, *47*, 1201-1209.

Ministry of Housing and Urban-Rural Development of the People's Republic of China. (2010). *Code for design of concrete structures, GB 50010-2010*. China: China Architecture & Building Press.

Nazari, A., Bagheri, A. & Riahi, S. (2011). Properties of geopolymer with seeded fly ash and rice husk bark ash. *Materials Science and Engineering A*, *528*, 7395-7401.

Pangdaeng, S., Phoo-ngernkham, T., Sata, V. & Chindaprasirt, P. (2014). Influence of curing conditions on properties of high calcium fly ash geopolymer containing Portland cement as additive. *Materials and Design*, *53*, 269-274.

Panias, D., Giannopoulou, I. P. & Perraki, T. (2007). Effect of synthesis parameters on the mechanical properties of fly ash-based geopolymers. *Colloids and Surfaces A:Physicochem.Eng.Aspects*, *301*, 246-254.

Phoo-ngernkham, T., Chindaprasirt, P., Sata, V. & Hanjitsuwan, S. (2014). The effect of adding nano-SiO_2 and nano-Al_2O_3 on properties of high calcium fly ash geopolymer cured at ambient temperature. *Materials and Design*, *55*, 58-65.

Rajamma, R., Labrincha, J. A. & Ferreira, V. M. (2012). Alkali activation of biomass fly ash-metakaolin blends. *Fuel*, *98*, 265-271.

Rattanasak, U. & Chindaprasirt, P. (2009). Influence of NaOH solution on the synthesis of fly ash geopolymer. *Minerals Engineering*, *22*, 1073-1078.

Rodriguez, E. D., Bernal, S. A., Provis, J. L., Paya, J., Monzo, J. M. & Borrachero, M. V. (2013). Effect of nanosilica-based activators on the performance of an alkali-activated fly ash binder. *Cement & Concrete Composites*, *35*, 1-11.

Ryu, G. S., Lee, Y. B., Koh, K. T. & Chung, Y. S. (2013). The mechanical properties of fly ash-based geopolymer concrete with alkaline activators. *Construction and Building Materials*, *47*, 409-418.

Somaratna, J., Ravikumar, D. & Neithalath, N. (2010). Response of alkali activated fly ash mortars to microwave curing. *Cement and Concrete Research*, *40*, 1688-1696.

Sukmak, P., Horpibulsuk, S. & Shen, S. L. (2013). Strength development in clay-fly ash geopolymer. *Construction and Building Materials*, *40*, 566-574.

Swanepoel, J. C. & Strydom, C. A. (2002). Utilisation of fly ash in a geopolymeric material. *Applied Geochemistry*, *17*, 1143-1148.

Temuujin, J., Riessen, A. V. & Williams, R. (2009). Influence of calcium compounds on the mechanical properties of fly ash geopolymer pastes. *Journal of Hazardous Materials*, *167*, 82-88.

Temuujin, J., Williams, R. P. & Riessen, A. V. (2009). Effect of mechanical activation of fly ash on the properties of geopolymer cured at ambient temperature. *Journal of Materials Processing Technology*, *209*, 5276-5280.

Tho-in, T., Sata, V., Chindaprasirt, P. & Jaturapitakkul, C. (2012). Pervious high-calcium fly ash geopolymer concrete. *Construction and Building Materials*, *30*, 366-371.

Vargas, A. S. D., Molin, D. C. C. D., Vilela, A. C. F., Silva, F. J. D, Pavão, B. & Veit, H. (2011). The effects of Na_2O/SiO_2 molar ratio, curing temperature and age on compressive strength, morphology and microstructure of alkali-activated fly ash-based geopolymers. *Cement & Concrete Composites*, *33*, 653-660.

Vora, P. R. & Dave, U. V. (2013). Parametric studies on compressive strength of geopolymer concrete. *Procedia Engineering*, *51*, 210-219.

Xie, J. & Kayali, O. (2014). Effect of initial water content and curing moisture conditions on the development of fly ash-based geopolymers in heat and ambient temperature. *Construction and Building Materials*, *67A*, 20-28.

Zivica, V., Palou, M. T. & Bagel, T. I. L. (2014). High strength metahalloysite based geopolymer. *Composites:Part B*, *57*, 155-165.

APPENDICES

APPENDIX A

EFFECT OF OPEN AND SATURATED CONDITION ON PHYSICAL PROPERTIES AND COMPRESSIVE STRENGTH OF FLY ASH-BASED GEOPOLYMER

Table A1 Compressive Strength

Activation temperature (℃)	Repeating number	Saturated time (day)	Average compressive strength (MPa)	Standard deviation (MPa)
60	#1	0	10.98	2.45
		1	15.60	2.48
		2	23.18	3.31
		3	38.11	6.08
	#2	0	21.89	4.17
		1	22.45	6.12
		3	27.46	4.88
	#3	0	13.75	2.54
		3	17.72	3.54
75	#1	0	12.72	0.96
		1	14.92	1.77
		2	18.79	1.87
		3	22.73	3.06
	#2	0	22.38	2.88
		1	22.79	3.25
		3	34.16	3.67
	#3	0	14.69	1.29
		3	24.05	1.59
90	#1	0	14.98	2.26
		1	11.24	2.11
		2	17.13	1.72
		3	21.63	1.59
	#2	0	16.89	2.02
		1	17.59	2.61
		3	25.23	2.77
	#3	0	12.71	0.60
		3	18.82	1.39

Table A2 Apparent Density

Activation temperature (℃)	Repeating number	Saturated time (day)	Average apparent density (g/cm^3)	Standard deviation (g/cm^3)
60	#1	0	2.35	0.05
		1	2.41	0.08
		2	2.44	0.11
		3	2.45	0.04
	#2	0	2.43	0.04
		1	2.38	0.02
		3	2.39	0.04
	#3	0	2.36	0.04
		3	2.42	0.01
75	#1	0	2.40	0.03
		1	2.42	0.05
		2	2.44	0.03
		3	2.41	0.03
	#2	0	2.38	0.02
		1	2.41	0.10
		3	2.38	0.02
	#3	0	2.37	0.06
		3	2.43	0.01
90	#1	0	2.41	0.02
		1	2.39	0.03
		2	2.39	0.02
		3	2.40	0.03
	#2	0	2.32	0.02
		1	2.33	0.04
		3	2.39	0.03
	#3	0	2.41	0.05
		3	2.36	0.02

Table A3 Bulk Density

Activation temperature (℃)	Repeating number	Saturated time (day)	Average bulk density (g/cm^3)	Standard deviation (g/cm^3)
60	#1	0	1.77	0.03
		1	1.82	0.03
		2	1.85	0.06
		3	1.86	0.03
	#2	0	1.71	0.02
		1	1.72	0.02
		3	1.71	0.01
	#3	0	1.73	0.03
		3	1.75	0.01
75	#1	0	1.78	0.02
		1	1.80	0.03
		2	1.79	0.03
		3	1.79	0.03
	#2	0	1.81	0.01
		1	1.81	0.06
		3	1.79	0.01
	#3	0	1.69	0.02
		3	1.71	0.01
90	#1	0	1.76	0.02
		1	1.75	0.03
		2	1.73	0.03
		3	1.74	0.01
	#2	0	1.68	0.02
		1	1.66	0.03
		3	1.67	0.01
	#3	0	1.72	0.04
		3	1.69	0.01

Table A4 Geometric Density

Activation temperature (℃)	Repeating number	Saturated time (day)	Average geometric density (g/cm^3)	Standard deviation (g/cm^3)
60	#1	0	1.85	0.02
		1	1.89	0.01
		2	1.90	0.01
		3	1.92	0.01
	#2	0	1.88	0.01
		1	1.89	0.04
		3	1.91	0.01
	#3	0	-	-
		3	-	-
75	#1	0	1.88	0.01
		1	1.91	0.01
		2	1.91	0.02
		3	1.93	0.02
	#2	0	1.92	0.02
		1	1.93	0.02
		3	1.95	0.01
	#3	0	-	-
		3	-	-
90	#1	0	1.90	0.01
		1	1.87	0.01
		2	1.89	0.01
		3	1.91	0.01
	#2	0	1.90	0.01
		1	1.90	0.01
		3	1.91	0.01
	#3	0	-	-
		3	-	-

Table A5 Porosity

Activation temperature (℃)	Repeating number	Saturated time (day)	Average porosity (vol%)	Standard deviation (vol%)
60	#1	0	24.71	0.30
		1	24.59	2.10
		2	24.10	1.15
		3	23.87	0.68
	#2	0	29.36	0.87
		1	27.80	1.23
		3	28.40	1.23
	#3	0	26.73	0.48
		3	27.51	0.14
75	#1	0	26.14	0.92
		1	25.55	0.41
		2	26.65	1.03
		3	25.77	0.92
	#2	0	23.89	0.64
		1	25.07	0.65
		3	24.47	0.23
	#3	0	28.68	2.23
		3	29.41	0.60
90	#1	0	27.06	1.22
		1	26.91	0.65
		2	27.68	1.21
		3	27.39	0.70
	#2	0	27.59	1.34
		1	28.70	0.78
		3	30.39	1.23
	#3	0	28.66	0.52
		3	28.43	0.68

APPENDIX B

EFFECT OF ACTIVATION TEMPERATURE ON PHYSICAL PROPERTIES AND COMPRESSIVE STRENGTH OF FLY ASH-BASED GEOPOLYMER

Table B1 Compressive Strength

Saturated time (day)	Repeating number	Activation temperature (℃)	Average compressive strength (MPa)	Standard deviation (MPa)
0	#1	60	10.98	2.45
		75	12.72	0.96
		90	14.98	2.26
	#2	60	21.89	4.17
		75	22.38	2.88
		90	16.89	2.02
	#3	60	13.75	2.54
		75	14.69	1.29
		90	12.71	0.60
1	#1	60	15.60	2.48
		75	14.92	1.77
		90	11.24	2.11
		60	22.45	6.12
	#2	75	22.79	3.25
		90	17.59	2.61
2	#1	60	23.18	3.31
		75	18.79	1.87
		90	17.13	1.72
3	#1	60	27.46	4.88
		75	34.16	3.67
		90	25.23	2.77
	#2	60	17.72	3.54
		75	24.05	1.59
		90	18.82	1.39

Table B2 Apparent Density

Saturated time (day)	Repeating number	Activation temperature (℃)	Average apparent density (g/cm^3)	Standard deviation (g/cm^3)
0	#1	60	2.35	0.05
		75	2.40	0.03
		90	2.41	0.02
	#2	60	2.43	0.04
		75	2.38	0.02
		90	2.32	0.02
	#3	60	2.36	0.04
		75	2.37	0.06
		90	2.41	0.05
1	#1	60	2.41	0.08
		75	2.42	0.05
		90	2.39	0.03
		60	2.38	0.02
	#2	75	2.41	0.10
		90	2.33	0.04
2	#1	60	2.44	0.11
		75	2.44	0.03
		90	2.39	0.02
3	#1	60	2.39	0.04
		75	2.38	0.02
		90	2.39	0.03
	#2	60	2.42	0.01
		75	2.43	0.01
		90	2.36	0.02

Table B3 Bulk Density

Saturated time (day)	Repeating number	Activation temperature (℃)	Average bulk density (g/cm^3)	Standard deviation (g/cm^3)
0	#1	60	1.77	0.03
		75	1.78	0.02
		90	1.76	0.02
	#2	60	1.71	0.02
		75	1.81	0.01
		90	1.68	0.02
	#3	60	1.73	0.03
		75	1.69	0.02
		90	1.72	0.04
1	#1	60	1.82	0.03
		75	1.80	0.03
		90	1.75	0.03
		60	1.72	0.02
	#2	75	1.81	0.06
		90	1.66	0.03
2	#1	60	1.85	0.06
		75	1.79	0.03
		90	1.73	0.03
3	#1	60	1.71	0.01
		75	1.79	0.01
		90	1.67	0.01
	#2	60	1.75	0.01
		75	1.71	0.01
		90	1.69	0.01

Table B4 Geometric Density

Saturated time (day)	Repeating number	Activation temperature (℃)	Average geometric density (g/cm^3)	Standard deviation (g/cm^3)
0	#1	60	1.85	0.02
		75	1.88	0.01
		90	1.90	0.01
	#2	60	1.88	0.01
		75	1.92	0.02
		90	1.90	0.01
	#3	60	-	-
		75	-	-
		90	-	-
1	#1	60	1.89	0.01
		75	1.91	0.01
		90	1.87	0.01
		60	1.89	0.04
	#2	75	1.93	0.02
		90	1.90	0.01
2	#1	60	1.90	0.01
		75	1.91	0.02
		90	1.89	0.01
3	#1	60	1.91	0.01
		75	1.95	0.01
		90	1.91	0.01
	#2	60	-	-
		75	-	-
		90	-	-

Table B5 Porosity

Saturated time (day)	Repeating number	Activation temperature (℃)	Average porosity (vol%)	Standard deviation (vol%)
0	#1	60	24.71	0.30
		75	26.14	0.92
		90	27.06	1.22
	#2	60	29.36	0.87
		75	23.89	0.64
		90	27.59	1.34
	#3	60	26.73	0.48
		75	28.68	2.23
		90	28.66	0.52
1	#1	60	24.59	2.10
		75	25.55	0.41
		90	26.91	0.65
		60	27.80	1.23
	#2	75	25.07	0.65
		90	28.70	0.78
2	#1	60	24.10	1.15
		75	26.65	1.03
		90	27.68	1.21
3	#1	60	28.40	1.23
		75	24.47	0.23
		90	30.39	1.23
	#2	60	27.51	0.14
		75	29.41	0.60
		90	28.43	0.68

APPENDIX C

EFFECT OF INITIAL WATER CONTENT ON PHYSICAL PROPERTIES AND COMPRESSIVE STRENGTH OF FLY ASH-BASED GEOPOLYMER

Table C1 Compressive Strength

Activation temperature (℃)	Initial water content (wt%)	Average compressive strength (MPa)	Standard deviation (MPa)
60	29	10.98	2.45
	34	7.02	0.77
	44	2.77	0.42
75	29	12.72	0.96
	34	7.47	0.44
	44	3.10	1.19
90	29	14.98	2.26
	34	9.60	0.35
	44	4.85	0.31

Table C2 Apparent Density

Activation temperature (℃)	Initial water content (wt%)	Average apparent density (g/cm^3)	Standard deviation (g/cm^3)
60	29	2.35	0.05
	34	2.35	0.04
	44	2.27	0.07
75	29	2.40	0.03
	34	2.41	0.09
	44	2.33	0.10
90	29	2.41	0.02
	34	2.37	0.04
	44	2.34	0.12

Table C3 Bulk Density

Activation temperature (℃)	Initial water content (wt%)	Average bulk density (g/cm^3)	Standard deviation (g/cm^3)
60	29	1.77	0.03
	34	1.66	0.02
	44	1.54	0.07
75	29	1.78	0.02
	34	1.71	0.06
	44	1.48	0.07
90	29	1.76	0.02
	34	1.66	0.02
	44	1.52	0.07

Table C4 Geometric Density

Activation temperature (℃)	Initial water content (wt%)	Average geometric density (g/cm^3)	Standard deviation (g/cm^3)
60	29	1.85	0.02
	34	1.74	0.02
	44	1.57	0.03
75	29	1.88	0.01
	34	1.81	0.01
	44	1.58	0.02
90	29	1.90	0.01
	34	1.78	0.01
	44	1.63	0.01

Table C5 Porosity

Activation temperature (℃)	Initial water content (wt%)	Average porosity (vol%)	Standard deviation (vol%)
60	29	24.71	0.30
	34	29.26	1.01
	44	32.21	3.17
75	29	26.14	0.92
	34	29.16	0.69
	44	36.40	1.35
90	29	27.06	1.22
	34	29.89	0.66
	44	34.95	1.80

APPENDIX D

EFFECT OF MILLING TIME AND PARTICLE SIZE ON PHYSICAL PROPERTIES AND COMPRESSIVE STRENGTH OF FLY ASH-BASED GEOPOLYMER

Table D1 Compressive Strength

Activation temperature (℃)	Saturated time (day)	Average particle size (μm)	Average compressive strength (MPa)	Standard deviation (MPa)
60	3	55	31.27	5.09
		25	44.67	7.33
	6	55	17.80	2.41
		25	44.32	8.77
	9	55	31.52	6.62
		25	49.71	3.07
75	3	55	22.24	2.06
		25	64.15	21.69

Table D2 Apparent Density

Activation temperature (℃)	Saturated time (day)	Average particle size (μm)	Average apparent density (g/cm^3)	Standard deviation (g/cm^3)
60	3	55	2.32	0.07
		25	2.32	0.07
	6	55	2.28	0.05
		25	2.47	0.02
	9	55	2.34	0.04
		25	2.38	0.05
75	3	55	2.34	0.05
		25	2.36	0.13

Table D3 Bulk Density

Activation temperature (℃)	Saturated time (day)	Average particle size (μm)	Average bulk density (g/cm^3)	Standard deviation (g/cm^3)
60	3	55	1.81	0.04
		25	1.88	0.05
	6	55	1.81	0.02
		25	1.94	0.02
	9	55	1.81	0.02
		25	1.87	0.03
75	3	55	1.72	0.01
		25	1.93	0.09

Table D4 Geometric Density

Activation temperature (℃)	Saturated time (day)	Average particle size (μm)	Average geometric density (g/cm^3)	Standard deviation (g/cm^3)
60	3	55	1.87	0.01
		25	2.00	0.03
	6	55	1.90	0.02
		25	2.02	0.02
	9	55	1.94	0.02
		25	2.02	0.01
75	3	55	1.78	0.02
		25	1.97	0.02

Table D5 Porosity

Activation temperature (℃)	Saturated time (day)	Average particle size (μm)	Average porosity (vol%)	Standard deviation (vol%)
60	3	55	22.00	0.65
		25	18.87	1.11
	6	55	20.36	0.94
		25	21.68	0.90
	9	55	22.86	0.53
		25	21.64	0.47
75	3	55	26.30	1.26
		25	18.37	1.11

APPENDIX E

CHEMICAL INFORMATION OF FLY ASH AND SODIUM SILICATE

Table E1 Chemical Composition of Fly Ash (FA: Mae Moh, Lampang, Thailand) Determined Using X-ray Fluorescence Spectrometer (HORIBA, MESA-500W)

Compo-sition	SiO_2	CaO	Fe_2O_3	Al_2O_3	SO_3	K_2O	TiO_2	Mn_2O_3	BaO
wt%	29.765	24.545	19.074	14.248	9.226	2.309	0.526	0.183	0.124

Table E2 Particle Size Distribution of Fly Ash Determined by Particle Distribution Analyzer (Malvern, Mastersizer 2000, Hydro 2000MU)

Distribution	D10	D50	D90	Average
Size (μm)	2	27	135	55

Table E3 Chemical Composition of Sodium Silicate (C. THAI CHEMICALS CO., LTD)

Composition	Na_2O	SiO_2	H_2O
wt%	15.50-17.50	34.25-36.25	46.25-50.25

CURRICULUM VITAE

CURRICULUM VITAE

NAME Mr. Hongsheng Cheng

DATE OF BIRTH 28 January 1987

ADDRESS 222 South Tianshui Road,
Lanzhou, Gansu, P. R. China
730000

EDUCATIONAL BACKGROUND

2011 Bachelor of Engineering
Nuclear Technology
Lanzhou University, P. R. China

WORK EXPERIENCE

2011-2013 Research Assistant
Institute of Modern Physics,
Chinese Academy of Sciences, P. R. China